The Formation of Tubulo-Vesicular Autophagosomes in Response to Non-Viral DNA Delivery Vectors

By Rebecca Louise Roberts

School of Medicine, Health Policy and Practice

University of East Anglia

June 2011

Abstract

Autophagy is activated in cells during nutrient deprivation and results in the formation of small double-membrane vesicles, known as autophagosomes. Autophagosomes deliver cytoplasmic contents to lysosomes for degradation. This provides a short term supply of amino acids that maintain cellular processes during starvation. Autophagosomes form following activation of the class III PI 3-kinase (Vps34), and translocation of the autophagy protein LC3 from the cytosol to the limiting membrane of the autophagosome. Autophagy can be visualised by following the redistribution of diffuse LC3 to small dots or 'LC3 puncta' in the cytoplasm. Interestingly, recent work has provided evidence for another pathway of LC3 translocation where LC3 becomes incorporated into large perinuclear tubulo-vesicular autophagosomes (TVAs). This thesis demonstrates that the formation of TVAs is triggered by the presence of non-viral DNA delivery vectors which include cationic liposomes frequently used for transfection.

In this study I have compared starvation-induced autophagosomes to TVAs. TVAs were induced by incubating cells with cationic liposomes. Live cell imaging experiments showed that TVAs formed from small LC3 positive punctae which became tubulated, and moved in a microtubule-dependent manner towards the perinuclear region of the cell. Incubation of cells with cationic liposomes impaired fusion of LC3 positive TVAs with lysosomes and slowed degradation and recycling of LC3. The TVAs therefore remained in the cytoplasm for prolonged periods. In common with starvation-induced autophagosomes, TVAs recruited lipidated LC3 and required Atg5 for their formation; however unlike autophagosomes they formed in absence of starvation. The TVAs were insensitive to wortmannin, and the knock-down of beclin-1, indicating that TVAs did not require the PI 3-kinase complex signalling.

TVA formation was prevented when clathrin-mediated endocytosis (CME) was inhibited, either by dominant negative Rab5 or by pharmacological inhibitors such as dynasore and chlorpromazine. These results indicted a role for the CME in TVA formation.

In conclusion, this thesis shows that TVA formation results from an overlap between autophagy and CME. The hypothesis that 'the autophagy pathway senses cationic liposomes entering cells via CME and forms modified autophagosomes that differ in composition, morphology and longevity to starvation-induced autophagosomes' is discussed.

TABLE OF CONTENTS

Abbreviations –

ALS – autophagic lysosome reformation

AMP – adenosine monophosphate

AMPK – AMP activated kinase

ATG/Atg – autophagy gene/protein

ATP – adenosine triphosphate

Baf A1 – bafilomycin A1

BCA - bicinchoninic acid

BSA – bovine serum albumin

CaPhos – calcium phosphate

$CaCl_2$ – calcium chloride

CHO cells – Chinese hamster ovary cells

CHX – cycloheximide

CCP – clathrin-coated pits

CCV – clathrin-coated vesicles

CME – clathrin mediated endocytosis

DAPI – 4'-6-diamidino-2-phenylindole

DEAE – diethylaminoethyl

DFCP1 - double FYVE-containing protein 1

DMEM - Dulbecco's modified Eagles media

DNA – deoxyribonucleic acid

ECL – enhanced chemiluminescence

EE – early endosome

EEA1 – early endosome antigen 1

eIF4E-BP1 – eukaryotic initiation factor 4E-binding protein 1

EM – electron microscopy

ER – endoplasmic reticulum

ERGIC – ER-to-Golgi intermediate compartment

ESCRT - endosomal sorting complex required for transport

FCS – foetal calf serum

FIP200 – focal adhesion kinase family interacting protein of 200 kDa

FYVE domain - Fab 1, YOTB, Vac 1 and EEA1 domain

GFP – green fluorescent protein

HBSS – Hanks balanced salt solution

HEK cells – human embryonic kidney cells

HEPES - 4-(2-hydroxyethyl)-1-piperazineethanesulfonic acid

HeBS – HEPES buffered saline

HRP - horseradish peroxidase

kDa – kilo Daltons

LAMP – lysosome associated membrane protein

LE – late endosome

MEF cells – mouse embryonic fibroblast cells

MEM - Minimum essential media

MES - 2-(N-morpholino)ethanesulfonic acid

mTOR – mammalian Target of Rapamycin

mTORC1/2 – mTOR complex 1 or 2

MTs – microtubules

MTOC – microtubule organising centre

MVB – multivesicular body

NaAs – sodium arsenate

NEAA – non-essential amino acids

Noc – nocodazole

NT siRNA – non-targeted siRNA

Oligo - oligomer

PBS – phosphate buffered saline

PCR – polymerase chain reaction

PEI - polyethylenimine

PFA – paraformaldehyde

PI – phosphatidylinositol

PI 3-K – phosphatidylinositiol 3-kinase

PI(3)P - phosphatidylinositol 3-phosphate

PKB – protein kinase B

POC chamber – perfusion open/closed chamber

P/S – penicillin-streptomycin

Raptor - regulatory associated protein of mTOR

RFP – red fluorescent protein

Rictor - rapamycin-insensitive companion of mTOR

RNA – ribonucleic acid

ROI – region of interest

S6K – S6 kinase

SDS – sodium dodecyl sulphate

SDS-PAGE – SDS polyacrylamide gel electrophoresis

siRNA - small interfering RNAs

TBS/TBST – Tris buffered saline/with Tween-20

TGN – trans-Golgi network

UBA – ubiquitin associated domain

Ulk – Unc-like kinase

UVRAG - UV irradiation resistance-associated gene

WIPI - WD-repeat protein interacting with phosphoinositides

List of Figures and Tables

Chapter 1:

Introduction

1.1 Aims of the Study –

Autophagy is a conserved pathway which plays a role in the supply of nutrients during starvation which is important for cell survival. There is recent evidence to support a role for autophagy in the innate immune response as it is activated during viral and non-viral entry into cell. There is evidence emerging from Gao *et al* (2008) that nanomaterials including non-viral DNA delivery vectors can activate autophagy. Cationic liposomes that are for transfection which activate autophagy produce autophagosomes that are morphologically different to starvation-induced autophagosomes.

The aims of this study –

- → To determine which markers can be use to indicate the induction of canonical autophagy in response to starvation, and characterisation of autophagic response using both fluorescence microscopy and Western blot analysis.
- → To establish which non-viral gene delivery vectors activate autophagy, using the above markers to monitor induction, and to characterise this response with respect to the canonical autophagic pathway.
- → To compare non-viral vector to other cellular responses to determine if they overlap with the autophagy pathway in producing a response.
- → To learn the mechanism by which non-viral gene delivery vectors enter cells and activate autophagy using pharmacological inhibitors to prevent cellular uptake to determine which route plays a role in entry and to see if this affects the response to the non-viral gene delivery vectors.

The introduction will illustrate canonical autophagy, and discuss the specifics of its activation, the signalling pathway and the formation of autophagosomes. Following this, the introduction will move into nanotheranostics, an area with increasing interest for using nanoparticles to imaging, diagnose and treat patients with various pathologies. This section will highlight how autophagy can be activated by a number of these particles and the importance of understanding its role.

Chapter 1 – Introduction:

1.2 Autophagy -

Autophagy is a catabolic process in which proteins and organelles are sequestered for degradation in lysosomes. It is conserved through from simple eukaryotes such as yeast to higher eukaryotes such as humans where it has developed multiple functions. Cells have a basal level of autophagy however autophagy increases dramatically following a number of intra- and extracellular stimuli such as nutrient deprivation, accumulation of mis-folded proteins, damaged organelles and oxidative stress (Yorimitsu and Klionsky 2005). Three forms of autophagy are described as macroautophagy, microautophagy and chaperone-mediated autophagy. Macroautophagy, commonly referred to as autophagy, is the subject of this study, involves the formation of double membrane vesicles known as autophagosomes which fuse with lysosomes (figure 1.1).

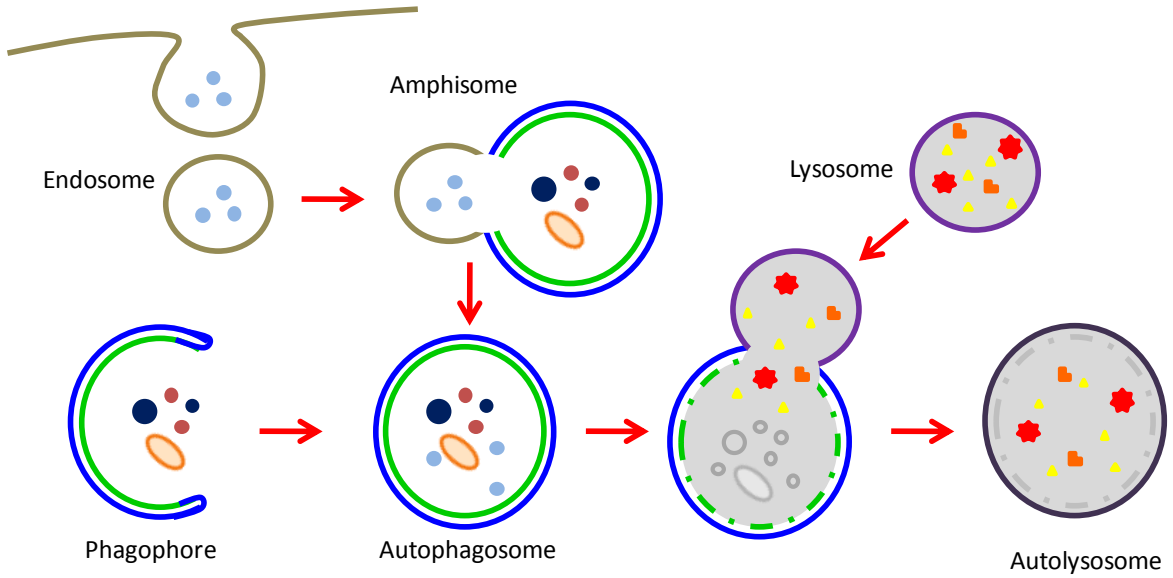

Figure 1.1 – the formation of autophagosomes and fusion with lysosomes

This pathway is triggered by a number of stimuli including starvation; resulting in digestion of the contents of the autophagic vesicle or autophagosome, and generates amino acids to counteract the effects of nutrient deprivation. In contrast, microautophagy occurs when the lysosomal membrane sequentially invaginates and sequesters portions of the cytoplasm for degradation (Kunz et al 2004). Chaperone-mediated autophagy also takes place at the

lysosomal membrane and requires chaperone proteins which interact with targeting sequences on cargo proteins in order for them to translocate across the lysosome membrane (Bandyopadhyay et al 2009). There is also growing evidence for autophagy involvement as an innate immune response in higher eukaryotes, whereby the process may have originally been implicated as a stress response to nutrient depravation, it has now evolved for the removal of invading pathogens and selective degradation of protein aggregates.

1.2.1 Origins and the Production of the Autophagosome Membrane -

Autophagy is a dynamic process involving a number of steps and numerous components. Genes implicated in autophagy are denoted ATG and their proteins are named using Atg for autophagy-related (Klionsky et al 2003, Klionsky 2005; Mizushima 2007). To date at least 30 genes involved in the different stages of autophagy have been identified from yeast genetic screens and many homologues have been identified in higher eukaryotic organisms where the autophagy pathway has developed multifaceted functions and overlaps with other pathways such as the ubiquitin-proteasome system, endocytosis and apoptosis. Autophagy has been intensively studied in yeast and much of its mechanics and signalling components have been identified in this system. A major challenge has been determining the origin of the autophagosome membrane in mammalian systems. The first electron microscopy (EM) studies from Dunn concluded that the membranes must be derived from pre-existing structures such as the ER (Dunn 1990a and b). This is supported by more recent electron tomography studies showing that the ER forms a scaffold, or cradle, for the growing autophagosome membrane (Axe *et al* 2008*,* Hayashi-Nishino *et al* 2009). Another paper by Hailey *et al* (2010) shows the mitochondria as a source for autophagosome membrane, suggesting this organelle contributes as much as the ER membrane to autophagosome formation. Similarly, inhibition of endocytosis has a detrimental effect on autophagy, reducing the number of autophagosomes; suggesting that the plasma membrane may provide membrane for autophagosomes (Ravikumar *et al* 2010). The contribution of membranes from several organelles to the phagophore need not be mutually exclusive; it is possible that depending on the conditions and the stimulus, they may all contribute to the formation of autophagosomes. It is possible that different stimuli will activate formation of autophagosomes from different sources, and this will also

determine the cargo which is sequestered. The current model proposed for the formation of autophagosomes from the ER is the 'cradle model' (Hayashi-Nishino *et al* 2009, Matsunga *et al* 2010). See figure 1.2 below. The induction of autophagy and the subsequent deformation of the ER membrane is due to the localisation of a number of autophagy proteins to the site, and begins with the recruitments of Atg14, and Atg6 also known as beclin-1 which is part of a PI(3)-kinase complex. It is the localisation of a PI(3)K complex to specific sites at the ER and an increase in PI(3)P production which recruits lipid binding proteins containing Fab 1, YOTB, Vac 1 (vesicle transport protein), and EEA1 (FYVE) domains such as double FYVE-containing protein 1 (DFCP1) and WD-repeat protein interacting with phosphoinositides (WIPI) (Atg18) to provide a scaffold for assembly of further Atg proteins.

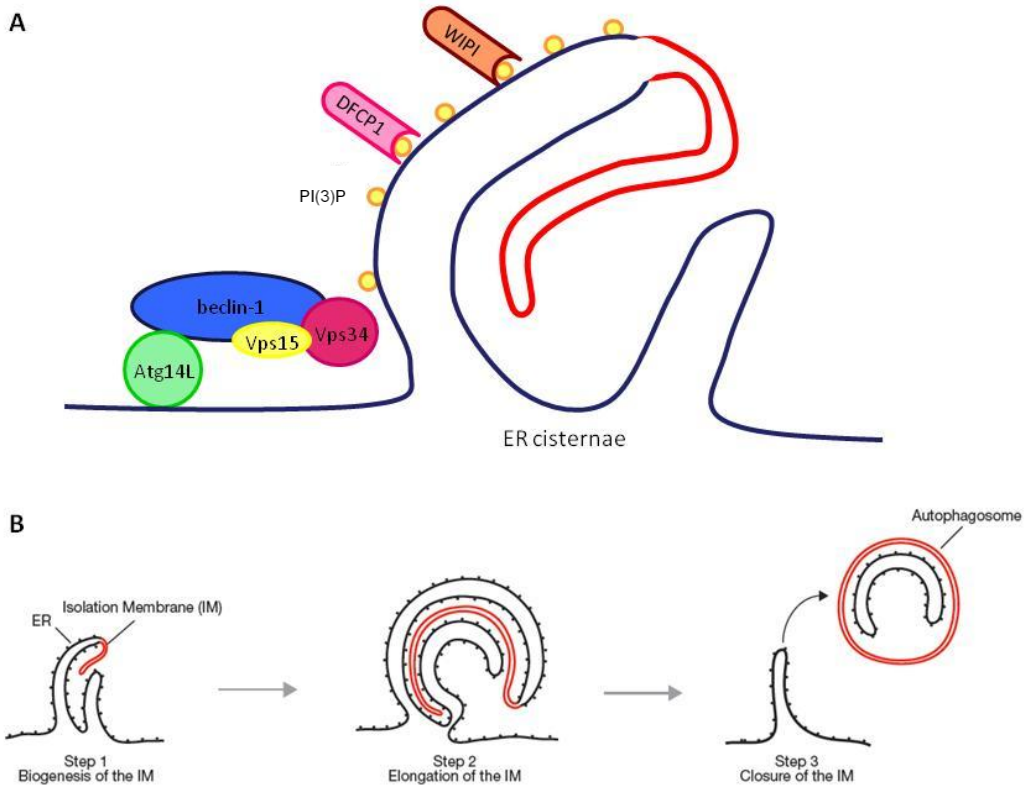

Figure 1.2 – Formation of Autophagsomes at the ER – (modified from Tooze and Yoshimori 2010) **-** induction of autophagy results in a localisation of the PI 3-kinase complex to specific sites at the ER and an increase in PI(3)P production which recruits DFCP1 and WIPI proteins to provide a scaffold for further Atg proteins to assemble (A). The formation of the isolation membrane and subsequent elongation is supported by the ER, and the formation of the omegasome. Once closure of the membrane has occurred the autophagosome can leave and traffic through the cytoplasm.

During nutrient depletion amino acid levels fall in the cytoplasm and this signals a starvation signal which will result in Atg14 localisation to the ER, recruiting the PI 3-kinase complex. Atg14 is an essential protein as part of the PI 3-K complex interacting with beclin-1, and localises this complex to the phagophore site for the localised generation of PI(3)P (Matsunaga *et al* 2010). The generation of PI(3)P will recruit proteins containing FVYE domain such as WIPI and DFCP-1 to the ER. This results in a fragment of the ER cisternae surrounds a portion of the cytoplasm. The isolation membrane (IM) then extends from the structure enriched in PI(3)P as it is cupped between the ER membranes. The machinery which closes the isolation membrane and results in the detachment of the autophagosomes is not yet known (Tooze and Yoshmori 2010). The elucidation of the membrane source of the autophagosomes in higher eukaryotes has illustrated that they have multiple site for autophagosomes formation termed sites for isolation membrane (IM) formation, whereas in yeast there are distinct site for the pre-autophagosome structure (PAS) to form (Orsi *et al* 2010).

1.2.2 The Core Sets of Proteins Required for Autophagy -

Autophagosome formation requires three core sets of proteins – a phosphatidylinositol 3-kinase (PI 3-K) complex; the ubiquitin-like protein (Ubl) system; and Atg9 and its recycling system (Klionsky 2005; Xie and Klionsky 2007). The PI 3-K complex, as described above, consists of beclin-1, Vsp34 (type III PI 3-kinase) and Vsp150. This complex is key in orchestrating the nucleation of other autophagy proteins to the site of phagophore formation by localised PI(3)P production.

The majority of the studies have been carried out in yeast to identify all the autophagy proteins, and in mammalian cells the homologs are currently being identified. The Ubl systems produces the Atg5-Atg12-Atg16 complex, and conjugates LC3/Atg8 to phosphatidylinositol (PE). Atg16 has a coiled-coil domain with a high degree of conservation of the essential residues that are crucial for autophagy (Fujita *et al* 2008). Whereas in higher eukaryotes Atg16L1 has addition domains known as WD40 domains at the C terminus and their function is currently unknown. It is possible that these domains confer other functions to Atg16L1, for example, in a recent paper by Ravikumar *et al* (2010), Atg16L1 is shown to localise to the cell membrane and participate in endocytosis. The coiled-coil domain of

Atg16L1 has a fundamental role during autophagosome formation and forms a larger complex with the smaller Atg5-Atg12 complex. Firstly, Atg12 is activated by Atg7 and then is transferred to the E2-like Atg10 and is subsequently covalently linked to Atg5. The Atg12-Atg5 interacts non-covalently with Atg16L1 and this complex mainly resides on the outer side of the membrane as it expands (Mizushima et al 1998, Xie and Klionsky 2007). Atg16L1 can also form non-covalent interactions with itself to form tetramers; it is possible that this is the scaffold that supports the formation and the expansion of the isolation membrane from the ER. Another important role for Atg16L1 is the correct localisation of Atg8, termed LC3 in mammalian cells.

LC3 is commonly used as a marker for autophagy as it associates with the inner and outer membranes of the autophagosome during formation and remains associated through to degradation in lysosomes. The LC3 which is on the inner membrane is degraded following fusion with lysosomes, and the LC3 that is on the outer leaflet is recycled. In humans, there are three families of Atg8-like proteins and these are known as microtubule-associated protein 1 light chain 3 (MAP1LC3 or LC3), GABARAP (γ-aminobutyric-acid-type-A ($GABA_A$) receptor-associated protein) and GATE-16 (Golgi-associated ATPase enhancer of 16 kDa). All of the Atg8 homologs undergo lipidation generating a lipidated form, known as LC3-II, and then move from the cytosol to the autophagosome membrane. The exact function of GABARAP and GATE-16 are currently being investigated and are thought to play a role downstream in autophagosome maturation rather than during formation (Weidberg *et al* 2010). LC3 has been found to exist in three isotypes known as LC3A, LC3B and LC3C, all of which participate in autophagy.

LC3 was originally described as a microtubule-associated protein and is synthesised in the pro-form where it rapidly becomes cleaved and forms a pool of cytosolic protein known as the LC3-I form, during autophagy activation it becomes cleaved at glycine 120 and lipidated with phosphatidylethanolamine (PE), forming LC3-II which can now associate with the isolation membrane. The process of conjugation requires a second set of ubiquitin-like proteins (figure 1.3B). Firstly, LC3 is cleaved by the Atg4 protease at its C terminus to expose a glycine residue at position 120. The E1-like activating enzyme Atg7 allows transfer of LC3 to Atg3 and then conjugation of LC3 to PE (Kabeya et al 2000).

Membrane expansion results in sequestration of cytosol, and/or organelles and damaged proteins, and eventually leads to closure of the membrane, and the fully formed vesicle will move away from the ER (Axe *et al* 2009). At this point LC3 remains associated with the autophagosome and the other Atg proteins involved in autophagosome formation are released.

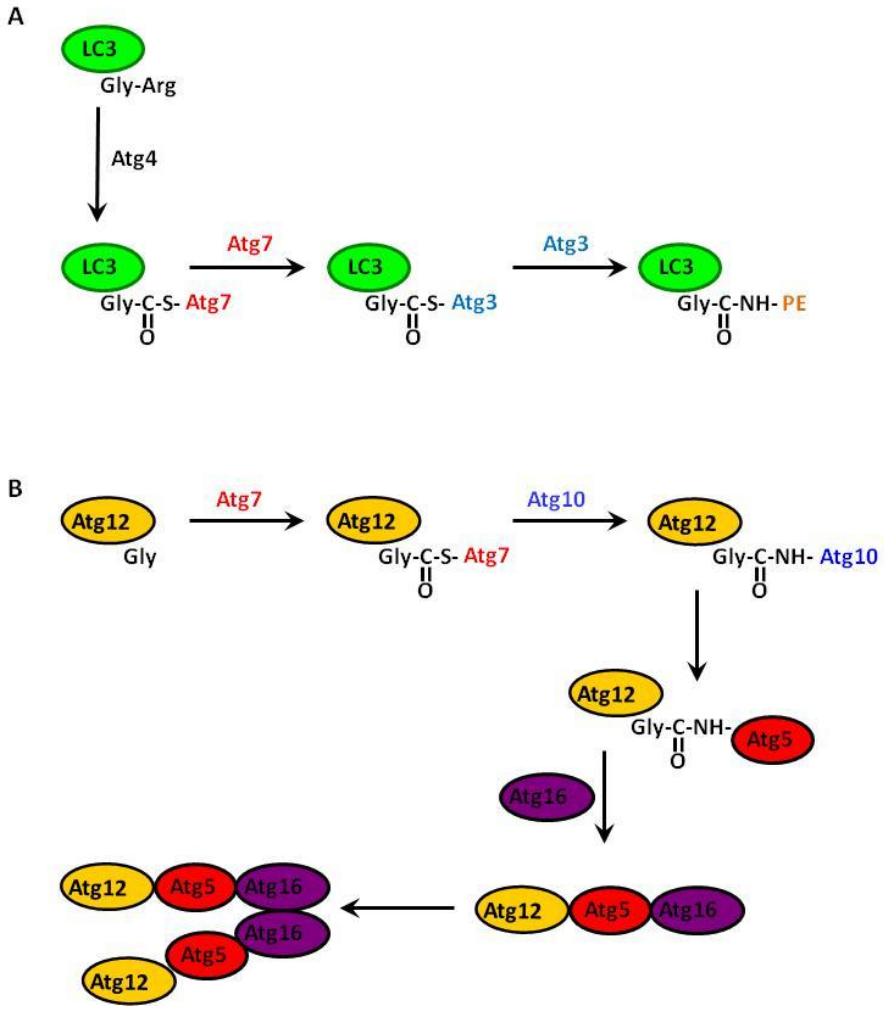

Figure 1.3 – The two ubiquitin-like (Ubl) conjugation systems involved in the formation of the autophagosome – (A) – LC3 is cleaved by Atg4 to expose a glycine residue which is conjugated to the E1-like Atg7 via a thioester link. Following this, LC3 is transferred to Atg3, an E2-like enzyme then conjugated to a PE molecule. **(B) –** a similar process occurs when Atg12 is activated and conjugated to Atg7 and Atg10. Following this, Atg12 is conjugated to Atg5 to form a complex, which then associates non-covalently with Atg16. This complex provides support and scaffolding for the forming autophagosome.

A number of autophagy proteins are recruited to the phagophore because they bind PI(3)P through FYVE domains. This includes DFCP1, Atg18 (WIPI-1/2), Atg20 and Atg24. The precise function of DFCP1 is currently unknown however; it contains two FYVE domains and

can be used as a marker for sites of autophagosome formation. Similarly, Atg18, termed WIPI in mammals can be used as a marker for induction of autophagy. Interestingly, a paper by Polson *et al* (2010) showed that WIPI-2 is recruited to autophagosomes in a PI(3)P dependent manner, however an interaction with another protein is responsible for anchoring it to the membranes.

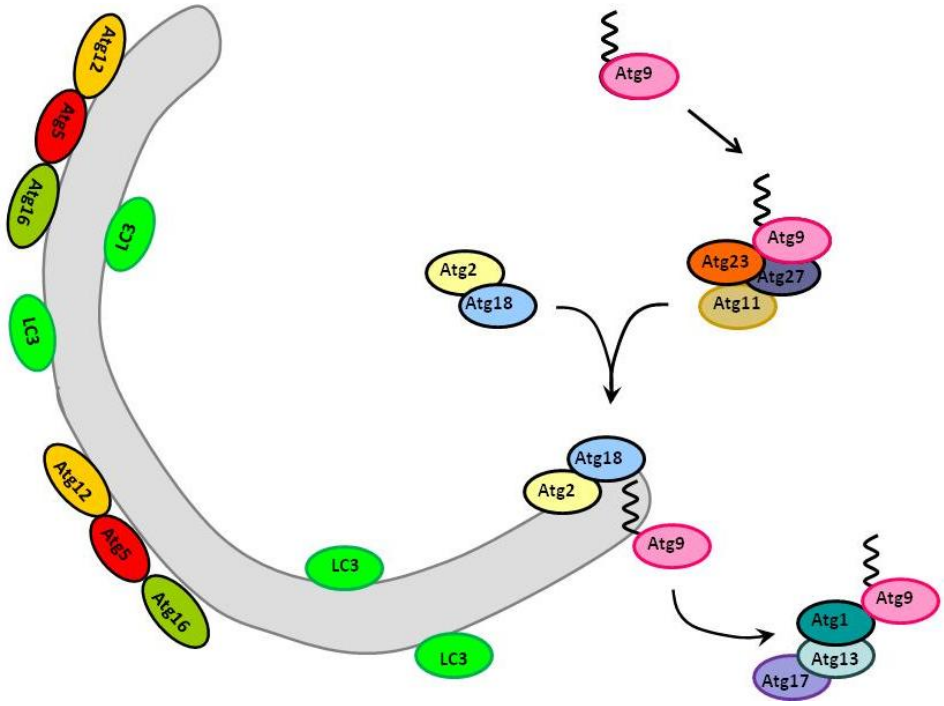

Figure 1.4 – Formation of the Phagophore – the localisation of Atg proteins to the PAS during autophagy induction includes the Atg12-Atg5-Atg16 and LC3 to the expanding membrane. Atg9 is thought to deliver lipids for the membrane to expand, and its cycling includes Atg2 and Atg18 at the PAS and Atg11, Atg23 and Atg27 to the membrane.

Many studies describe the formation of a 'pre-autophagosome structure' or 'phagophore assembly site' (PAS) in yeast (Figure 1.4). PAS may be analogous to the isolation membrane seen in higher eukaryotes. In common with mammalian cells formation of PAS involves the Atg12-Atg5:Atg16 complex, lipidation of LC3/Atg8 and recruitment of LC3/Atg8 II to membranes. Yeast genetic screens have identified further proteins involved including Atg20 and Atg24. Further work is required to determine their roles in autophagy (He and Klionsky 2010). Atg9 is the only transmembrane Atg protein and has been shown to localise to the PAS, where it is thought to deliver lipids (He et al 2008, Young et al 2006). Transport of proteins to the PAS involves Atg11, Atg23 and Atg27, and retrieval depends on Atg1 kinase:Atg13 complex as well as Atg2 and Atg18, and retrieval of Atg9 recycling

pathway is necessary for autophagosome formation, as illustrated in figure 1.4 (Xie and Klionsky 2007, Young et al 2006, He *et al* 2009).

1.2.3 Recycling of LC3 -

Once the autophagosome is formed, it traffics through the cytoplasm via microtubules to fuse with lysosomes. To prevent the movement of autophagosomes on microtubules, cells can be incubated with nocodazole, this prevents the tubulin subunits from polymerising and forming tubes. Atg4 is the cysteine protease which is responsible for the initial cleavage of LC3 to allow lipidation. Atg4 is also responsible for the cleavage of the PE conjugate from LC3 and release from the autophagosomes membrane and recycling for further rounds of lipidation (Noda *et al* 2009). There are 4 mammalian homologs of Atg4, and Atg4B has the broad specificity for LC3 and its mammalian paralogs GATE-16 and GABARAP. The active site consists of catalytic triad Cys74, His 280 and Asp278 residues, and the protease deficient mutant $Atg4B^{C74A}$ or $Atg4B^{C74S}$ prevent the formation of autophagosomes (Fujita *et al* 2008). Atg4 is required at both the initial stage and the end stage of autophagy following interactions with the lysosomes.

1.2.4 mTOR the Master Regulator of Autophagy Signaling -

The sections above described how the isolation membrane and autophagosome are formed. The next section describes how this process is activated in response to starvation. One of the key regulators of autophagy is the target of rapamycin (TOR) kinase. Mammalian TOR kinase (mTOR) is a serine/threonine kinase that plays a central role in many complex cell signalling pathways which regulate cell growth, cell cycle, protein translation and autophagy (Pattingre et al 2008, Weichhart and Saemann 2009). TOR is found in two evolutionarily conserved complexes - mTORC1 and mTORC2. mTORC1 consists of mTOR and regulatory associated protein of mTOR (raptor). The mTORC1 complex incorporates signals from nutrients and hormones and promotes protein translation through the phosphorylation of the downstream effectors S6 kinase (S6K) and eIF4E-BP1. mTORC1 inhibits autophagy through phosphorylation of Atg13. mTORC2 contains the rapamycin-insensitive companion of mTOR (rictor) and participates in regulation of assembly of the cytoskeleton (Inoki and Guan 2006, Pattigre *et al* 2008). mTORC1 is inhibited by rapamycin, and therefore activates autophagy. Another inhibitor, known as Torin1 is a second

generation inhibitor of mTOR with specificity for mTORC1 (Thoreen *et al* 2009). Torin1 is an ATP-competitive inhibitor of mTOR, whereas rapamycin binds to a hydrophobic pocket and prevents mTORC1 complex formation. There is also evidence that mTOR inhibits bulk endocytosis and can promote endocytic degradation of proteins to supply nutrients during starvation (Hennig *et al* 2006). Similarly mutants of the Rab5 protein that impair early endosome transport and also early to late endosome maturation also have an inhibitory effect on mTOR (Flinn *et al* 2010). There is increasing evidence emerging that mTOR has a role in the endocytic pathway, as well as being a key regulator of autophagy and protein translation.

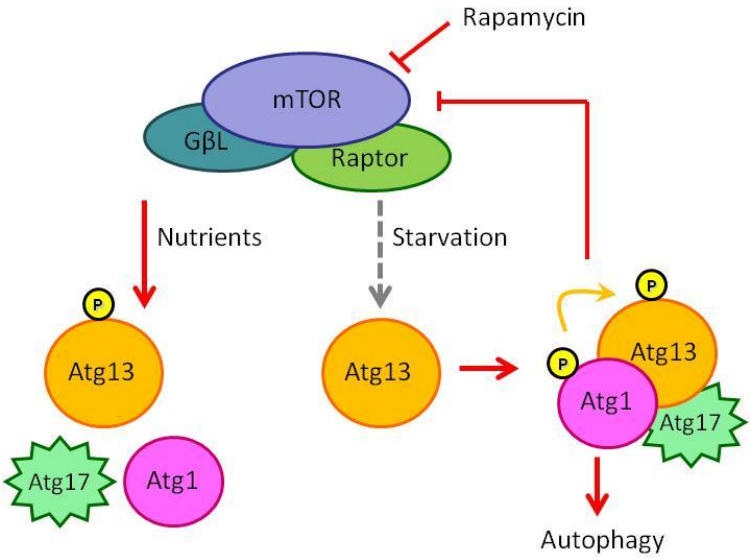

Figure 1.5 – mTOR regulation of Atg1-Atg13-Atg17 complex during nutrient-rich and starvation conditions.

In nutrient rich conditions amino acid levels in cells are high and phosphorylation of Atg13 by mTORC1 prevents an interaction with Atg1 (figure 1.5). During starvation amino acid levels drop, mTOR is inhibited allowing the formation of an Atg13-Atg1-Atg17 complex (see figure 1.4 above). This results in activation of Atg1, promoting its auto-kinase activity and phosphorylation of Atg13. Atg1 also inhibits mTOR as a negative feedback loop (Chang and Neufeld 2009, Chan and Tooze 2009). Atg1 localises to the PAS and is crucial in the recruitment of other key autophagy proteins as discussed above. In mammalian systems there are five isoforms of Atg1 known as Unc-like kinases (Ulk) 1-5(Chan and Tooze 2009). Similarly, Ulk-Atg13 have been found to interact with (focal adhesion kinase family interacting protein of 200 kDa (FIP200) which although has no sequence homology, is

thought to be the mammalian counterpart of Atg17, and it is the Ulk-mAtg13-FIP200 complex which is required in mammalian cells for autophagosome formation (Hara *et al* 2009, Ganley *et al* 2009). Recent evidence by two groups has further highlighted mTOR regulation of Ulk-1. Kim *et* al (2011) have shown the mTOR directly phosphorylates Ulk-1 and prevented it from interaction with AMPK. Phosphorylation of Ulk-1 by AMPK is on different serine residues, and this activates Ulk-1 and allows it to form the complex with Atg13 and FIP200 (Kim *et al* 2011, Hsu *et al* 2011).

1.2.5 Upstream and Downstream Effectors of mTOR -

A number of stimuli, such loss of nutrients, insulin and growth factors trigger signalling pathways that converge to either activate or inhibit mTOR. The insulin receptor, for example, activates phosphoinositide 3-kinases (PI 3-Ks), Akt (PKB) and Rheb proteins leading to increased mTOR activity and inhibition of autophagy (Manning and Cantley 2003). The localisation of mTOR has been discussed in many papers, and evidence suggests it can localise to the ER, Golgi, late endosomes and most recently to the lysosome membranes (Liu and Zheng 2007). Sancak *et al* (2010) demonstrated that mTOR in the presence of amino acids will redistribute to Rab7 positive structures in the perinuclear region. The upstream effectors TSC2 and Rheb are localised endosome membranes, and this localisation is important in mTOR activity. Sancak *et al* (2010) showed that the Ras-related GTPases (Rag GTPases) A-D and another protein complex known as the Ragulator are important regulators of mTORC1. During nutrient rich conditions the Ragulator complex induces redistribution of mTOR and Rag GTPases to the late endosomes and lysosomes (Kim *et al* 2009, Sancak *et al* 2008 and 2010). There is also recent evidence from Yu *et al* (2010) to demonstrate that mTOR is important in controlling the reformation of lysosomes once they have fused with autophagosomes (see below).

Other regulators of autophagy include insulin and cellular energy levels which depend on the ratio of ADP to ATP. Insulin signals through the insulin receptor increasing the uptake of glucose for glycogen synthesis and generates $PI(3,4,5)P_3$ which inhibits the TSC1/2 complex, activating Rheb and mTOR thus inhibiting autophagy.

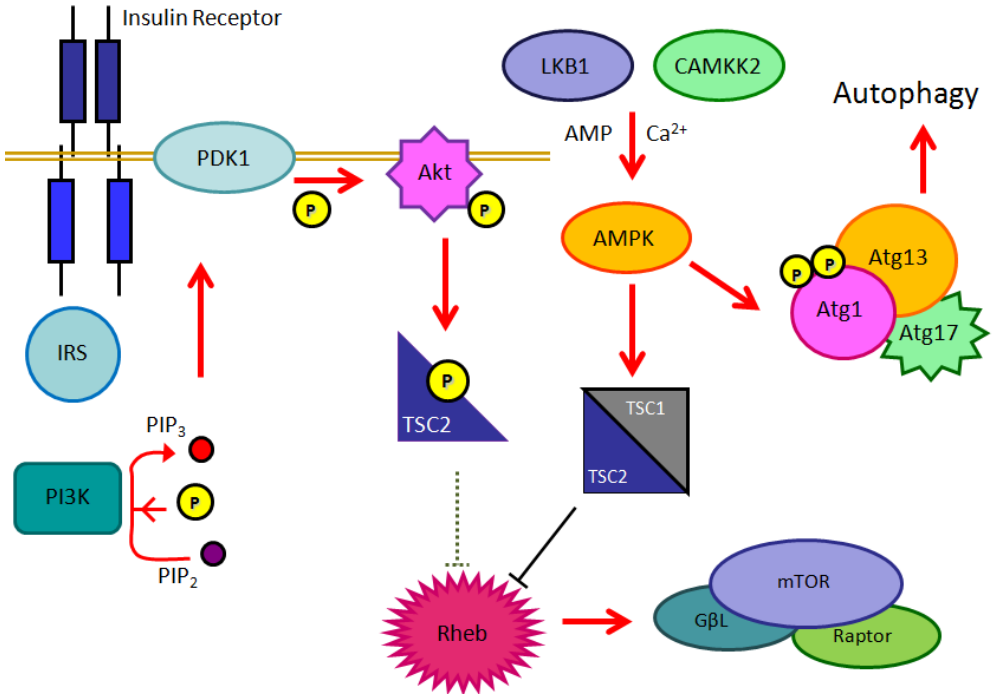

Figure 1.6 – Insulin and AMPK Regulation of mTOR – stimulation of the insulin receptor and the IRS generates the production of PIP_3 by PI3K which activates PDK1. PDK1 phosphorylates and activates Akt which phosphorylates TSC2 preventing its inhibitory effects on Rheb. Rheb activates mTOR which inhibits autophagy. High levels of AMP or calcium will activate AMPK which activates TSC1/2 complex which inhibits Rheb and mTOR, thus activating autophagy.

AMP-activated protein kinase (AMPK) monitors cellular energy levels by sensing the AMP:ATP ratio. AMPK phosphorylates raptor and also TSC2, both of these have an inhibitory effect on Rheb, and thus mTOR. Similarly, AMPK can dircctly phosphorylates Atg1/Ulk-1 and activate autophagy (Kim *et al* 2011). The upstream control of AMPK is through the kinase LKB1, and also through the CamKK2 which is regulated by calcium flux. One of the downstream targets of AMPK is the transcription factor FoxO which also promotes the induction of autophagy, and is linked to longevity in both *Drosophila* and Rhesus monkeys (Greer *et al* 2009). Overall it is not just nutrient levels which impact on the induction of autophagy but also cellular energy levels and when these are low, autophagy is activated. Both of these pathways converge on mTOR to decrease unnecessary energy consumption and protein synthesis to conserve and increase cell survival in times of stress.

Beclin-1, the mammalian homolog of Atg6, is an important regulator of autophagy and apoptosis. Under nutrient rich conditions, autophagy is inhibited due to beclin-1 binding to Bcl-2 family members. However, during starvation, the Bcl-2 proteins can become

phosphorylated by kinases such as JNK and no longer bind beclin-1, allowing autophagy to occur (Wei *el al* 2008). There may also be competitive binding with other BH3 domain proteins which prevents Bcl-2 binding to beclin-1, and there is growing evidence that activation of other pathways can regulate this interaction. Once beclin-1 is free from Bcl-2 interactions it can bind to other proteins such as UVRAG, Ambra-1, Atg14L or Rubicon to regulate autophagy (Itakura *et al* 2008, Matsunaga *et al* 2009, Zhong *et al* 2009). The multiple beclin-1:Vsp34 complexes that can be formed highlight the complexity of regulation of autophagy. UVRAG (UV irradiation resistance-associated gene) and Atg14L binding is mutually exclusive and evidence suggests that both are involved in the early stages of autophagosome formation. UVRAG also functions independently of beclin-1 binding; it has been shown to induce Rab7 activity which functions in endocytic trafficking events, and is also required for autophagosome maturation. Rubicon has been shown to bind to the beclin-1 complexes containing UVRAG and this inhibits autophagosome maturation (Matsunaga *et al* 2009, Zhong *et al* 2009). The central role of the core beclin-1 complex is to regulate autophagy, and through different binding partners it is possible to have opposing effects. Similarly, interaction with different partners may also connect and regulate the complex to other cellular trafficking pathways such as apoptosis. Beclin-1 is a key player in autophagy regulation and during viral infection appears to be the common target protein.

1.3 Other Cellular Pathways of Degradation – The Proteasome

There are two ways to degrade cellular constituents in higher eukaryotes such as mammals; these are the fusion of autophagosomes with lysosomes, as previously discussed, and through the ubiquitin-proteasome system (UPS) (Klionsky and Emr 2000, Huang and Klionsky 2002). The proteasome is a compartmentalized structure, consisting of a 20S central core unit and two 19S cap units at either end, with its enzymatic activities embedded inside the central chamber (Alberts *et al*. 2002, Korolchuk *et al* 2010). As a result the degradative capacity is confined to partially denatured protein substrates that can access its proteolytic subunits, whereas autophagic vesicle can form and capture any portion of the cytoplasm. However between the two pathways all misfolded or damaged component can be removed from the cell. Initially due to the diversity of the pathways there was thought to be no communication, however recent evidence has highlighted the cross-talk between

them (Korolchuk *et al* 2010). Proteins destined for the proteasome are tagged with ubiquitin, a 76 amino acid molecule by undergoing a series of reactions through enzymes known as E1 (ubiquitin activating enzyme), E2 (ubiquitin conjugating enzyme) and E3 (ubiquitin protein ligase) which conjugate the ubiquitin to the protein, much like the conjugation of LC3 to the lipid component phosphatidylethanolamine (PE). Different combination of E2 and E3 allow the recognition of specific signals in the targeted protein (Myung *et al* 2001).

Ubiquitin can be ubiquitinylated in different ways due the presence of a number of lysine residues in the molecule, and depending on the position of ubiquitin, different conformations of chain can be formed (Fushman and Walker 2010). A protein targeted for degradation maybe mono-ubiquitinated, multi-monoubiquitinated or poly-ubiquitinated. Also the ubiquitin molecule contains 7 different lysine residues that can be ubiquitinated (Wong and Cuervo 2010). The canonical chain is through polyubiquitination of the K48 residues, and this is a signal for degradation through the proteasome. However, the other non-canonical chains through the other residues such K63, are thought to have other functions, such as signalling for degradation by autophagy (Korolchuk *et al* 2010, Wong and Cuervo 2010). There is a growing amount of evidence that inhibition of UPS leads to activation of autophagy, which compensates for the loss of the pathway, however the loss of autophagy leads to a decrease of UPS degradation (Ding *et al* 2007). The evidence suggests it is due to the molecule known as p62, also known as sequestersome 1, which is bound to the proteins destined for degradation (Korolchuk *et al* 2009). It is this molecule which links autophagy and the UPS. p62 has the ability to bind to ubiquitin through its ubiquitin-associated (UBA) domain and is incorporated into protein aggregates seen during various disease pathologies (Seibenhener *et al* 2004). p62 binds to ubiquitinated proteins and directs them to the autophagosome through an association to LC3. p62 and its cargo will be incorporated into the autophagosome, however it is not crucial for the formation (Pankiv *et al* 2007, Shvets *et al* 2008). p62 was identified as a scaffold protein for signalling networks including atypical protein kinase C (PKC) and NF-κB. Although it has a role in autophagy it can still signal through these pathways, and may serve to link autophagy to them. Similarly, other molecules similar in structure to p62 have been identified such as neighbour of BRCA1 gene 1 (NBR1) and nuclear dot protein 52 (NDP52) (Kirkin *et al* 2009).

These also have LC3-interacting regions (LIRs) and there is growing evidence these participate as cargo receptors targeting specific organelles and pathogens for degradation through autophagy. Despite the additional roles of p62 in other cellular activities, it can be used to monitor the activation of autophagy. In other words increased turnover of p62 is an indicator of activation of autophagy. Clearly, p62, NBR1 and NDP52 play a role in cargo selectivity and targeting to autophagosomes, however, further work is required to detail their roles.

1.4 Endocytosis, the Endomembrane System and Autophagy –

Endocytosis is the cellular uptake of materials and liquids across the plasma membrane and this can occur in a number of ways such as clathrin-mediated or caveolae-termed endosome. Most endosomes have the same destination as an autophagosome and that is fusion with lysosomes where the contents are degraded. There is evidence to suggest an overlap of the endocytic pathway and the autophagy pathway, and some of the Rab GTPases that are involved in regulation of endocytosis are also important for autophagy.

It has become increasingly clear from the various studies that cells have a number of different mechanisms by which they can ingest materials from the extracellular environment. Clathrin-mediated endocytosis (CME) is the best characterised endocytic pathway as clathrin is conserved throughout tissues and also across different species (Young 2007, Edeling *et al* 2006). Clathrin and associated adapter proteins (APs) are required for the formation of clathrin-coated pits (CCPs) on the cytoplasmic side of the plasma membrame. There have been a number of APs discovered, some of which have more specialised roles than others such as AP-3 and AP-4, and the two best characterised is AP-1 and AP-2. AP-1 is involved in forming clathrin coats for transport for the trans-Golgi network (TGN) whereas AP-2 is involved with transport from the plasma membrane.

The process begins with the nucleation of clathrin, and its adapter proteins, AP-2, at the surface of the plasma membrane where it binds and begins to form a clathrin-coated pit (CCPs). This region of the plasma membrane recruits receptors and bound ligands which will invaginate. The pits continue to grow in size to 60-90 nm diameter and bud inwards into the cytoplasm (Huang *et al* 1999). Scission of the vesicle from the plasma membrane requires a GTPase known as dynamin, which binds around the neck of the CCP, and through GTP

hydrolysis removes the CCP from the plasma membrane, producing a clathrin-coated vesicle (CCVs) free in the cytoplasm. The process also includes cooperation with the actin cytoskeletal components which provide the momentum to move the CCPs and CCVs away from the plasma membrane into the cell (Edeling *et al* 2006, Doherty and McMahon 2009). CCVs exist for a very short period before the clathrin and the accessory proteins are removed, allowing the vesicles to fuse with early endosomes and begin trafficking through the cell. Removal of the clathrin coat involves heat shock cognate 70 kDa (Hsc70) and auxilin. As well as removing the coat, the accessory proteins must be removed, and this is done through phosphorylation of the AP complex (Kirchhausen 2000, Young 2007). Clathrin is important in not only vesicle transport from the plasma membrane but also in the intracellular traffic of vesicles from the trans-Golgi and endosomes, and it is not the only coat protein which is important is forming vesicles. Other coat proteins include COP-I and COP-II protein coats. COPI complex has been shown to function in both anterograde and retrograde transport of the Golgi complex, and also in early endosome formation (Razi *et al* 2009)

Sorting of molecules can occur in early endosomes, and some of these have tubular extension, where molecules are packed and transported back to the plasma membrane (Doherty and McMahon 2009). The maturation of early endosomes into late endosomes means they lose their tubular nature and also become increasingly acidic through the pathway. Evidence suggest that microtubules play a role in the maturation of early endosomes to late endosomes, and also the acidification of the vesicles by the vacuolar ATPases (V-ATPases) is required (Bayer *et al* 1998). Inhibition of microtubules using nocodazole, prevents not only the movement of early endosomes but also the localisation of late endosomes and lysosomes. Maturation of endosomes is also important for receptor-mediated endocytosis, whereby specific ligands, such as the iron-carrying molecule transferrin and its receptor, bind at the cell surface and are taken-up into CCVs which enter the endocytic pathway. The maturation of the early endosome to late endosome, and subsequent lowering of the luminal pH means the iron can dissociate from transferrin, now known as apotransferrin, and both receptor with ligand bound are recycled back to the plasma membrane. The fusion of endosomes with other vesicles is regulated by the Rab GTPases which switch between an active GTP-bound state and an inactive the GDP bound

state. Fusion of early endosomes requires Rab5 proteins. Rab5 is recruited to membranes by Rabex5, guanine exchange factor (GEF) which also recruites Vsp34 to produce PI(3)P and subsequent recruitment of other Rab5 effectors (Poteryaev *et al* 2010). A key effector of Rab5 is early-endosomal autoantigen (EEA-1) which is known to bind to early endsomes in a PI(3)P dependent manner and mediated fusion (Simonsen *et al* 1998). Rab5 is also important in autophagy because its depletion decreases the number of autophagosomes formed (Ravikumar *et al* 2008). Fusion of early endosomes and late endosomes requires Rab7. Interestingly, expression of a dominant negative Rab7 causes accumulation of LC3-positive vesicles in the cytoplasm (Gutierrez *et al* 2004) suggesting that Rab7 is important for autophagosome maturation and fusion with lysosomes.

The overlap between the endocytic pathway and autophagy is becoming increasingly evident from studies by Razi *et al* (2009) and Ravikumar *et al* (2010). It is thought that late endosomes and multivesicular bodies fuse with autophagosomes as part of autophagosome maturation. Razi *et al* (2009) show that depletion of the COP-I α, β, and β' subunits hinder the maturation of autophagosomes and leads to an accumulation of not only autophagosomes but also p62-positive structures indicating a block in autophagy. Similarly there was also a block in CME, as seen through a block in transferrin up-take after COP-I depletion. This highlights that autophagosomes fuse with early endosomes and the block in early endosome formation also effects autophagosomes maturation.

1.5 Lysosome Biogenesis

Lysosomes are important degradative organelles inside cells and up until recently it was generally believed they were the endpoint of endocytic and autophagy pathways. A recent study by Yu *et al* (2010) demonstrated that one aspect of lysosome biogenesis occurs after fusion of autophagosomes with lysosomes. During starvation mTOR is initially inhibited as amino acid levels drop in the cells. Autophagy is activated and this delivers proteins to the lysosome for degradation. Passage of amino acids from the lysosome into the cytoplasm activates mTOR. This reactivation correlates with the formation of tubular membranes extending from the surface of lysosomes. Many of the lysosomes appear docked with LC3 positive autophagosomes 4 hours post-starvation and at 8 hours post-starvation tubules positive for LAMP1, but negative for LC3 are present in the cytoplasm. The new tubules

pinch off to form new vesicles called proto-lysosomes, which mature to form lysosomes however these structures are not acidic, and require further maturation before they can function as lysosomes. This process is termed autophagic lysosome recovery (ALS) and is important for the regeneration of the lysosome (Yu *et al* 2010).

1.6 Cationic Liposomes, Nanoparticle, and Nanotheranostics –

The delivery of nanomaterials into cells for imaging or therapeutics use is a growing area of interest. The entry route of nanomaterials into cells is endocytosis, and as previous discussed there is an overlap between endocytosis and autophagy. Non-viral DNA delivery vectors also use endocytosis for cell entry; however these must escape before degradation in lysosomes in order for transfection to occur. The role of autophagy in the cellular processing of these molecules is important to determine, and in understanding how seemingly inert nanomaterials can active this pathway.

There are a number of different ways to introduce a plasmid containing a gene of interest into cells; these include the classical method of using calcium phosphate and diethylaminoethyl-dextran (DEAE-dextran) and also the newly developed cationic liposomes, dendrimers and PEI methods. The method of using HEPES-buffered saline, containing phosphate ions, with a calcium chloride solution will form a calcium phosphate precipitate composed of the positive calcium ions and negative phosphate ions, and this will also cause the DNA to precipitate. This precipitate can then be added to a range of cells type and will be taken up by cells through a poorly understood endocytic mechanism (Jordan and Wurm 2004). However the size of the precipitate and amount of DNA incorporated can vary in each transfection. Similarly DEAE-dextran has been used for transfections for the ability to replicate transfection conditions. This molecule is positively charged and can form a complex with DNA, and entry into cells is through endocytosis (Sambrook and Russell 2000). Following this, cationic liposomes have been used to transfect plasmid DNA into a range of cell lines since their introduction by Felgner *et al* 1987. A range of different composition and types are commercially available, and many of these include the addition of the helper lipid dioleoyl phosphatidylethanolamine (DOPE) to improve transfection efficiency. DOPE affects the packing properties of the cationic lipid and improves membrane fluidity in liposome formation (Zuhorn *et al* 2002). On addition to an aqueous environment the hydrophobic

lipid chain will form multi-lamellar liposomes, with the polar head group interacting with the aqueous environment. The negative charge of DNA will interact with the cationic liposomes, and thus be incorporated into the structures on formation. The complex of DNA-liposome is known as a lipoplex, and entry of liposomes into cells is through clathrin-mediated endocytosis (CME) (Rejman *et al* 2005). Once inside the endosome the cationic lipid interacts and forms neutral charge pairs with the anionic endosomal membrane, releasing the DNA in the endosome (Xu and Szoka 1996, Hafez *et al* 2001). The presence of DOPE will aid in inducing a change in phase of the lipid from lamellar to the inverted hexagonal phase, which essentially flips the endosomal membrane inside out and allowing the release of the DNA into the cytoplasm (Tresset 2009). The theory of the "flip-flop" mechanism is illustrated in figure below. The progression of lipoplexes through the endocytic pathway, if they do not escape, will lead to their destruction when the endosomes fuse with lysosomes and are degraded (Medina-Kauwe *et al* 2005).

Following the requirement of the development of non-viral gene delivery methods to use in diagnostics and also in therapeutics, other cationic and anionic molecules have been explored including polyethylenimine (PEI) and dendrimers. PEI is a cationic molecule that will form polymers that incorporate the DNA in a complex known as a polyplex which is then taken up by cells. In contrast to liposomes, evidence suggests that these polyplexes enter cells through caveolin-mediated rather than clathrin-mediated endocytosis (Rejman *et al* 2005). The polyplex escape from the endosome relies on the PEI proton buffering capacity and the "proton sponge effect". PEI can become protonated inside the endosome and results in endosomal uptake of protons and chloride ions, and the end result is the osmotic swelling of the endosome. This causes the vesicle to swell and rupture, thus releasing its contents into the cytoplasm. The other advantage of PEI is that the vesicles that results from caveolar endocytosis do not fuse with lysosomes (Rejman *et al* 2005, Won *et al* 2009).

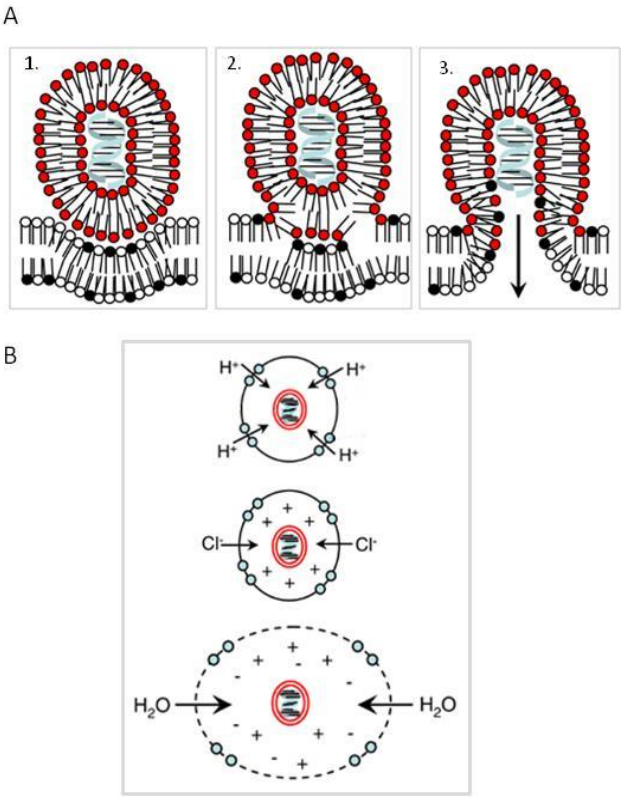

Figure 1.7 – Mechanism of DNA Escape into the Cytoplasm from Cationic Non-Viral Vectors – (A) – 1. Cationic liposomes (red membrane) enter through clathrin-mediated endocytosis into anionic endosomes (black membrane), 2. These will form charge pairs releasing the DNA. 3. The presence of DOPE (not shown) inverts the membrane causing a "flip flop" allowing release of DNA into the cytoplasm. (B) – the PEI/DNA polyplex (red) will enter cells through caveolae-mediated endocytosis. The PEI will become protonated, and result in the osmotic swelling of the vesicle which results in rupture and release of DNA.

PEI is not the only cationic molecule which has been developed for transfection methods, dendrimers have also been extensively examined in their ability as non-viral gene delivery vectors. Dendrimers are commercially available and the most popular available is based on a core of ethylenediamine which branch to form the aminoamide branches, termed Starburst PAMAM dendrimers (Kukowska-Latallo *et al* 1996). The positive charge of surface of the dendrimers allows them to interact with negatively charged DNA and thus developed for use as a transfection reagent. However, data by Li *et al* (2009) illustrates that the cationic properties, not the anionic generation of dendrimers, also increase their toxicity and reduce cell viability, and an activation of autophagy is seen from LC3 rearrangement and the presence of double membrane vesicle in the cytoplasm of cells treated with the cationic generations. Similarly, quantum dots (QDs) which are used in fluorescent imaging for their intrinsic fluorescence and small size have been found to activate autophagy.

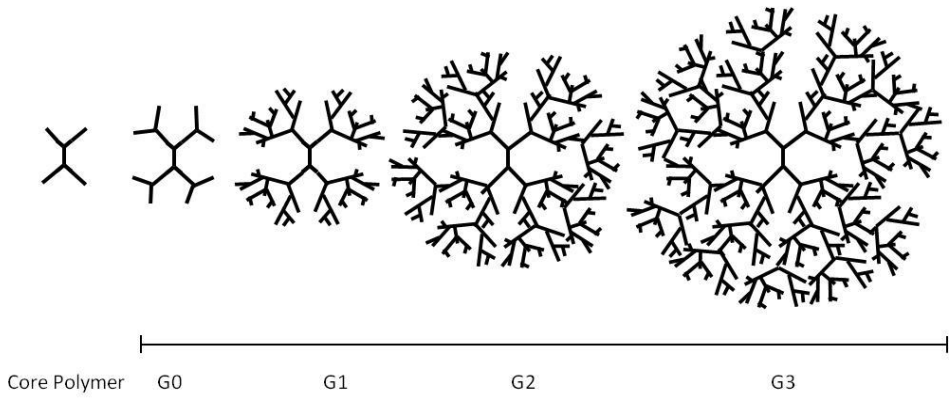

Figure 1.8 – Generations (G) of Dendrimer Molecules – cationic and anionic dendrimer molecules are available for transfection of DNA into cells, and the defined increase in size and shape arises from additional conjugation of polymers to the core and branches of each generation (Li *et al* 2009).

In a paper by Seleverstov *et al* (2006) the data indicates that incubation with small QDs activated autophagy, and these were rapidly cleared from the cell. With the increase use of nanoparticles such as liposomes, dendrimers and QDs in diagnostics and therapeutics it is essential to correctly understand the mechanisms by which they affect cells, and also the cellular events which are activated during incubation with them. Whilst not all effects are detrimental to cell viability it is important to understand any undesired side effects they might have in cellular and *in vivo* to prevent unwanted consequences. It is clear from the recent data that whilst non-viral gene delivery vectors are the best choice in terms of low immunogenicity, they require investigation to understand how cells may respond to them, and they are not inert as previously once thought.

Chapter 2:

Materials and Methods

Chapter 2 - Materials and Methods

2.1 Tissue Culture Media, Reagents and Buffers

All media solutions and reagents were purchased from Invitrogen (Paisley, UK) and all chemical compounds were purchased from Sigma (Dorset, UK) unless otherwise stated.

2.1.1 Cell Lines **–**

African green monkey kidney epithelial cells or Vero cells (ECACC 84113001), human embryonic kidney epithelial 293 cells or HEK 293 cells (ECACC 85120602), human cervix carcinoma (HeLa) cells (ECACC 96112022) and Chinese Hamster Ovary cells or CHO cells (ECACC 85051005), were obtained from European Collection of Cell Cultures (ECACC) (Porton Down, UK).

The CHO cell line stably expressing the plasmid eGFP-LC3 (CHO-LC3) and the mutant CHO cell line expressing GFP-LC3G120A (CHO GFP-LC3G120A) were a kind gift from Dr Zvulun Elazar of the Weizmann Institute of Science, as described in Fass *et al* 2006. The stable HEK 293 cell line expressing the eGFP-LC3 plasmid was a kind gift from Sharon Tooze of Cancer Research UK, London Research Institute, as described in Kochl *et al* 2006. MEF wild-type (WT) and MEF Atg $5^{-/-}$ cell lines were a kind gift from Noboru Mizushima of Tokyo Medical and Dental University, as described in Mizushima *et al* 2001. HEK 293 cells stably expressing the double FYVE domain-containing protein 1 (DFCP1) were a kind gift from Nicholas Ktistakis, as described in Axe *et al* 2008. All cells were grown in stated media below at 37^{o}C and 5% CO_2.

2.1.2 Tissue Culture Media **-**

Unless stated all cells were cultured in Dulbecco's Modified Eagles Media (DMEM) with GlutaMAX supplemented with 10% foetal calf serum (FCS) and 1% (100 units/µl) penicillin-streptomycin (p/s). FCS was purchased from Biosera (Sussex, UK). Additional supplements for culturing HEK 293 and HEK 293 GFP-LC3 in DMEM were 100x non-essential amino acids (NEAA) and 100 mM sodium pyruvate, final concentrations for culturing were 1x and 1 mM respectively. Minimum essential media Eagle with alpha modification (MEM-α) containing

10% FCS and 1% p/s was used to culture CHO eGFP-LC3 and CHO eGFP-LC3 G120A stable cell lines. Opti-MEM reduced serum with GlutaMAX, was used for all transfections and for cell culture in the POC chamber. Hank's Balanced Salt Solution (HBSS) was used as a starvation media (Sigma, Dorset).

2.1.3 Tissue Culture Additives **–**

The following table shows the final working concentrations for the compounds which were added to Opti-MEM, stocks were prepared in DMSO unless otherwise stated –

Compound name	**Final Concentration**
Bafilomycin A1	100 nM
Cycloheximide	20 µg/ml
E64d	30 µM
Nocodazole	5 µM
Pepstatin A	150 µM
Puromycin (in dH_2O)	10 µM
Sodium arsenate (in dH_2O)	5 µg/ml
Wortmannin	100 nM

Table 2.1 – the final concentration of additive used in cell culture

2.1.4 DNA plasmids -

The tdTomato-p62 plasmid was a kind gift from Terje Johansen, as described in Bjorkoy *et al* 2005. GFP, RFP-tagged or dsRed Rab proteins wild-type and dominant negatives (DN) were purchase from Addgene (Cambridge MA, USA). The mCherry-tagged construct TIA-1 were a kind gift from T. Eisinger-Mathason University of Virginia, as described in Eisinger-Mathason *et al* (2008).

2.1.5 Antibodies and Fluorescent Dyes -

Rabbit anti-LC3b was purchased from Sigma (Dorset, UK). Guinea pig anti-p62 was purchased Progen (Heidelberg, Germany). Anti-ubiquitin mouse monoclonal antibody, clone FK2, was purchased from BioMol (Exeter, UK). Monoclonal antibodies to the cytoskeleton α-tubulin (clone B512), γ-tubulin (clone GTU-88) and vimentin (clone V9) purchased from Sigma, were used as directed see table 2.2 below. Alexafluor 350 nm, 488 nm and 594 nm were used 1:500 from Invitrogen (Paisley, UK).

Antibody Name	Clone	Working Dilution	Company
Rabbit anti-LC3	-	1:1000	Sigma (L7543)
Guinea Pig anti-p62	-	1:100	Progen Biotechnik (GP62-N)
Mouse anti-β actin	AC-15	1:20,000	Sigma (A5441)
Mouse anti-LAMP1	UH1	1:2	Hybridomas - DSHB University of Iowa
Rabbit anti-Atg5	-	1:1000	Cell Signalling (2630)
Rabbit anti-beclin-1	-	1:1000	Cell Signalling (3738)
Mouse anti-α tubulin	B512	1:1000	Sigma (T5168)
Mouse anti-γ tubulin	GTU-88	1:500	Sigma (T6557)
Mouse anti-vimentin	V9	1:1000	Sigma (V6630)
Mouse anti-ubiquitin	FK2	1:500	BioMol (PW8810-0500)
Rabbit anti-β COP	-	1:500	See Rouiller *et al* (1998) J Virol 72:2373
Rabbit anti-ERp60	-	1:500	As above
Rabbit anti-TGN 46	-	1:500	AbD Serotec (AHP1586)
Rabbit anti-mannosidase II	-	1:500	AbCam (ab12277)
Mouse anti-EEA1	14	1:200	BD Bioscience (610457)
Mouse anti-clathrin	23	1:200	BD Biosciences (610499)

Table 2.2 – Working Dilutions for Antibodies used for Immunofluorescence and Western Blot

Transferrin AlexaFluor 594 conjugate was purchased from Invitrogen, and cells were pre-incubated in 5 μg/ml in Opti-MEM for 30 minutes prior to experimentation. For lipid staining Nile red was used, purchased from Sigma (Dorset, UK). Cell nuclei were stained with 4',6-diamidino-2-phenylindole (DAPI) or Hoechst 33258 dye from Sigma (Dorset, UK) in PBS for

working concentrations of 10 µg/ml. All coverslips were mounted onto glass slides using Fluoromount G (Cambridge Biosciences, Cambridge, UK) and stored at 4^{o}C.

2.2 Methods

2.2.1 Transfection Methods –

Cells cultured on glass coverslips, or in plates for transfections and immunofluoresence at 37^{o}C and 5% CO_2 in the appropriate media for 24 hours prior to transfection. Transfections were carried out for 6 hours before changing media. Cells seeded at the following densities according to plate growth area, see table 2.3. Transfections were carried out in OptiMEM media with either Transfast (Promega, Southampton, UK), Lipofectamine (Invitrogen), JetPRIME and INTERFERin (Autogen Bioclear, Wiltshire, UK), Nanojuice (Merck Chemicals, Nottingham, UK), Fugene (Roche Applied Bioscience, West Sussex, UK), HiPerFect (Qiagen, West Sussex, UK), TurboFect (Fermentas Life Science, York, UK), DharmaFect (Dharmacon, Lafayette, CO) or calcium phosphate ($CaPO_4^-$) (Sigma). Transfection protocol volumes stated for 24 well plates, scaled up or down depending on culture vessel. Cells were washed twice in Opti-MEM prior to transfection, and transfection mix was replaced with fresh media after 6 hours. In cases where transfection reagent alone was used, the volumes were made up with Opti-MEM.

Culture Vessel	Growth Size (cm^2)	Cell Density (Per Well)	Plating Media (ml)	Relative Area
48 well plate	1	10,000	0.2	0.5x
24 well plate	2	20,000	0.4	1x
12 well plate	3.8	50,000	1	2x
6 well plate	9.5	250,000	2	5x
6 cm dish	21	300,000	3	10x

Table 2.3 – Cell Densities for Different Culture Plates For Transfections

2.2.1.1 Transfast Transfection – per well of 24 well plate - 0.5 µg DNA diluted in 200 µl Opti-MEM, followed by 1.5 µl of Transfast reagent and mixed gently, left to incubate at room

temperature before placing on cells. After 1 hour, 100 µl of complete media added to each well.

2.2.1.2 Lipofectamine Transfection – cells seeded in antibiotic-free media prior to transfection. In a tube 2 µl Lipofectamine in 50 µl Opti-MEM, and incubated at room temperature for 5 minutes before adding to a tube containing 0.8 µg DNA in 50 µl Opti-MEM and then incubated at room temperature for a further 20 minutes before adding to 500 µl antibiotic free media.

2.2.1.3 Calcium Phosphate Transfection – transfection carried out in complete media, changed prior to addition of the transfection mix. In one tube 5 µg DNA, 49 µl sterile water and 6 µl 2.5 M $CaCl_2$ which was added to bubbled 60 µl 2x HEPES buffered saline (HeBS), and incubated at room temperature for 20 minutes before addition of 30 µl dropwise to each well. Glycerol shock was required for some plasmid expression, per well – 20 µl 50% (w/v) glycerol, 50 µl 2x HeBS and 30 µl sterile water. Cells shocked for 2 minutes and washed twice in PBS before fresh complete media added.

2.2.1.4 JetPRIME Transfection – 0.5 µg DNA into 50 µl JetPRIME buffer, mixed gently and added 1 µl JetPRIME, vortex briefly, spin down and incubate at room temperature for 10 minutes before adding to 500 µl complete media.

2.2.1.5 Fugene HD Transfection Protocol – 0.5 µg DNA and 1.25 µl Fugene HD diluted and mixed in 25 µl Opti-MEM, incubated at room temperature for 15 minutes before added to 475 µl complete media.

2.2.1.6 Nanojuice Transfection – cells seeded in antibiotic-free media prior to transfection. In 100 µl Opti-MEM, 1 µl NanoJuice core reagent and 0.5 µl booster was added, and incubated for 5 minutes before 0.5 µg DNA was added. The transfection mix was left for 15 minutes at room temperature before adding to the cells dropwise. After 1 hours 100 µl media with serum, no antibiotics, was added.

2.2.1.7 TurboFect Transfection – 1 µg DNA and 2 µl of TurboFect was added to 100 µl Opti-MEM and incubated for 20 minutes at room temperature before adding dropwise to 500 µl complete media.

2.2.2 siRNA Transfections –

HeLa cells were seeded and cultured overnight in antibiotic-free media, and media was replaced with fresh prior to transfection. All siRNA oligomers were pre-designed and purchased from Dharmacon (Lafayette, CO), the sequences as described in table 2.4 and 2.5 below.

siRNA Oligo	**Oligo Sequence**
J004374-07	GGCAUUAUCCAAUUGGUUU
J004374-08	GCAGAACCAUACUAUUUGC
J004374-09	UGACAGAUUUGACCAGUUU
J004374-10	ACAAAGAUGUGCUUCGAGA

Table 2.4 – Sequences of siRNA targeting Atg5 mRNA

siRNA Oligo	**Oligo Sequence**
J055895-05	CUAAGGAGUUGCCGUUAUA
J055895-06	GAGAGGAGCCAUUUAUUGA
J055895-07	GGGAGUAUAGUGAGUUUAA
J055895-08	GGACAAAAGCGCUCAAGUU

Table 2.5 – Sequences of siRNA targeting beclin-1 mRNA

The siRNA was reconstituted in siRNA buffer to a stock solution of 20 µM. This was further diluted in Opti-MEM for a working concentration of 2 µM and the final concentration of siRNA per well was 100 nM. The siRNA oligos were transfected into cells using Lipofectamine 2000, following the manufacturer's guidelines for siRNA transfections.

Lipofectamine siRNA Transfection – cells were 50-60% confluency at time of transfection. For 12 well format, 50 µl siRNA was added to 50 µl Opti-MEM, incubated for 5 minutes before gently mixing with 2 µl Lipofectamine in 50 µl Opti-MEM and incubated further for 20 minutes before adding to 800 µl antibiotic-free media on the cells.

2.2.3 Microscopy and Immunofluorescence -

2.2.3.1 Live Cell Imaging -

Before entering the sterile POC chamber for the live cell imaging, the 40 mm coverslips were washed in PBS, secured in the chamber and 2 mls media was added. The cells were then place into the microscope stage, incubated at 37^{o}C and 5% CO_2 for the duration of the experiment.

2.2.3.2 Paraformaldehyde Fixation – Cells were fixed in 4% PFA for 15 minutes and washed twice in PBS before blocking for 10 minutes in 30% goat quench solution, and then permeabilised for 30 minutes in 30% goat quench solution with 0.2% Triton-X 100. Primary antibody incubation was 1 hour and secondary antibody incubation was 40 mins, with 3x 5 minutes washes in-between. Cells were DAPI stained for 15 minutes and mounted using Fluoromount G.

2.2.3.3 Methanol Fixation - Cells were fixed in 100% methanol for 5 minutes and blocked for 30 minutes in 30% goat quench solution. Antibodies were diluted in blocking buffer and primary antibody incubation was 1 hour and secondary antibody incubation was 40 mins, with 3x 5 minutes washes in between**.** Cells were DAPI stained for 15 minutes and mounted using Fluoromount G. For cytoskeletal antibodies, cells were fixed in methanol with 10% MES buffer for 5 minutes, and blocked and stained as above. For the details regarding concentrations of the different antibodies see the above table 2.1.

2.2.3.4 Immunofluorescence with anti-LC3b (Sigma) - Cells were fixed in 100% methanol for 5 minutes and blocked for 10 minutes in 2% BSA in PBS solution. Antibodies were diluted in blocking buffer and primary antibody incubation (1:1000) was 1 hour and secondary antibody incubation was 40 mins, with 3x 5 minutes washes in-between with 2% BSA in PBS solution. Cells were DAPI stained for 15 minutes and mounted using Fluoromount G

2.2.3.5 Nile Red Staining - to increase lipid storage and lipid droplet formation, CHO eGFP-LC3 cells were cultured in complete media supplemented with 1x oleic acid (stock solution 100x Sigma) for 24 hours prior to fixation. Following treatment, cells were fixed in 4% PFA as usual. Stock solution of Nile Red prepared in 150 mM NaCl at 1 mg/ml, diluted in dH_2O to a working solution of 0.1 µg/ml. Cells were incubated with 500 µl of the working solution per

well in 24 well plate, for 10 minutes in the dark. Coverslips were washed again with 1x PBS and mounted onto coverslips.

2.2.3.6 Filter Sets and Microscopes -

Live cell images were obtained on a Zeiss inverted microscope at x40 magnification. All fixed cell images were obtained at x63 magnification on a Zeiss Axioplan 2 microscope unless otherwise stated. Images were analysed and deconvolved using the Axioplan software version 4.7.1.

Filter Set (Zeiss)	*Ex. Wavelength (nm)*	*Em. Wavelength (nm)*
15	546	590
25	400, 495, 570	460, 530, 625
38	470	525
43	545	605
49	365	445

Table 2.6 – excitation and emission wavelength ranges of filter sets

2.2.4 Western Blot Analysis -

Cells were lysed in hot SDS buffer, scraped and pipetted into a clean tube and stored at -20^{o}C. Samples were allowed to defrost on ice, sonicated and assayed using the BCA kit according to manufacturer's instruction and then the appropriate volumes were incubated for 3 minutes at 95^{o}C in sample preparation buffer before loading.

2.2.4.1 BioRad SDS-PAGE System -

Gels were prepared at 12% or 15% acrylamide as described in table 2.6 below. Gels were washed and run at 70-80 V until the samples reached the resolving gel then ran at 100 volts until reaching the near bottom of the gel. Gels were semi-dry blotted for 15 minutes at 25 volts or two gels for 30 minutes at 25 volts. Membrane washed and blocked in 5% Marvel TBST for 30 minutes followed further washing in TBST. Primary antibody in 5% Marvel TBST,

left overnight at 4^{o}C shaking. Subsequent washing, incubation with secondary antibody for 1 hour before developing using the X-Ograph.

2.2.4.2 Invitrogen X-Cell NuPAGE System – Precast gels were washed and prepared according to manufacturer's instructions. Gels run in 1x MES buffer at 200 V for 35 minutes before semi-dry blotted for 15 minutes at 25 V or 30 minutes at 25 V. Membrane washed and blocked in 5% Marvel TBST for 30 minutes followed further washing in TBST. Primary antibody in 5% Marvel TBST, left overnight at 4^{o}C shaking. Subsequent washing, incubation with secondary antibody for 1 hour before developing.

Development of HRP-tagged antibodies (Jackson ImmunoResearch Laboratories, West Grove, PA, USA) was carried out using SuperSignal West Pico chemiluminescent substrate (Pierce, Rockford IL), incubating the blots for the 5 minutes in the solutions and subsequent development in the X-Ograph Imager using x-ray film to capture the signal. Imaging of infra-red tagged antibodies (LI-COR Biosciences UK, Cambridge UK) on the Odyssey machine (LI-COR Biosciences) and associated imaging software. To enable subsequent blotting with another primary antibody, the membrane could be stripped of antibodies by incubating the membrane in 1x Reblot solution (Millipore, Watford, UK) for 15 minutes at room temperature. After this the membrane was washed, blocked, probed and developed as described above.

2.2.4.3 *Gel and Buffer Compositions for Western Blot Analysis*

Cell lysis buffer for all cell lysates: 200 µl 10% SDS and 1 ml 0.5 M Tris, pH 6.8 in 8.8ml dH_2O

Sterile 1x phosphate buffered saline (PBS) prepared from 10x stock – 80g NaCl, 2g KCl, 26.8g Na_2HPO_4 and 2.4g KH_2PO_4 in 1 litre H_2O.

Running buffer and transfer buffer prepare at 1x concentration from a 10x stock – 10x running buffer pH 8.3 (30 g Tris base, 140 g glycine, 10 g SDS in 1 litre) and 10x transfer buffer pH 9.2 (390 mM Glycine, 480 mM Tris, 0.3% SDS). Blocking in 5% Marvel solution – 5g powered milk in water and washing in 1x TBS 0.5% Tween (1 ml Tween 20 in 1 litre 1x TBS (6.05g Tris and 8.76g NaCl in distilled water))

Preparation of 12% gel and 15% gel – 30% acryl-bisacrylamide and TEMED were purchased from BioRad (Hemel Hempstead, UK). Ammonium persulphate – 1 mg dissolved in 1 ml, 10% SDS – 100 g SDS dissolved in 1 litre and 1.5 M Tris – 182 g dissolved in 1 litre distilled water and pH adjusted accordingly.

Reagent	Resolving Gel Volume (ml) 12% or 15%	Stacking Gel Volume (ml)
H_2O	1.6 or 1.1	0.68
30% acryl-bisacrylamide mix	2.0 or 2.5	0.17
1.5 M Tris (pH 8.8)	1.3	-
1.5 M Tris (pH 6.8)	-	0.13
10% SDS	0.05	0.01
10% ammonium persulphate	0.05	0.01
TEMED	0.002	0.001

Table 2.7 – Volumes of Solution required for 10% or 12% gels in Western Blot analysis

Chapter 3:

Assays for Autophagy

Chapter 3 – Assays for Autophagy

3.1 Aims

The aims of this chapter are to describe the assays which will be used to study autophagy. The proteins of interest are LC3, the mammalian homolog of Atg8, and p62 which is also known as sequestersome 1 (SQSM1).

3.2 Introduction

Autophagy is the process of cellular degradation in which double membrane vesicles form, engulfing portions of the cytoplasm and fuse with lysosomes. Many of the autophagy (Atg) proteins involved in the formation of the autophagosome associate with the expanding membrane in the early steps. However they dissociate after autophagosome closure and are not incorporated into the fully formed autophagosome. One protein known as Atg8 or LC3 remains associated with the autophagosome membrane through to degradation in the lysosome, and this can be used to follow vesicle maturation. LC3 plays a vital role in the formation and the maturation of the autophagosome (Kirisako *et al* 1999, Kabeya *et al* 2000). LC3 has a cytoplasmic distribution in normal growth conditions, and undergoes rapid redistribution to punctuate structures during starvation. These LC3 'punctae' indicate recruitment of LC3 to autophagosome membranes (Kabeya *et al* 2000) and can be studied using GFP fused to the N-terminus of LC3 or by immunostaining of endogenous LC3. Translocation to the autophagosome membrane requires conjugation of phosphatidylethanolamine (PE) molecule to the C terminus of LC3. The attachment site for PE to LC3 is generated by the Atg4 protease which cleaves at Arg119 to expose Gly120. The glycine binds to Atg7 and is subsequently transferred to Atg3 before its final conjugation to PE, as illustrated in figure 3.1 below. Importantly, conversion of LC3-I to LC3-II results in a more rapid migration on SDS-PAGE gels which can be detected by Western blot.

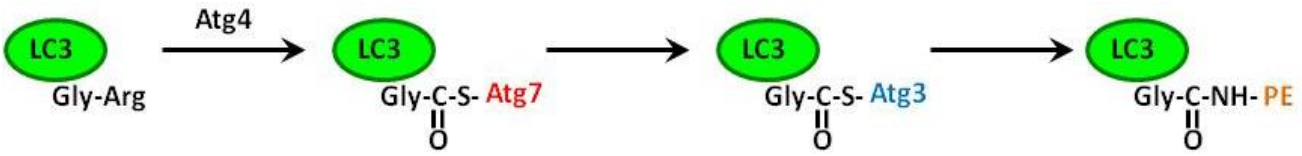

Figure 3.0 – the process of LC3 lipidation which changes the localisation of LC3 during autophagy.

The Atg12-Atg5-Atg16 conjugate (Atg16 complex) plays an important role in localising LC3 on the membrane for the forming autophagosome. In support of this, in the $Atg5^{-/-}$ cells LC3 is not recruited to autophagosome membranes and over expression of Atg12 or Atg16 inhibits autophagosome formation (Fujita *et al* 2008, Mizushima *et al* 1998 and 2001). Once the membrane closes and a complete double membrane forms, then the Atg16L complex dissociates and the autophagosome continues on route to the lysosomes, LC3 remains with the membrane and can be used as a marker for the formation and progression of autophagosomes.

Sequestersome 1/p62 can also be used as a marker for autophagy. p62 binds to ubiquitinated proteins through the ubiquitin-associated (UBA) domain and directs them to the autophagosome by binding to LC3. p62 and its cargo is incorporated into the autophagosome; however p62 is not crucial for the formation of autophagosomes (Pankiv *et al* 2007, Shvets *et al* 2008). Despite the additional roles of p62 in other cellular activities, it can be used to monitor the activation of autophagy through binding to LC3 and subsequent degradation in lysosomes. In other words increased turnover of p62 is an indicator of activation of autophagy.

3.3 Results

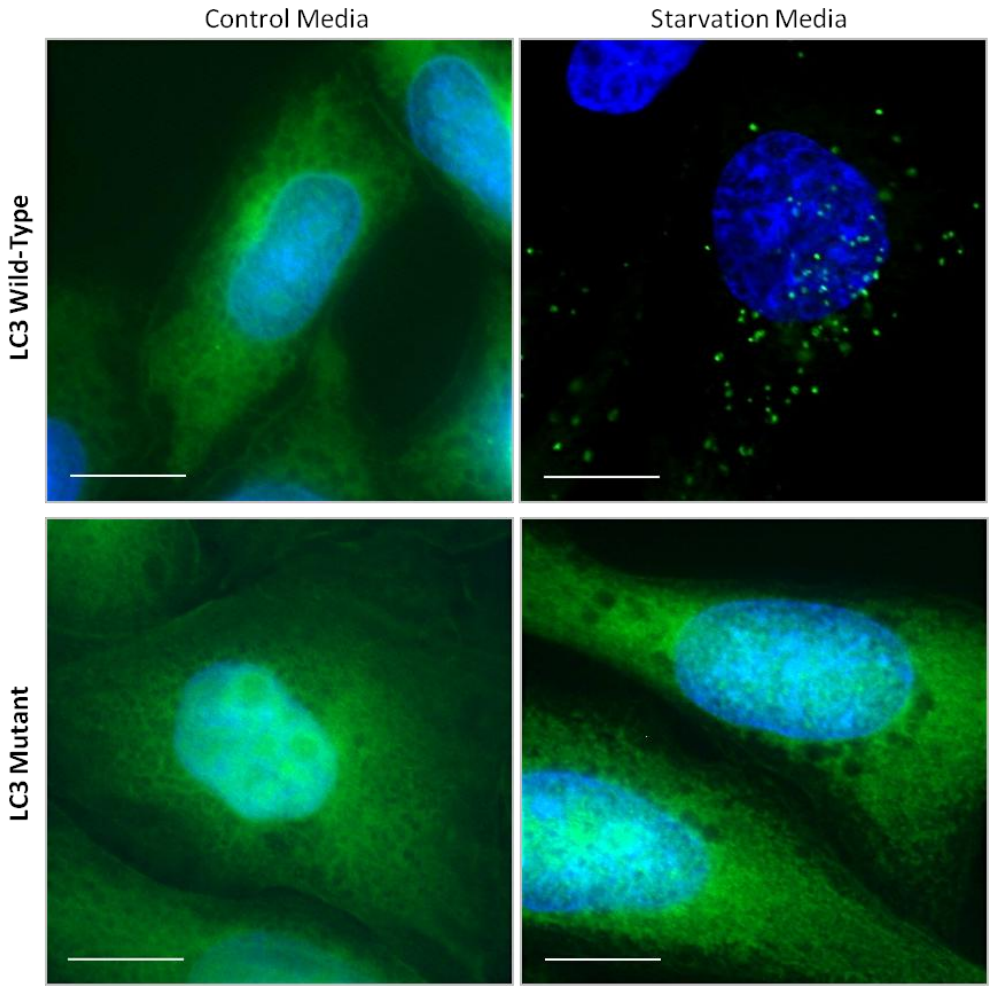

Figure 3.1 – Starvation Reorganises LC3 but not LC3 G120A to Autophagosomes - CHO cells stably expressing eGFP-LC3 (top panels, green) or the mutant eGFP-LC3 G120A (bottom panels, green) were cultured overnight in full nutrient media on glass coverslips. Cells were maintained in nutrient media (left panels) or starved (right panels) for 4 hours before fixation. Nuclei were stained with DAPI (blue). Bar is 10 µm.

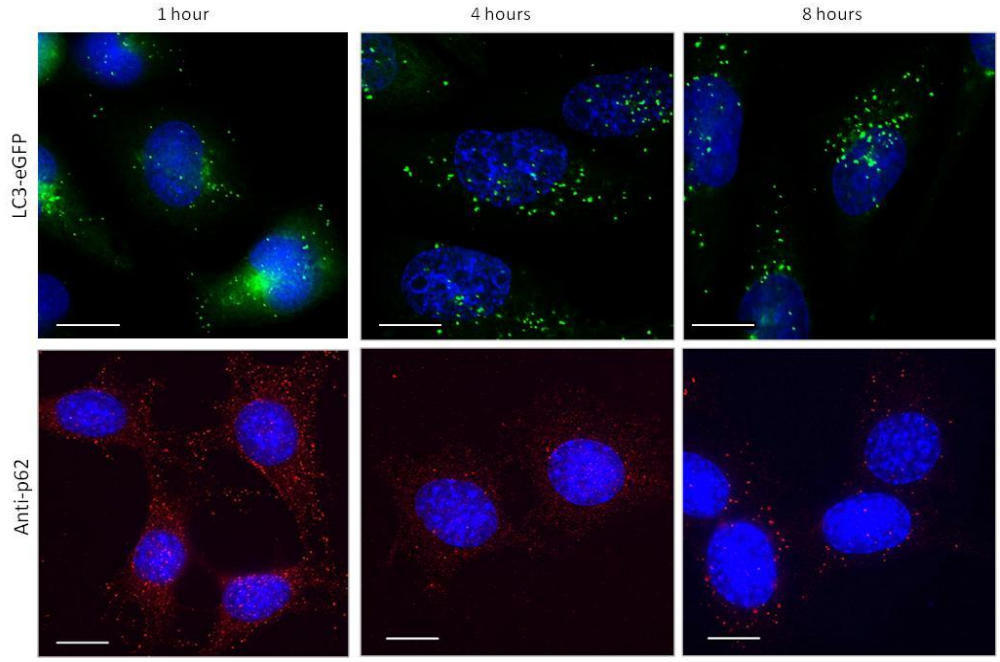

Figure 3.2 – Time Course of LC3 and p62 Redistribution after Induction of Autophagy – CHO cells stably expressing eGFP-LC3 (top panels, green) were starved in HBSS then fixed at time points stated. MEF cells (bottom panels) were starved for 4 hours prior to fixation and stained with anti-p62 antibodies (red) and the nuclei with DAPI (blue). Bar is 10 µm.

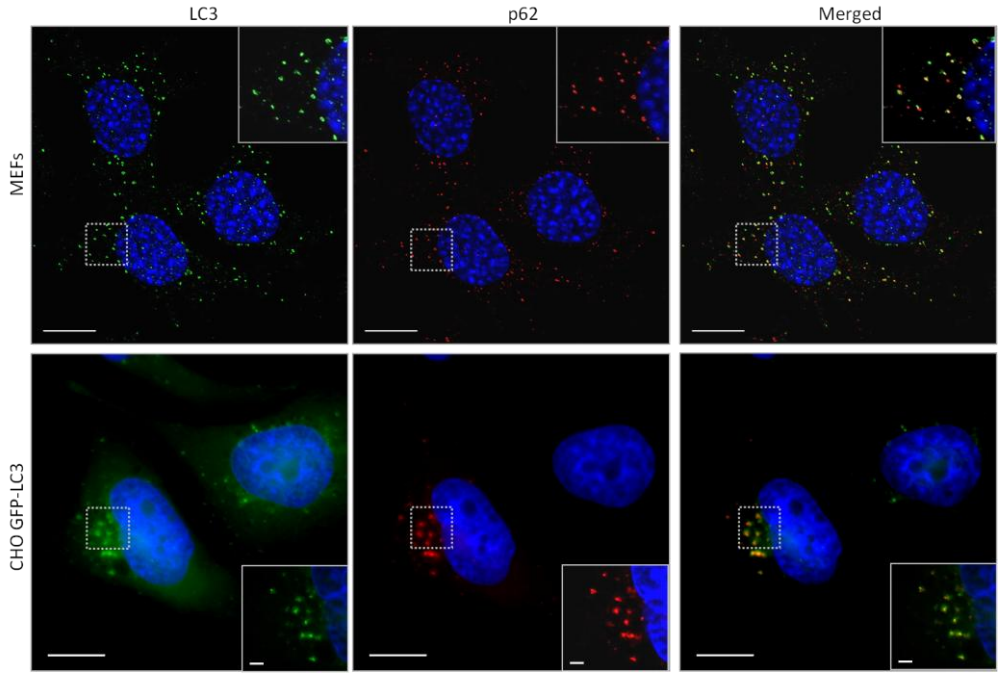

Figure 3.3 – Autophagy Results in the Colocalisation of LC3 and p62 to autophagosomes – MEF cells (top panels) were starved for 4 hours prior to fixation and stained with anti-LC3 (green) and anti-p62 (red). CHO cells stably expressing eGFP-LC3 (bottom panels, green) were transiently transfected using calcium phosphate with a plasmid expressing p62-tomato (red). 24 hours after transfection cells were starved for 4 hours. Cells were fixed and the nuclei stained with DAPI (blue). Bar is 10 µm.

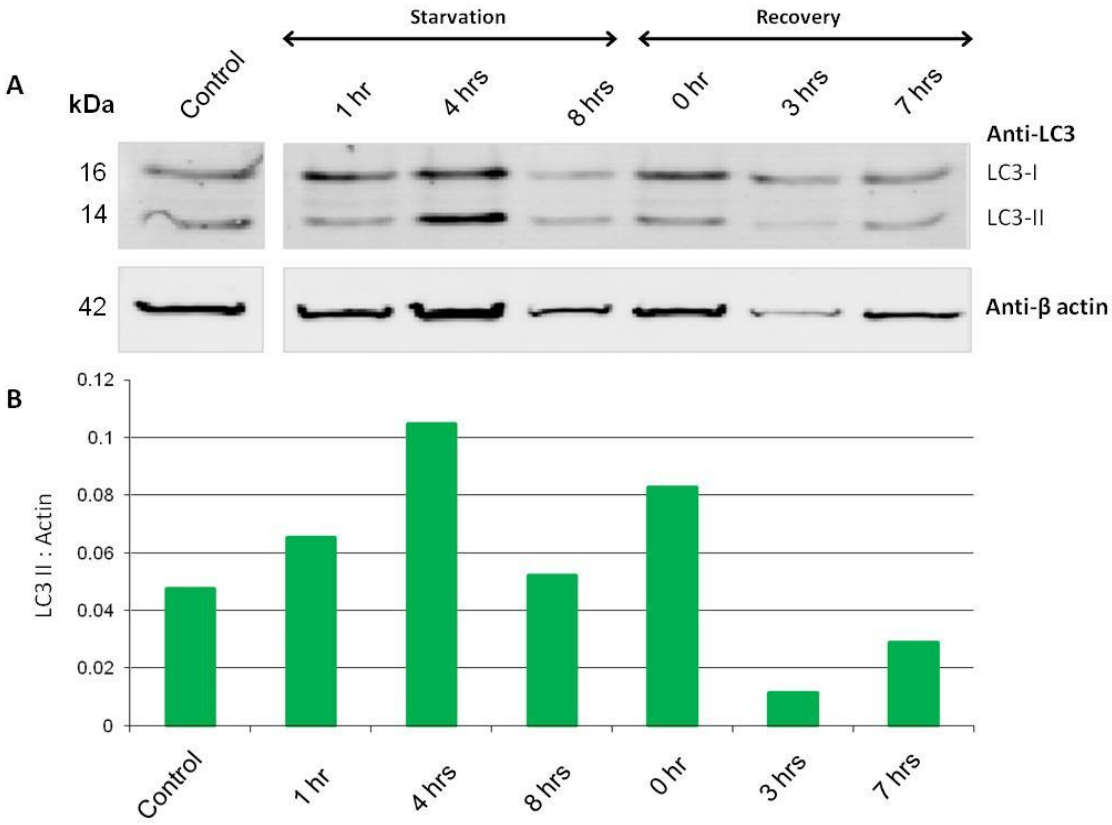

Figure 3.4 – Increase of LC3-II Following Starvation and the Recovery After Feeding – (A) MEF cells were grown in complete media (control), or incubated HBSS for 1, 4 or 8 hours (starvation). In separate experiments MEF cells were starved for 1 hour and allowed to recover for 3 or 7 hours in full nutrient media (recovery). Cell lysates were separated by SDS-PAGE and levels of LC3 and β actin determined by Western blot. Secondary antibodies were detected using infra-red light at 680nm (β-actin) and 800nm (LC3). (B) LC3-II signal normalised to β-actin using the Odyssey software.

3.3.1 Use of LC3 and p62 to Determine Induction of Autophagy

A stable CHO cell line expressing a chimeric form of LC3, eGFP-LC3, allows for the distribution of LC3 to be followed using the inherent fluorescence of the GFP molecule. Figure 3.1 shows that LC3 has a diffuse cytoplasmic distribution in control nutrient rich media and on induction of autophagy, following replacement of media with starvation media, the GFP-LC3 signal becomes punctate. The small LC3 'puncta' represent autophagosomes and indicated the activation of autophagy. In the bottom panels of 3.1, CHO cells stably expressing the mutant LC3, eGFP-LC3 G120A, where the glycine residue is replaced with an alanine and therefore cannot be conjugated to the PE molecule. In these cells there is no change in distribution of LC3 in starvation media compared to the controls media. In both conditions the LC3 remains cytoplasmic.

Figure 3.2 shows analysis of LC3 punctae can change due to the progression of the pathway over an eight hour time course. The number of LC3 vesicles will increased between 1 and 4 hours and reached a peak with a slight decrease can be seen by 8 hours. LC3 punctae were concentrated closer to the perinuclear region at 8 hours. Similar results were recorded for p62 (figure 3.2) with a cytoplasmic distribution at 1 hour, followed by a small number of punctate vesicles at 4 hours and 8 hours. The experiment was repeated using MEF cells. Endogenous LC3 and p62 and the fluorescently tagged proteins showed similar changes in distribution on induction of autophagy and double labelling experiments showed colocalisation of p62 and LC3.

3.3.2 Lipidation of LC3 and Degradation of p62 Can Be Monitored Using Western Blots

The lipidation of LC3 results in faster migration on a SDS-PAGE gel. The fast migrating form known as LC3-II can be detected as a separate band at 14 kDa compared to the 16 kDa unlipidated form (LC3-I). The faster migration of LC3-II is thought to be due to the negative charge of the PE molecule. During starvation levels of LC3-II increase, but then LC3-II is delivered to lysosomes and degraded. This complicates interpretation of Western bots and makes it difficult to use LC3-II levels as an absolute indicator of autophagy. A semi-quantative assay is possible by comparing the levels of cellular LC3-II relative to actin. In the Western blots of figure 3.4 LC3-I and LC3-II are seen at 16 and 14kDa respectively in control cells, due to basal autophagy. The levels of both forms of LC3 increased after 4 hours

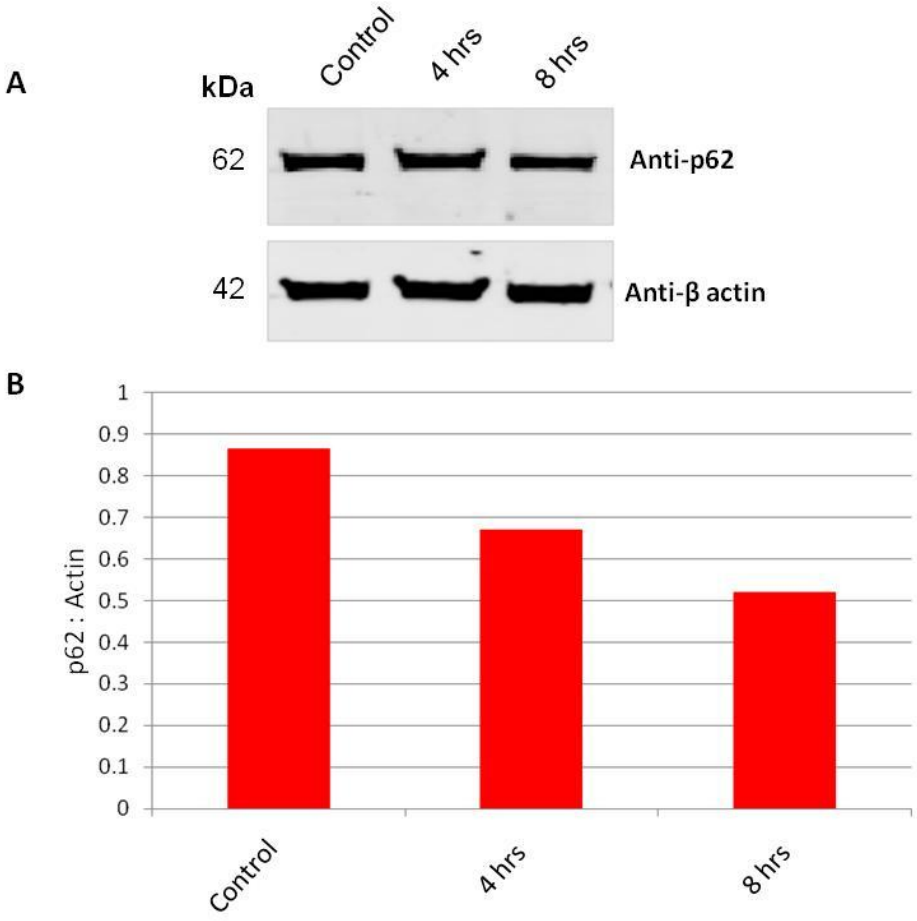

Figure 3.5 – Decrease in the Levels of p62 After Activation of Autophagy – (A) MEF cells were incubated HBSS for 4 or 8 hours then lysed. Cell lysates were separated by SDS-PAGE and levels of LC3 and β actin determined by Western blot. Secondary antibodies were detected using infra-red light at 680nm (β-actin) and 800nm (LC3). (B) p62 signal normalised to β-actin using the Odyssey software.

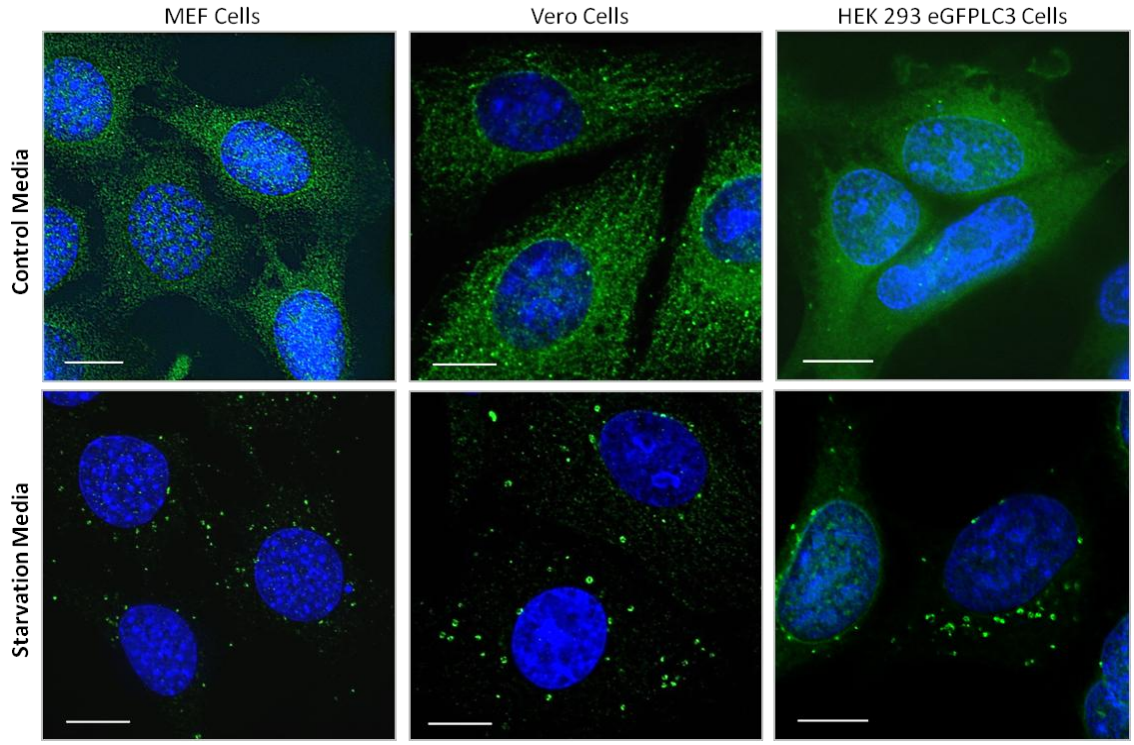

Figure 3.6 – Redistribution of cytoplasmic LC3 to Punctate Autophagosomes in Cell Lines from Different Species After Activation of Autophagy – Cells were cultured overnight on glass coverslips, and were left untreated in full media (top panels) or starved for 4 hours prior to fixation and immunostaining for endogenous LC3 (green) in MEF and Vero cells. LC3 was detected in the HEK 293 cells from the natural fluorescence of GFP (green). Nuclei were stained with DAPI (blue). Bar is 10 µm.

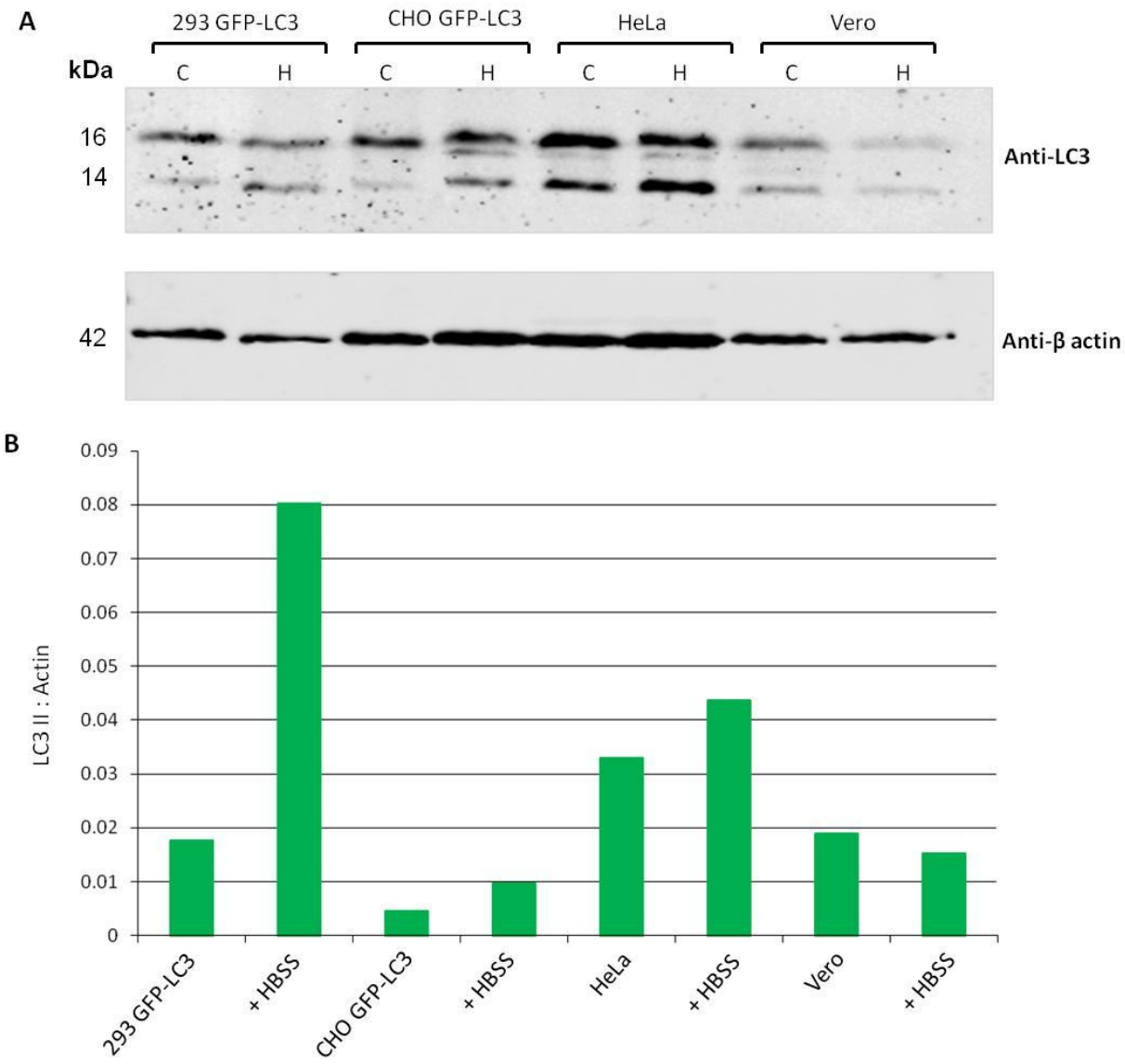

Figure 3.7 – The Increase in LC3-II in Response to Autophagy in Different Cell Lines – (A) Cells were grown in full nutrient media (C, control), or starved in HBSS for 4 hours (H, HBSS). Cells lysates were separated by SDS-PAGE and analysed by Western blot using anti-LC3 and anti-β actin. Secondary antibodies were detected using infra-red light at 680nm (β-actin) and 800nm (LC3). (B) LC3 signal normalised to β-actin using the Odyssey software.

following transfer to HBSS and declined at 8 hours. Densitometric analysis of bands after adjustment for gel loading is shown in panel B. The ratio of LC3-II to actin increased at 4 hours indicating an overall increase in LC3-II, and then declined. In a separate experiment cells were starved for 1 hour and then allowed to recover in complete media. Again the ratio of LC3-II to actin was high after starvation and then declined during recovery. A gradual decrease in the levels of LC3-II can be seen between 3 and 7 hours possibly due to the delivery and degradation in lysosomes. The levels of p62 can be used to monitor the induction of autophagy (Bjorkoy *et al* 2005) since autophagy results in degradation of p62 in lysosomes (figure 3.5). In this experiment induction of autophagy for 8 hours resulted in a slight fall in p62 levels of p62 in comparison to the control level in full media. This is further highlighted by figure 3.9 shown later.

3.3.3 Induction of Autophagy in Different Cell Lines

Autophagy is a conserved response in eukaryotic organisms. The distribution of LC3 used to assess autophagy in different mammalian cells lines in subsequent experiments is shown in figures 3.6 and 3.7. In MEF and Vero cells, the LC3 was identified by immunostaining of endogenous LC3 rather that following eGFP-LC3. As seen with the CHO cells expressing eGFP-LC3, the unlipidated LC3 staining was predominantly cytoplasmic in all cell lines grown in nutrient media. There were some LC3 punctae in Vero cells suggesting there may be a higher level of basal autophagy in these cells. LC3 punctae were distributed through-out the cytoplasm when the cells were starved in HBSS. LC3 processing was analysed by Western blots of the unstarved control and starved cells (figure 3.7). The cells showed different levels of basal LC3-II on the Western blot. There was no obvious relative increase in LC3-II over LC3-I. The LC3-II levels were therefore normalised to actin to generate the bar cart in panel B. During 4 hours of starvation, the 293 GFP-LC3 cells have a large increase in the amount of LC3-II in comparison to the other cell lines. The CHO GFP-LC3 and HeLa show an increase in LC3-II under starved conditions. The Vero cells showed a slight decrease and this correlates with the LC3 punctae seen by fluorescence. In conclusion it looks as if different cells have different levels of basal autophagy depending on their own cellular metabolism, highlighted by the different LC3 levels on the western blot. This makes LC3-II processing difficult to use as an assay for activation of autophagy, the results are

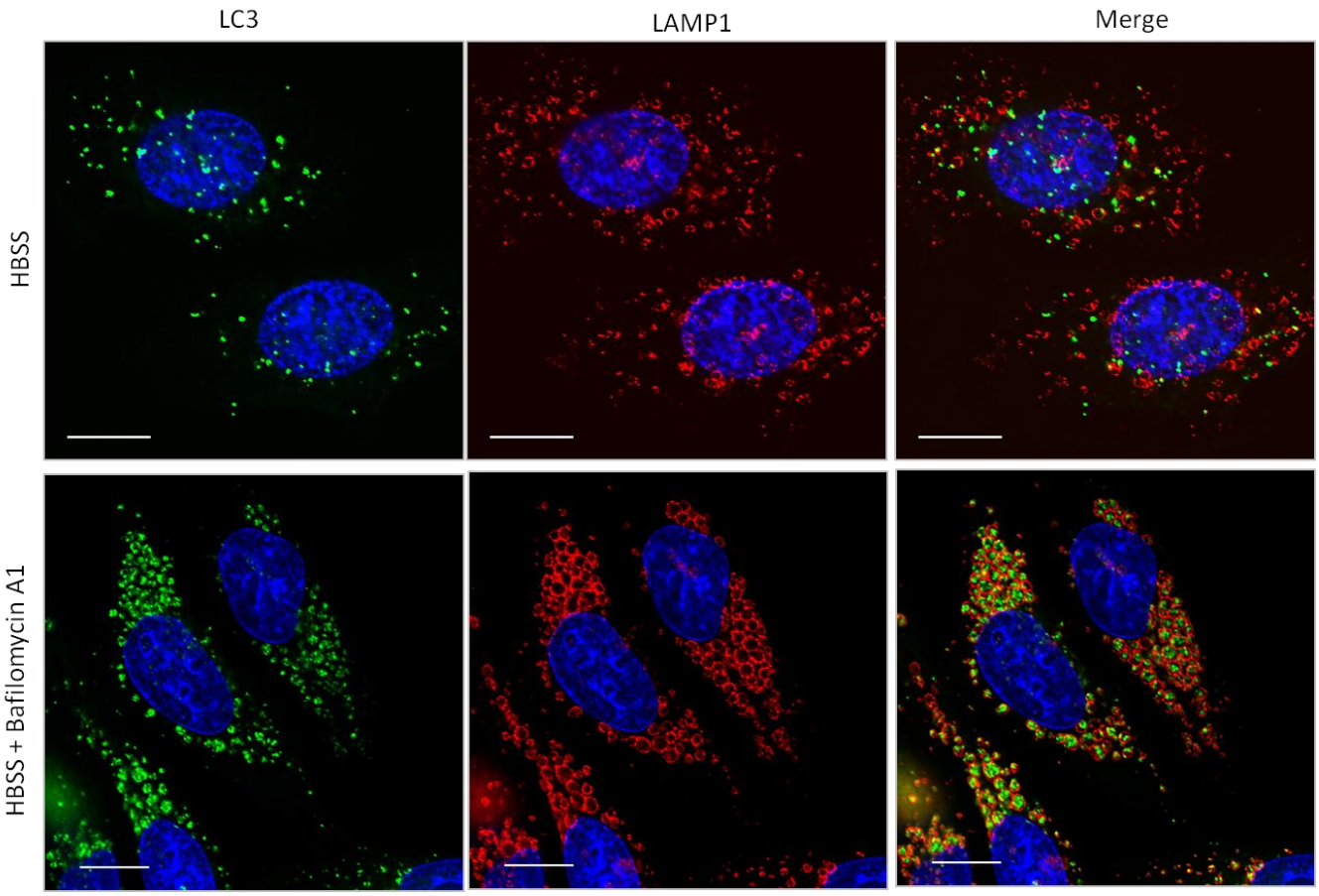

Figure 3.8 - Inactivation of Lysosomal Degradation Results in Accumulation of LC3 - CHO cells stably expressing eGFP-LC3 (green) were cultured overnight on coverslips and then starved in HBSS for 8 hours without (top panels) or with bafilomycin (bottom panels) and then fixed. Cells were stained with anti-LAMP1 (red) and the nuclei with DAPI (blue). Bar is 10 µm.

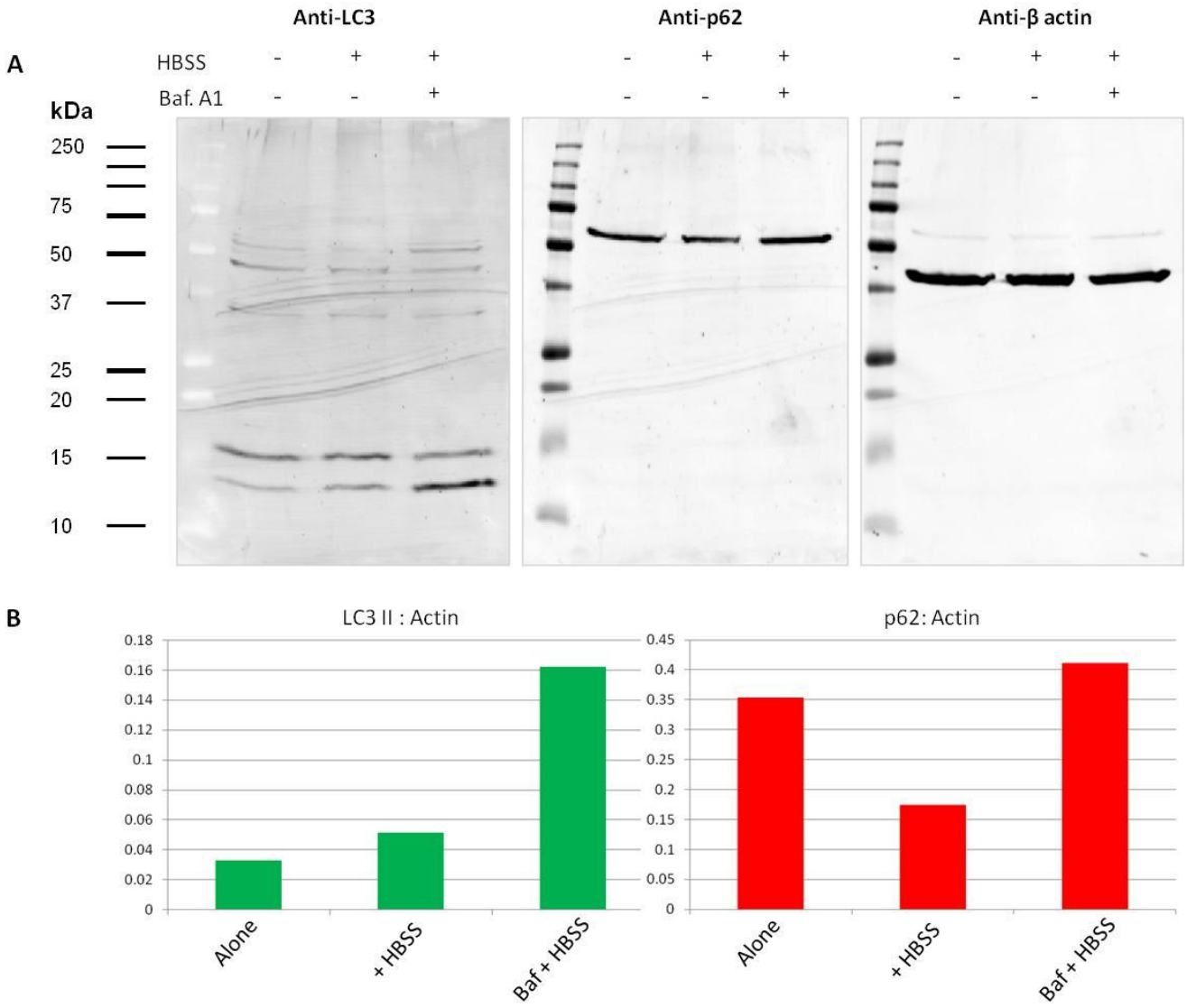

Figure 3.9 – Effect of bafilomycin on levels of LC3-II and p62 during Autophagy (A) HeLa cells were cultured in complete nutrient media or starved in HBSS for 4 hours (HBSS), or HBSS with 100 nM bafilomycin A1. Cell lysates were separated by SDS-PAGE and analysed by Western blot using anti-LC3 and anti-β actin. Secondary antibodies were detected using infra-red light at 680nm (β-actin) and 800nm (LC3). (B) LC3 and p62 signals normalised to β-actin using the Odyssey software.

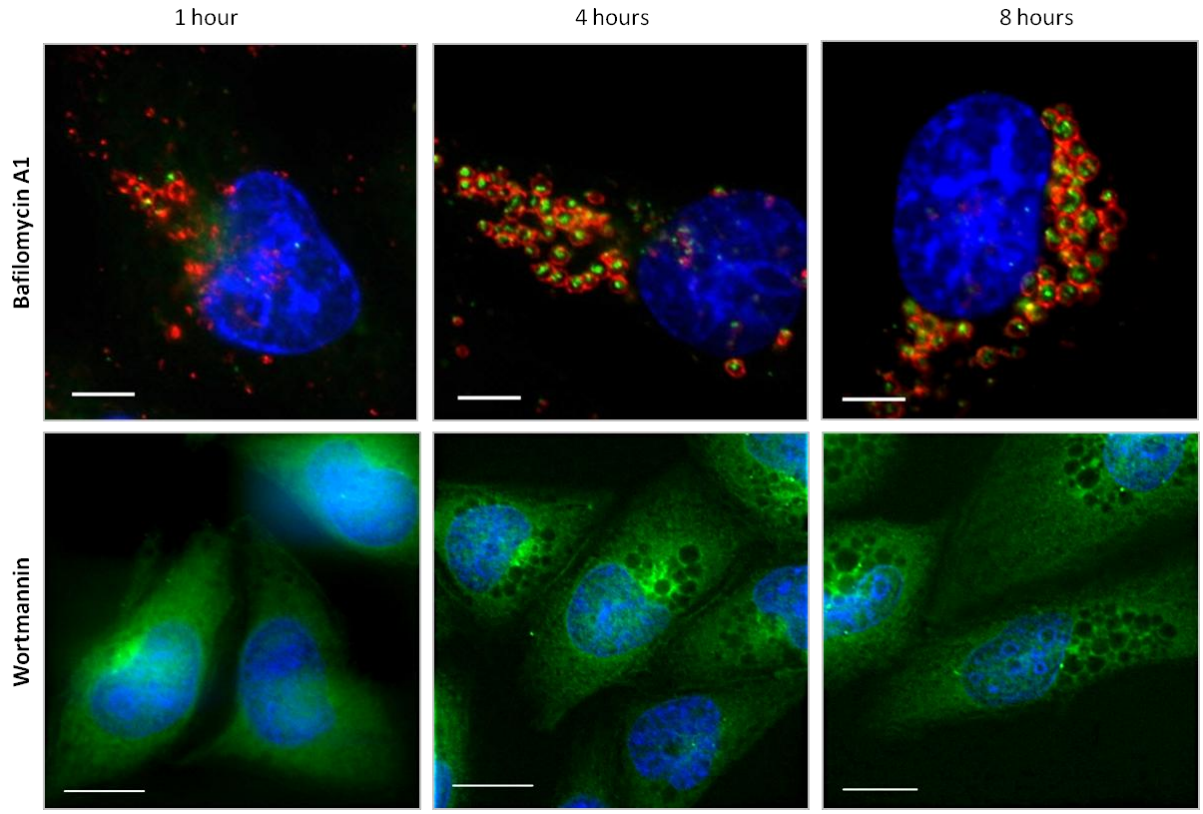

Figure 3.10 – Comparison of the Inhibitory Effects of Bafilomycin and Wortmannin on Autophagy - CHO cells stably expressing eGFP-LC3 (green) were grown on coverslips for 24 hours. Cells were then starved in HBSS in the presence of 100 nM bafilomycin A1 (top panels) or 10 nM wortmannin (bottom panels). Cells were then fixed at 1, 4 or 8 hours. Cells incubated with bafilomycin (top panels) were subsequently counter stained for LAMP1 (red) Bar is 10 μm.

easier to interpret when LC3-II bands were normalised to β-actin levels in each cell type rather than to LC3-I levels.

3.3.4 Autophagosomes Fusion with Lysosomes

The transfer of autophagosomes to lysosomes was studied in figure 3.8. The CHO cells stably expressing eGFP-LC3 were starved for 8 hours and autophagosomes followed by the distribution of LC3 formed LC3 punctae and lysosomes were identified using the lysosomal marker LAMP1. The top panel shows that many eGFP punctae which localised near to the lysosomes but there were few double positive structures in the merged image. GFP is not stable in acidic conditions and therefore will not be stable inside the lysosomes (Kimura *et al* 2007). Bafilomycin A1 is an inhibitor of the vacuolar ATPase that delivers H^+ to the lysosomes prevents the acidification of the lysosomes, and hence proteolysis. When cells were incubated with bafilomycin during starvation eGFP-LC3 punctae were observed inside the swollen lysosomes indicating fusion of autophagosomes and lysosomes. The GFP signal is retained as the lysosome is no longer able to acidify. Use of bafilomycin A1 to determine the autophagy flux is important mechanistically to see if autophagosome production is increased or if degradation in lysosomes is inhibited. If the end point of the flux is inhibited, then incubation with bafilomycin A1 will not yield any differences in LC3-II on a Western, or the number of LC3 puntae. However, if the stimulus increased the number of autophagosomes, then a larger LC3-II band is seen on a Western blot and increased number of puntae. This is an important assay to use for determining how a stimulus can affect autophagy.

Cell incubated with bafilomycin A1 were analysed by Western blot. Consistent with the immunofluorescence study (figure 3.9), bafilomycin A1 increases the levels of LC3-II, by decreasing degradation in lysosomes. Similarly the degradation of p62 is hindered and this also accumulates in the cytoplasm, and can be seen by an intense band running between the 50 and 72 kDa standards.

3.3.5 Inhibitors of Autophagy

Figure 3.10 compared the effects of bafilomycin A1 and wortmannin, a PI-3 kinase inhibitor, on autophagy. As recorded above bafilomycin A1 inhibited the degradation of LC3

in lysosomes. LC3 punctae first appeared at one hour when they were separate from LAMP1 positive lysosomes. Cells observed at 4 and 8 hours showed LC3 signals inside the lysosomes indicating fused autophagosomes with lysosomes, however as the GFP signal is retained. In contrast, in the presence of wortmannin, cells did not form LC3 punctae in response to starvation and LC3 remained in the cytoplasm.

3.4 Discussion

The aim of this chapter has been to describe standard assays of autophagy and show that these can be carried out in cell lines used in subsequent studies. Autophagy was monitored using the proteins LC3 and p62 as markers for induction and progression to fusion with lysosomes. The results also showed that autophagy can be inhibited by the incubation with wortmannin, and bafilomycin A1 can be used to prevent the degradation of LC3 in lysosomes.

The use of LC3 and p62 as markers in this study highlighted that both proteins can be used to examine the process as they localise the autophagosomes. LC3 is a useful protein to use to measure autophagy. The formation of LC3 punctae can be monitored by microscopy as its location changes within the cell, and correlated with addition of PE to produce LC3-II which can be measured independently on a Western blot. Cells expressing the form of LC3 carrying the G120A mutation, which prevented addition of PE, can be used as an additional control. A change in the amino acid sequence can prevent the lipidation and hence the formation of autophagosomes. A stable cell line is also an important tool, as autophagy is a response which can be induced by a number of stress stimuli, which include starvation. It is important to have the cells in the least stress conditions prior to experimentation in order to achieve accurate results. Kuma *et al* (2007) have, for example reported LC3 incorporation into protein aggregates independently of autophagy causing doubts as to autophagy induction (Korkhov 2009). Although these aggregates are particularly large and localised to the perinuclear region of the cell they are not characteristic of autophagosomes. It is noted that other methods to validate autophagy are required such as immunoblots also have to be interpreted carefully. The levels of LC3-I and LC3-II are detected using specific anti-LC3 antibodies; however, it is possible that the antibody will recognise the LC3-II form more than

the LC3-I due to unmasking of epitopes during the autophagy (Mizushima and Yoshimori 2007). For this reason, the normalisation of LC3-II to actin provides a more accurate indication of autophagy than the ratio of total levels of LC3, LC3-I and LC3-II (Tanida *et al* 2005). The levels of LC3-I and LC3-II can, as seen in this study, vary between cell types depending on cellular metabolism and basal autophagy which may also yield results that are difficult to interpret (Tanida *et al* 2005).

With the rising interest in autophagy alternative markers to LC3 are being developed to verify the induction of autophagy. Whilst many of the autophagy (Atg) proteins are removed after the closure of the autophagosomal membrane, p62 can be used in parallel with LC3. The data presented in this study indicates that p62 localises to the autophagosomes during autophagy, and a decrease in the levels of p62 can be used as an indicator of autophagy induction because p62 is degraded following fusion with the lysosomes. It is important to study the levels and location of endogenous p62 in parallel to studies of fluorescently-tagged p62. Transient expression of a fluorescent-tagged p62 can lead to the formation of inclusion bodies rather than autophagosomes (Bjorkoy *et al* 2005, Pankiv *et al* 2007). However, caution must be employed as p62 is not crucial for the formation of the autophagosome. When used in tandem with other methods it provides a useful tool to monitor autophagy.

In summary, these studies on LC3 and p62 indicated that both proteins can be used to follow the induction and the progression of autophagy to fusion with lysosomes, and also that this process can be inhibited using bafilomycin A1 or wortmannin.

Chapter 4:

The Formation of Large Tubulo-Vesicular Autophagosomes and the Comparison to Autophagic Components

Chapter 4 – The Formation of Large Tubulo-Vesicular Autophagosomes (TVAs) and the Comparison to Autophagic Components

4.1 Aims –

The aims of this chapter are to describe the nature of the large tubulo-vesicular autophagosomes (TVAs) that formed when cells are incubated with cationic liposomes, and also to compare these structures to typical autophagosomes formed following starvation. The principal marker used to define the large tubulo-vesicular structure is LC3, and the study also aims to establish if other autophagy proteins are activated or required during the formation of these structures.

4.2 Introduction

During experiments in the previous chapter it was noted that cationic liposomes commonly used as transfection reagents resulted in the formation of novel autophagosomes. Generally, autophagosomes are double membrane vesicles 300-900 nm in diameter. This can vary between different cell lines and tissues. However a well-defined change in the location of LC3 is always seen during autophagy where cytoplasmic LC3 moves punctate structures distributed throughout the cytoplasm as previously discussed (Mizushima *et al* 1998). Originally, autophagy was described as a cellular response to lack of nutrients, however, many recent examples have highlighted that autophagy can adapt to new challenges. Interestingly, a recent study by Nishida *et al* (2009) has provided an example of non-canonical autophagy, whereby a knock-out or loss of function mutations in the key autophagy proteins Atg5 and Atg7 reveal Atg5/Atg7 independent pathways. These Atg5/Atg7 independent pathways are still PI 3-kinase dependent and they have a functional role in higher eukaryotes. Similarly, Zhou *et al* (2011) has shown a Vps34-independent form of autophagy that exists in neurons, yet this type of autophagy still depends on Atg7 for LC3 punctae to form. Emerging in the literature is evidence for non-canonical autophagy pathways and how they play a role in cellular survival and adaptation when canonical autophagy cannot function.

The experiments at the start of this thesis work showed that autophagosomes formed following DNA transfection using cationic liposomes. During the same period, papers appeared in the literature (Gao *et al* 2008, Sarkar *et al* 2009) that confirmed the non-viral DNA delivery vectors such as cationic liposomes and calcium phosphate precipitates, previously thought inert, could induce autophagy. Liposomes are formed when a lipid in an aqueous environment generates single or multi-lamellar structures, and cationic liposomes are used to deliver DNA to cells. The positive charge of the lipids allows incorporation of the negatively charged DNA into the liposomes see figure 3.1 below.

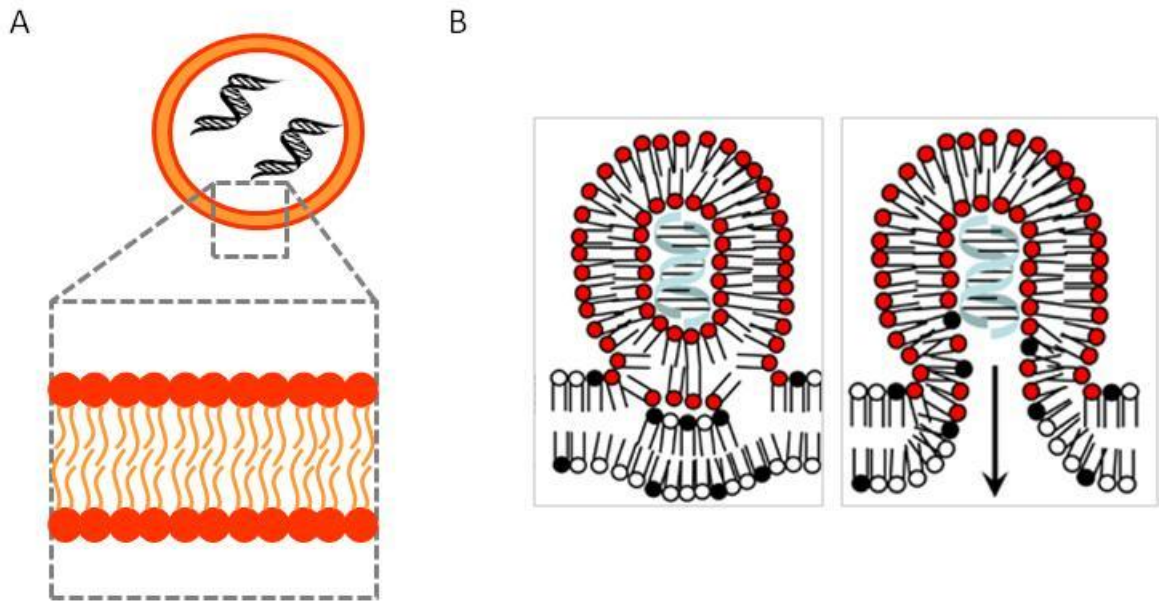

Figure 4.0 – (A) the arrangement of lipid in a liposome – the hydrophobic tail and the polar head group of the lipid will arrange so the head group is in contact with the aqueous environment whilst the chains form a aqueous-free layer **(B) fusion with cellular membranes –** cationic lipid bilayers will fuse with endocytic vesicle membranes and result in the release of DNA (adapted from Medina-Kauwe *et al* 2005).

Commercially, there are a number of liposomes available that vary in composition, many of which have the neutral helper lipid DOPE to improve transfection efficiency. DOPE affects the packing properties of the cationic lipid and improves membrane fluidity in liposome formation (Zuhorn *et al* 2002). Liposomes enter the cell through endocytosis and fuse with the endosome membrane to release the DNA into the cytoplasm, as shown above. Viral vectors such as the lentivirus or adenovirus vectors which can be used as an alternative to liposomes can potentially activate other cellular and innate immunity during the delivery

of DNA to cells (Kufe *et al* 2003, Tresset 2009). This can lead to undesired side effects or cellular responses to the viral vectors.

In this chapter, the autophagosomes generated by cationic liposomes are compared with autophagosomes formed during starvation. Autophagy is monitored by following LC3 redistribution. The studies also investigate the role played by beclin-1 and Atg5. Beclin-1 is part of the PI 3-kinase: Vps34 complex involved in the initiation of autophagy, and DFCP1 will be used as a marker for the generation of PI (3)P required for autophagy. Atg5 functions as a complex with Atg12 and Atg16 to provide support for the forming autophagosome, and to ensure correct lipidation of LC3.

4.3 Results

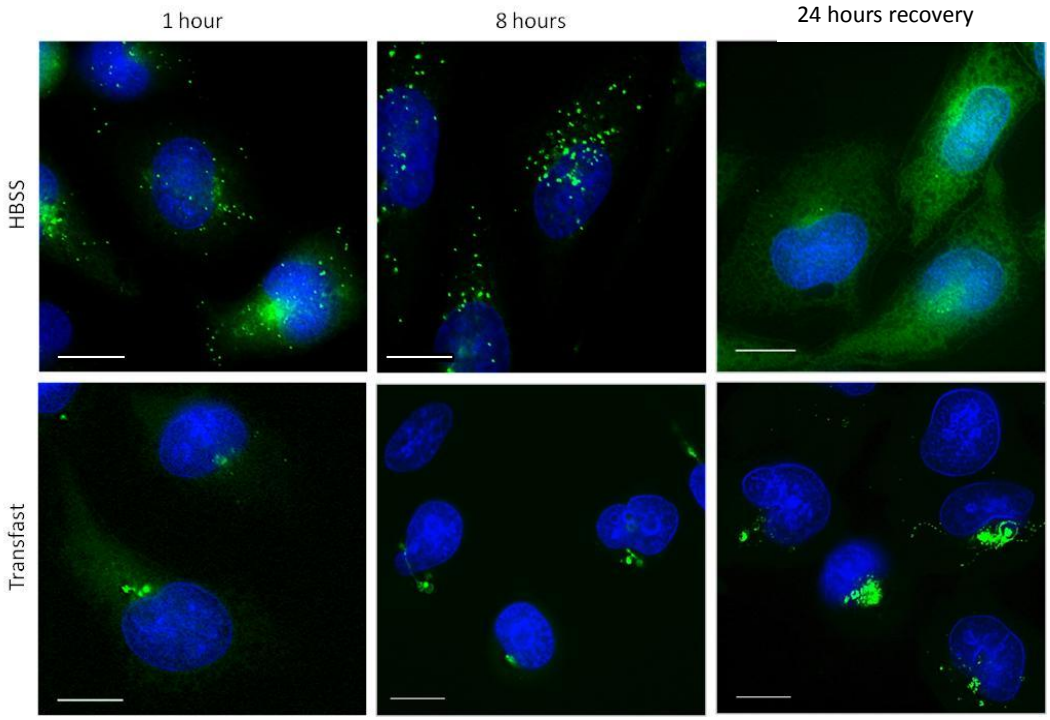

Figure 4.1 – Cells Incubated with Cationic Liposomes Rearrange eGFP-LC3 into Large Perinuclear Structures - CHO cells stably expressing eGFP-LC3 were cultured overnight on glass coverslips. Cells were starved by incubation in HBSS (top panels) or incubated with the cationic transfection reagent Transfast (bottom panels) for the indicated times and then fixed. At 8 hours, cells were washed, and fed in complete media overnight. These cells were fixed at 24 hours post incubation. Nuclei were stained with DAPI (blue). Bar is 10 µm.

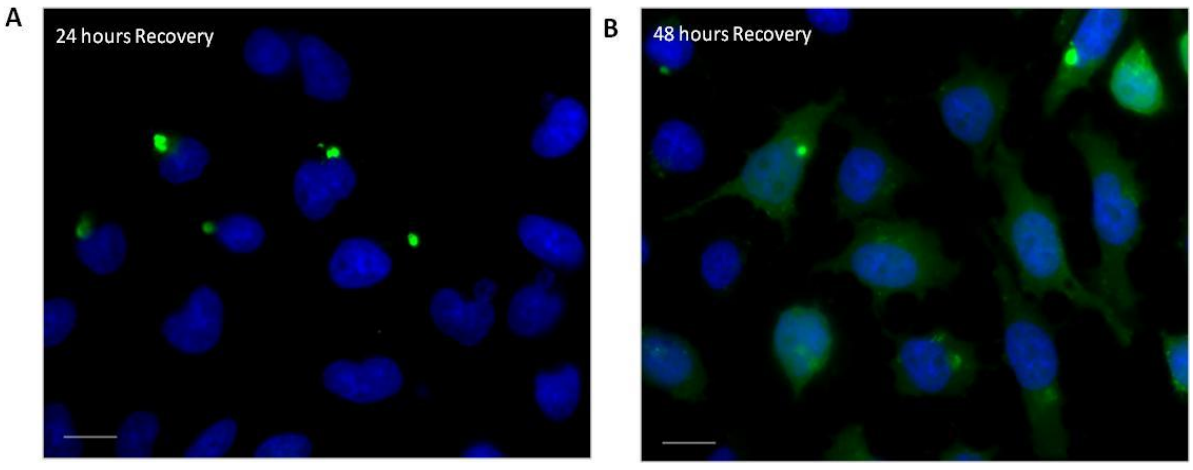

Figure 4.2 – Tubulo-Vesicular Autophagosomes (TVAs) Remained in the Cytoplasm for at Least 48 hours - CHO cells stably expressing eGFP-LC3 were cultured overnight on glass coverslips and processed as described for figure 4.1. Cells were incubated with Transfast for 8 hours and allowed to recover for 24 hours (A) or 48 hours (B) before fixation, and stained the nuclei with DAPI (blue). Bar is 10 µm.

Reagent	Rearrangement of LC3	Type
Transfast	✓	Liposome-based
Lipofectamine	✓	Liposome-based
Nanojuice	✓	Liposome-based
HiPerfect	✓	Liposome-based
Fugene HD	✓	Non-Liposome
Turbofect	✓	Non-Liposome
JetPrime	✓	Non-Liposome
Interferin	✓	Non-Liposome
Calcium Phosphate	✓	Non-Liposome

Table 4.1 – Incubation with a Variety of Liposomes Generated Tubulo-Vesicular Autophagosomes (TVAs) - CHO cells stably expressing eGFP-LC3 were cultured overnight on glass coverslips. Cells were incubated with the transfection reagents stated in the table for 4 hours before fixation, and analysed using fluorescence microscopy to monitor LC3 distribution.

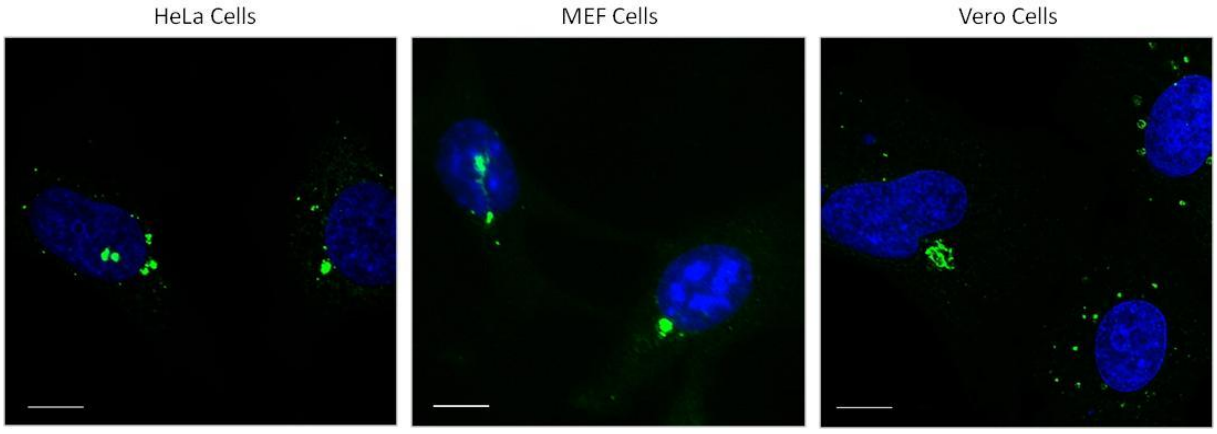

Figure 4.3 – Formation of Tubulo-vesicular Autophagosomes (TVAs) in Different Cell Lines - HeLa cells, MEF cells or Vero cells were cultured overnight on glass coverslips. Cells were incubated with Transfast for 4 hours before fixation. Cells were then stained with anti-LC3b bodies to detect endogenous LC3 and the nuclei were stained with DAPI (blue). LC3 was visualised using secondary antibodies conjugated to Alexa 488 (green). Bar is 10 µm.

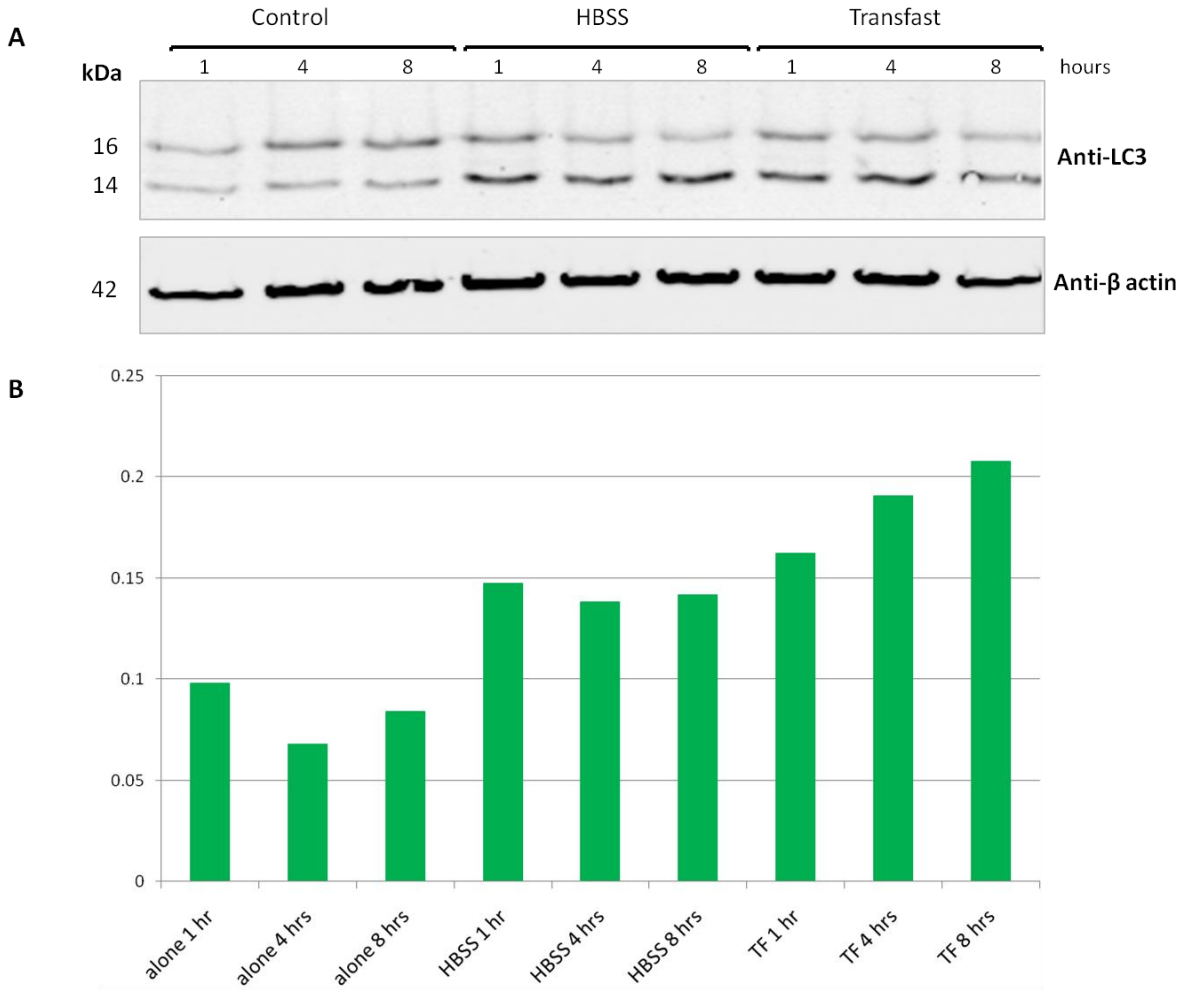

Figure 4.4 – Increase of LC3-I Processing Following Starvation or Incubation with Cationic Liposomes – (A) MEF cells were cultured in complete nutrient media (control), or starved by transfer to HBSS, or incubated with Transfast transfection reagent. Cells lysates generated at the indicated times were separated by SDS PAGE and analysed by Western blot using antibodies recognising LC3 or β actin. Secondary antibodies were detected detection using infra-red light at 680nm (β-actin) and 800nm (LC3). (B) Densitometry of the LC3-II signal which was normalised to β-actin using the Odyssey software.

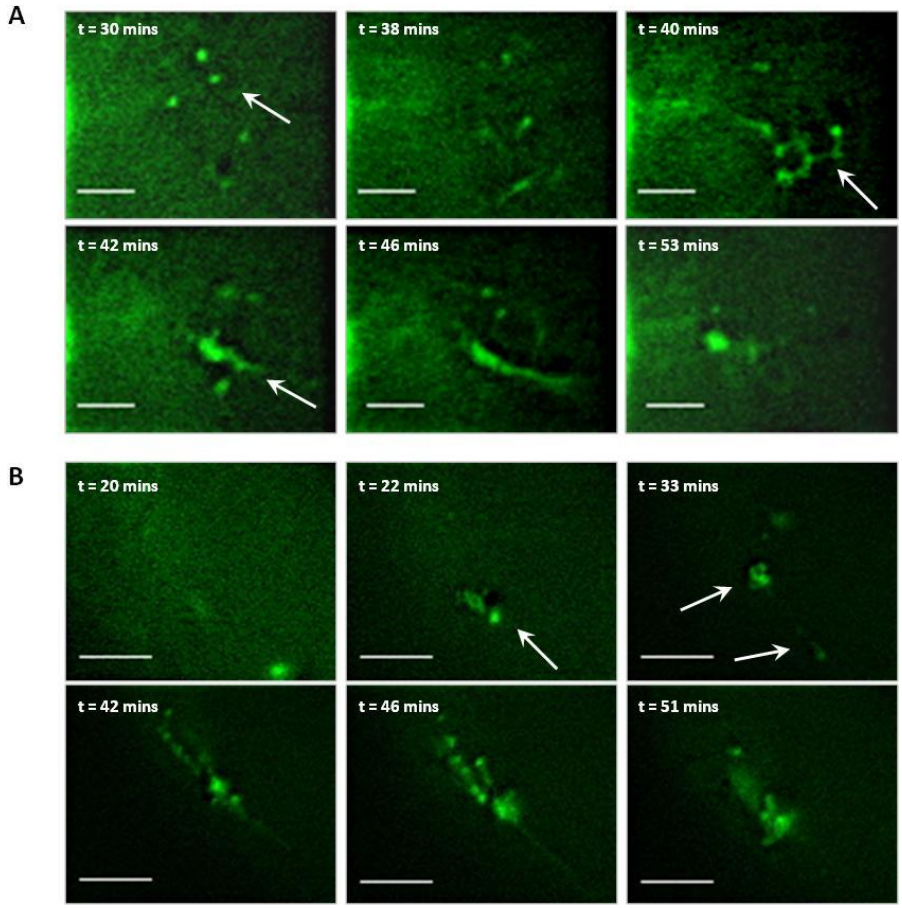

Figure 4.5 – The Formation of Tubulo-Vesicular Autophagosomes (TVAs) in Response to Cationic Liposomes - CHO cells stably expressing eGFP-LC3 (green) were grown on coverslips overnight prior to placing in a POC chamber and incubated in Transfast in OptiMEM for a further 2 hours whilst imaging. Bar is 2 µm.

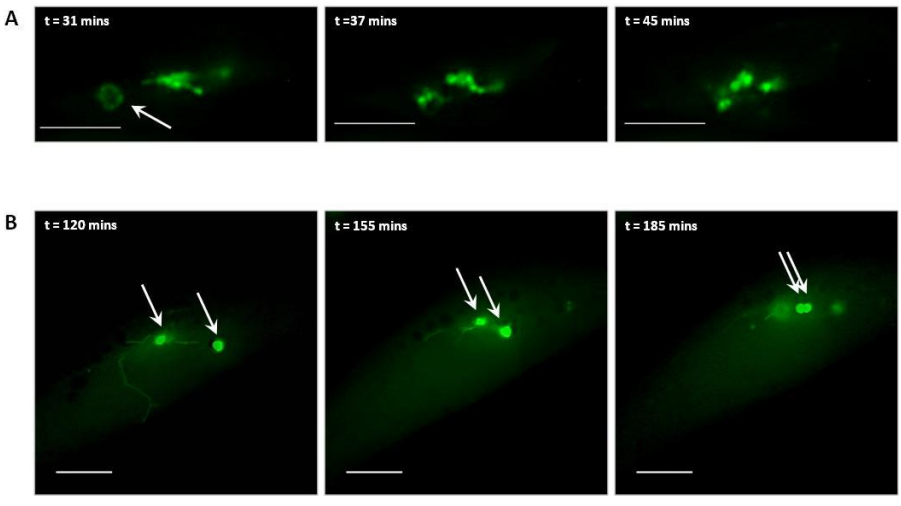

Figure 4.6 – New Tubulo-Vesicular Autophagosomes (TVAs) are Incorporated into Pre-Existing Structures - CHO cells stably expressing eGFP-LC3 (green) were grown on coverslips overnight prior to incubating in Transfast in OptiMEM for a further 4 hours, imaging at the time point stated. Bars are 5 and 10 µm respectively. White arrows show TVA incorporation into pre-existing LC3-positive structure.

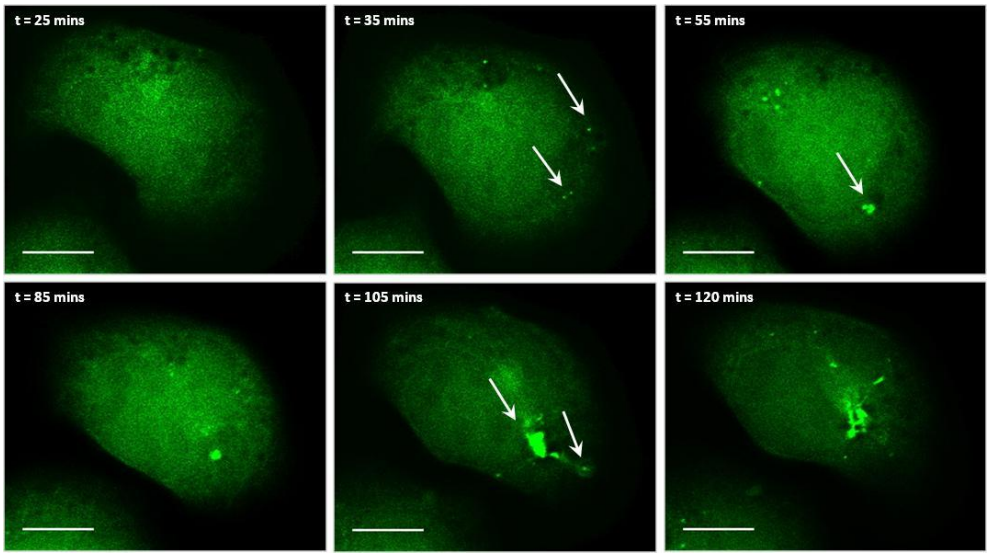

Figure 4.7 – Tubulo-Vesicular Autophagosome (TVAs) Formation Does Not Require Ongoing Protein Synthesis- CHO cells stably expressing eGFP-LC3 (green) were grown on coverslips overnight prior to placing in a POC chamber and incubated in Transfast in OptiMEM and in the presence of 20µg/ml cyclohexmide for a further 2 hours, imaging at the time point stated. Bar is 10 µm. White arrows show the formation of TVAs from punctate vesicles and tubular elements.

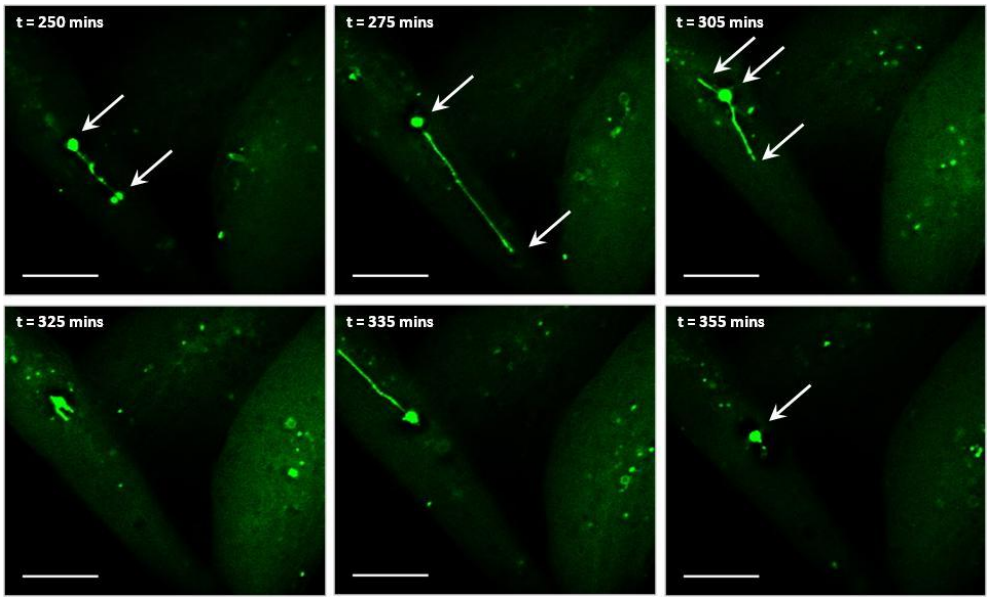

Figure 4.8 – Dynamic Tubules Extending from the Tubulo-Vesicular Autophagosomes (TVAs) Do Not Require Ongoing Protein Synthesis- CHO cells stably expressing eGFP-LC3 (green) were grown on coverslips overnight prior to placing in a POC chamber and incubated in Transfast in OptiMEM in the presence of 20µg/ml cyclohexmide for a further 6 hours, imaging at the time point stated. Bar is 10 µm. White arrows indicate connecting TVAs, and the dynamic tubules which extend outwards.

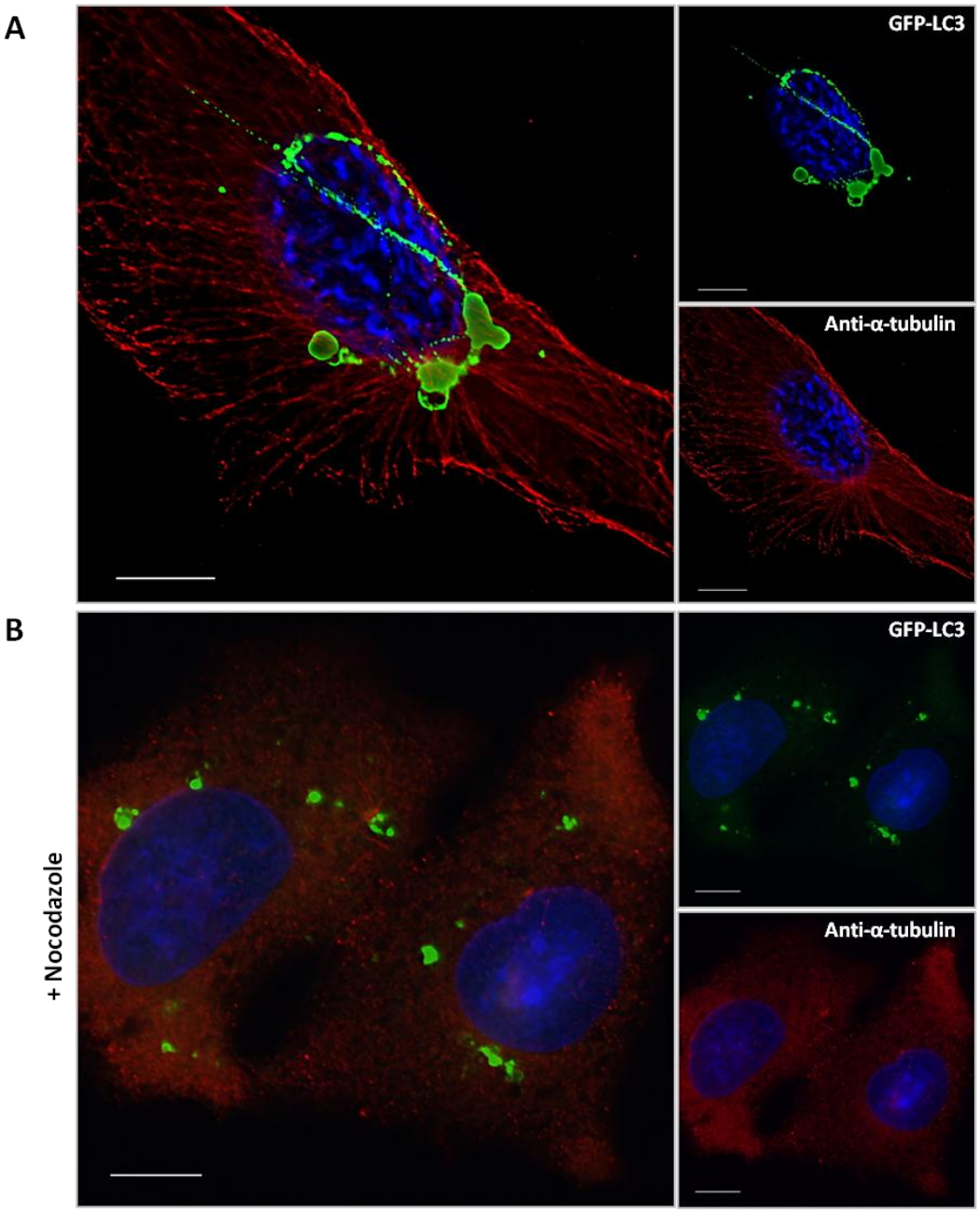

Figure 4.9 – Role of Microtubules in the Formation of Tubulo-Vesicular Autophagosomes (TVAs) - CHO cells stably expressing eGFP-LC3 (green) were incubated in completed media (A) or pre-treated with 5µM nocodazole for 30 mins (B) before addition of Transfast. Cells were incubated for a further 4 hours in OptiMEM before fixation in methanol/MES solution. Cells were stained using an antibodies against α tubulin (Alexafluor 594, red) and nuclei were stained with DAPI (blue). Bar is 10 µm.

4.3.1 Cationic Liposomes Induce the Formation of Large LC3-Positive Perinuclear Structures -

Autophagy was monitored by following the formation of LC3 punctae as discussed previously in chapter 3. The top panels in figure 4.1, showed this change in LC3 distribution over time during starvation, using the stable CHO cell line expressing eGFP-LC3. When cells were fed at 8 hours, and allowed to recover for 24 hours the eGFP-LC3 signal had returned to a cytoplasmic distribution. Incubation of the same cell line with the transfection reagent Transfast induced a different rearrangement of LC3 into large perinuclear structures. This novel rearrangement of LC3 was induced in almost the entire population of cells and, in contrast to LC3 punctae induced by starvation, large LC3 positive structures remained in the cytoplasm for a substantial period. In spite of an overnight recovery in complete media, the large LC3 positive structures could still be detected in some cells (figure 4.2) at 48 hours. The experiment was repeated with a number of different transfection reagents including liposomes and non-liposome based formulations (table 4.1), and all of the reagents tested induced a similar redistribution of LC3 to perinuclear structures. This response was not restricted to eGFP-tagged LC3. Figure 4.3 shows endogenous LC3 staining in human (HeLa), mouse (MEF) and monkey (Vero) cells following incubation with Transfast. HEK 293 stably expressing GFP-LC3 (data not shown) also showed the same response. Similarly, LC3-II production is increased following starvation, and also incubation with liposomes, as shown in figure 4.4. The Western blot show the levels of endogenous LC3 increased with starvation over an 8 hour time course, and also increased further when incubated with the transfection reagent Transfast.

4.3.2 Large LC3-positive Perinuclear Structures form Tubular and Vesicular Intermediates -

In order to determine how these large LC3 positive structures form in the cytoplasm, CHO stably expressing eGFP-LC3 were imaged in real time by live cell microscopy. At the early time points monitored over the first hour (figure 4.5 panels A) a number of small eGFP-positive vesicles appeared at 30 minutes which formed a network of tubular structures that collapsed back towards the nucleus between 40 and 53 minutes, as highlighted by the white arrows. In figure 4.5, panels B, a similar process occurred whereby vesicles, indicated by the white arrows, were present at 20 minutes and tubular structures appeared at 42 minutes

which collapsed into large perinuclear at 51 minutes. The structures have both tubular and vesicular components and will be referred to as tubulo-vesicular autophagosomes (TVAs).

Figure 4.6 monitored the dynamics of pre-existing TVAs in the cytoplasm, in panels A, a ring-like structure, indicated by the white arrow, appeared next to the TVA at 30 minutes which became incorporated into the large TVA at 45 minutes. Similarly panel B shows cells 2 hours post incubation with Transfast. Two large TVAs, highlighted by the two white arrows, are connected by a tubule which extended towards the structure on the right, the two then moved close to each other and concentrate in the perinuclear region.

4.3.3 The TVAs Recruit Pre-Synthesised LC3 and Require Intact Microtubules for Tubular Structures

The experiment shown in figure 4.7 investigates whether TVAs are maintained by a continuous supply of LC3. The experiment used cycloheximide to inhibit new protein synthesis and only the pre-existing pool of LC3 protein can be used for LC3 processing and incorporation into TVAs. As before small vesicles were seen within 35 minutes and at 55 minutes a larger structure appeared as indicated by the white arrow. This developed further into TVA at 2 hours indicating that TVAs can be formed from small vesicles through incorporation of pre-existing LC3. In figure 4.8 CHO eGFP-LC3 cells were incubated with Transfast in the presence of cycloheximide for 6 hours. As seen in the control experiments long tubules extended outwards in both directions from the centre of the structure, and eventually retracted back to the central structure. Taken together the results showed that TVA formation and tubulo-vesicular dynamics did not require continuous delivery of newly-synthesised LC3 from the cytoplasm.

The results suggested that TVAs form from the fusion of smaller eGFP-LC3 positive vesicles which are transported to the perinuclear region of the cell. It is possible that the tubular structures which extended from the centre of the TVAs are transported along components of the cytoskeleton, whilst remaining attached to the central structures. To determine if microtubules play a role in either the formation of the central structure or the tube-like elements, the experiments were repeated in the presence of nocodazole, a

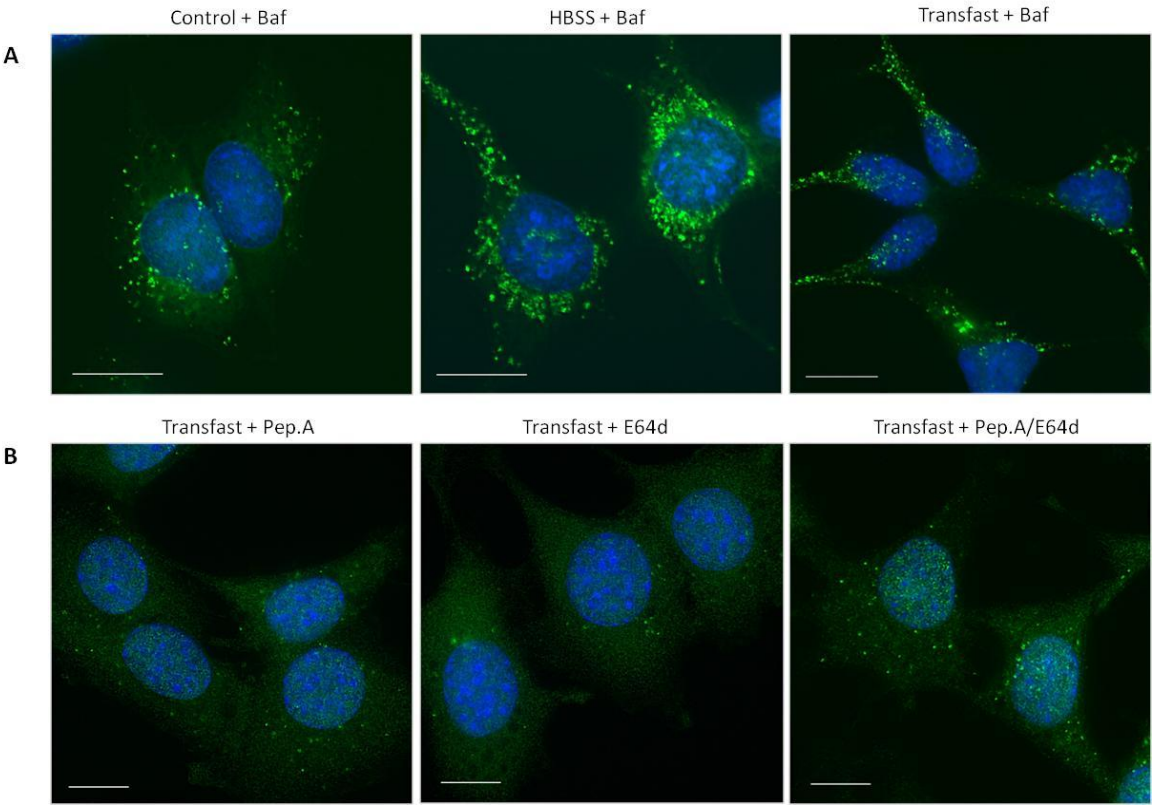

Figure 4.10 – Inhibitors of Lysosome Function Prevent the Formation of Tubulo-Vesicular Autophagosomes (TVAs) – HEK 293 cells stably expressing eGFP-LC3 (green) were grown on coverslips overnight prior to incubation. (A) HEK 293 cells were incubated with 100 nM bafilomycin A1 in either complete nutrient medium as control, HBSS or with Transfast in OptiMEM. Cells were fixed at 4 hours and nuclei stained with DAPI (blue). MEF cells (B) were grown on coverslips overnight and incubated for 4 hours with Transfast in OptiMEM the presence of 150 µM pepstatin A, 30 µM E64d or both 150 µM pepstatin A, 30 µM E64d. Cells were fixed and stained using an anti-LC3 antibody (Alexafluor 488, green) and the nuclei stained with DAPI. Bar is 10 µm.

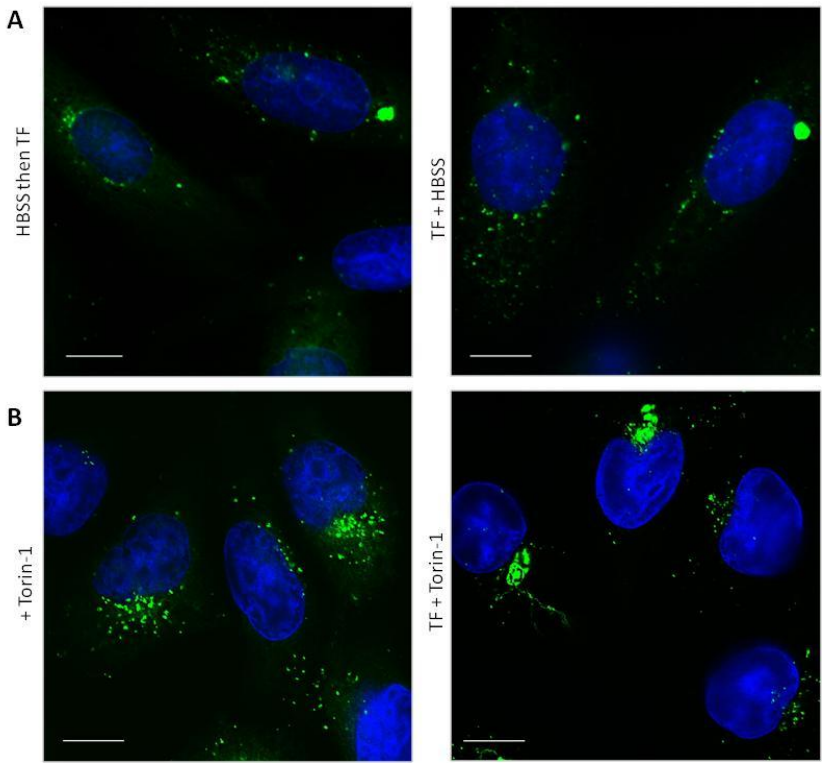

Figure 4.11 – Induction of Autophagy by Starvation or with Torin-1 Does Not Prevent Tubulo-Vesicular Autophagosomes (TVAs) Formation - CHO cells stably expressing eGFP-LC3 (green) were cultured overnight on coverslips. Cells were subsequently pre-incubated in HBSS for 1 hour followed by incubation with Transfast for a further 3 hours (A – left panel) or were incubated simultaneously in HBSS containing Transfast for 4 hours (A – right panel). In panels B, cells were incubated with 250 nM torin-1 in complete media for 4 hours (B- left panel) or with torin-1 and Transfast (B – right panel) for 4 hours. Cells were fixed and the nuclei stained with DAPI (blue). Bar is 10 µm.

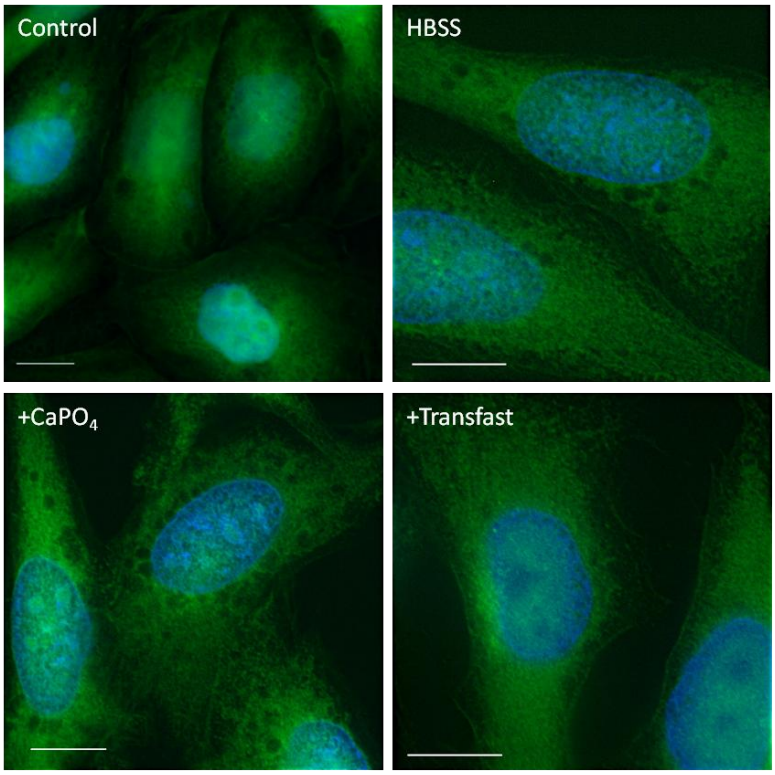

Figure 4.12 – Recruitment of LC3 to Tubulo-Vesicular Autophagosomes (TVAs) Requires Lipidation of LC3 - CHO cells stably expressing the mutant eGFP-LC3G120A were cultured overnight on glass coverslips. Cells were incubated in complete nutrient media (control) starved by transfer to HBSS (HBSS), or incubated with calcium phosphate ($CaPO_4$) or Transfast for 4 hours before fixation. Nuclei were stained with DAPI (blue). Bar is 10 µm.

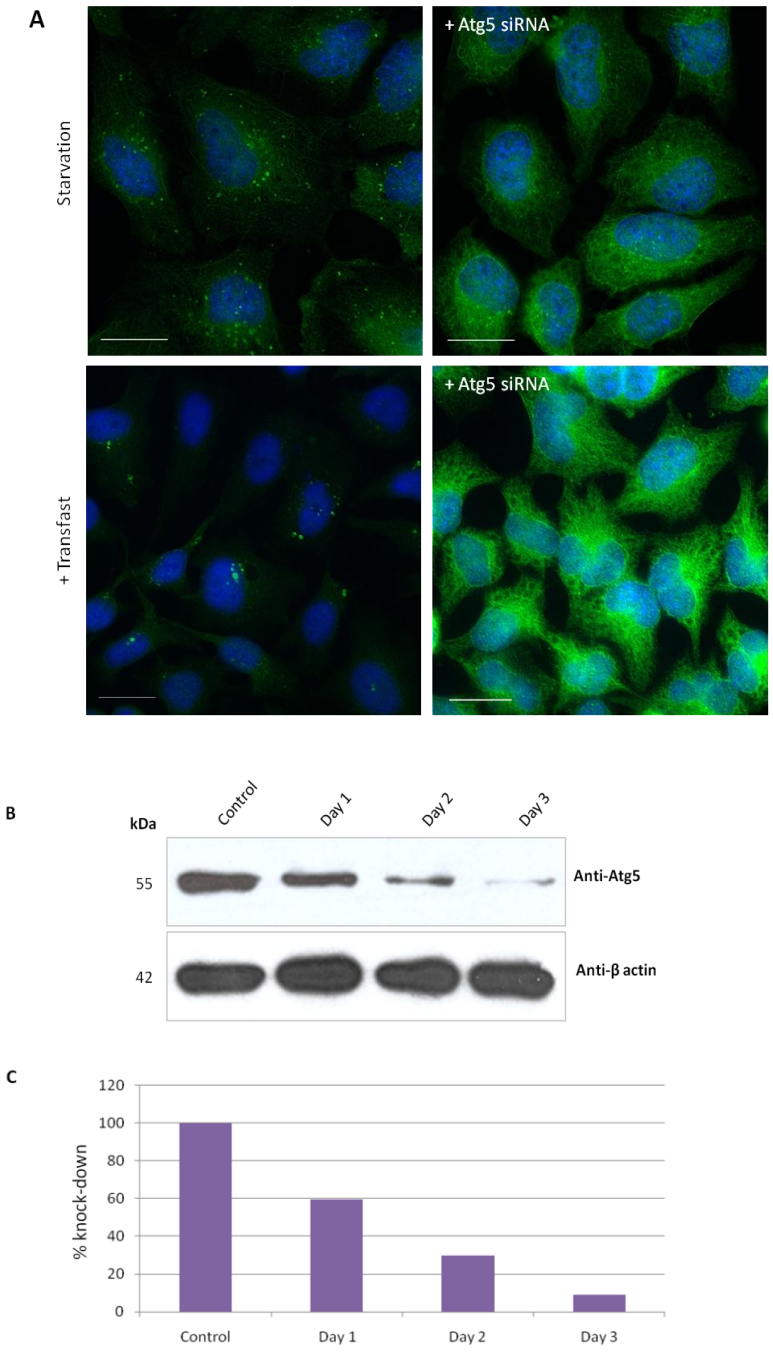

Figure 4.13 – Formation of Tubulo-Vesicular Autophagosomes (TVAs) requires Atg5 - HeLa cells were transfected with oligonucleotides siRNA specific for Atg5 using Lipofectamine 2000 and were further cultured and assayed at the time points stated to determine level of Atg5 knock-down. (Panel B) Control cells (left) or cells incubated with siRNA for Atg5 for 72 hours (Atg5 siRNA) were starved by transfer to HBSS media (top of panel) or incubated with Transfast (bottom of panel) for 4 hours prior to fixation in 100% methanol. Cells were stained using antibodies specific for LC3 (green) and the nuclei with DAPI (blue). Bar is 10 µm. Cell lysates were separated by SDS-PAGE and analysed by Western blot using antibodies specific for Atg5, or β-actin followed by a chemiluminescent detection with a secondary antibodies conjugated to HRP. (Panel C) Densitometric analysis of Western blots was used to calculate Atg5 expression normalised to actin.

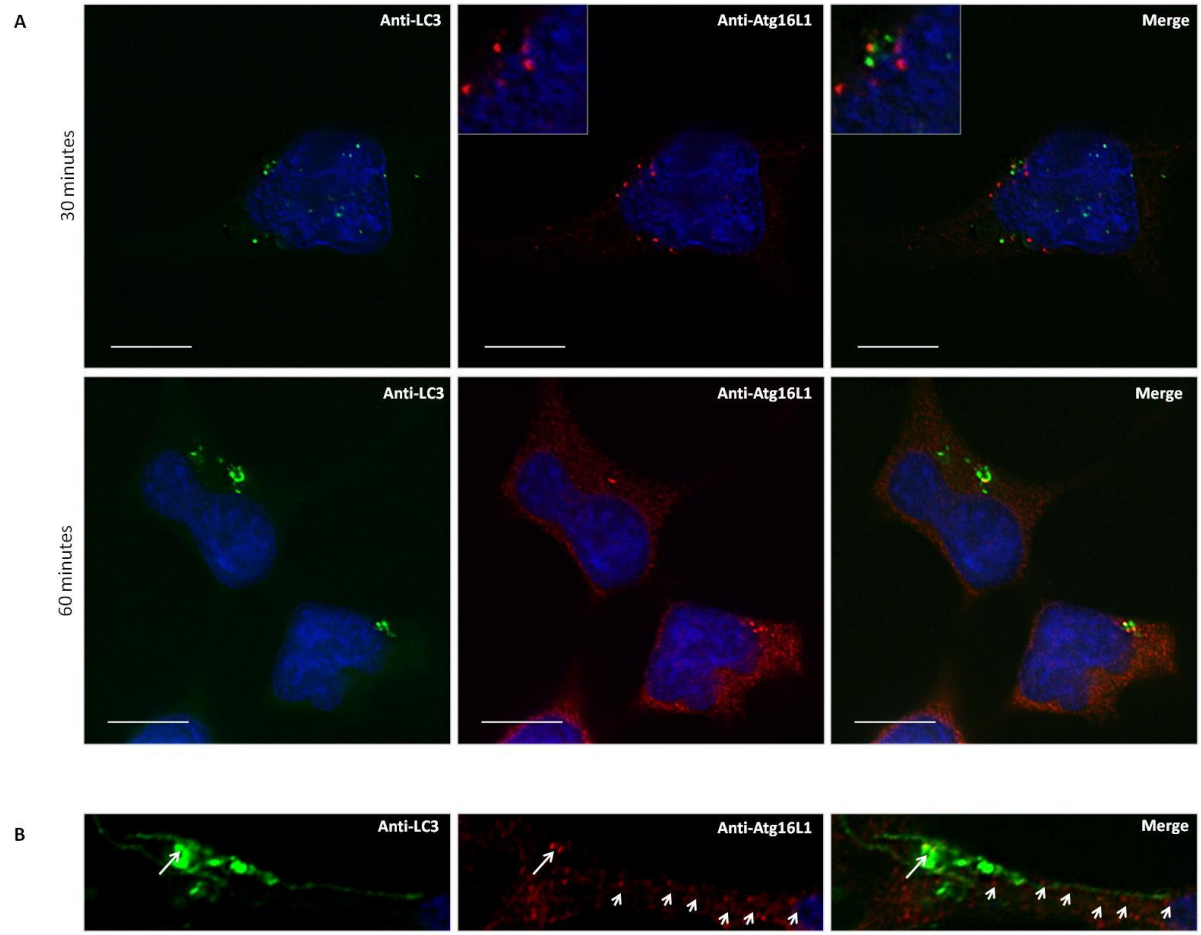

Figure 4.14 – Atg16L1 Is Partially Recruited During Tubulo-Vesicular Autophagosomes (TVAs) Formation – HEK-293 stably expressing GFP-LC3 (green) were cultured overnight on coverslips prior to incubation with Transfast in OptiMEM. Cells were subsequently fixed at 30 minutes and 60 minutes, and stained with anti-Atg16L1 antibody (red) and the nuclei with DAPI (blue). White arrows indicate the central TVA structure, whilst the arrow heads indicate Atg16L1 positive vesicles. Bar is 10 µm.

microtubule depolymerisation drug. Figure 4.9A shows the distribution of microtubules in CHO eGFP-LC3 cells which have been incubated with Transfast. Intact microtubules (red) are clearly visible, as are the tubular elements containing GFP-LC3 extending from the TVA. Following treatment with nocodazole (panel B) intact microtubules were lost, and there were still several large LC3-positive structures. The structures showed loss of interconnecting tubules and were less concentrated in the perinuclear region. The result showed that formation of large vesicular structures containing LC3 structures does not require intact microtubules; however the accumulation of TVAs in the perinuclear region and the formation of the tubular elements was dependent on microtubules.

4.3.4 Inhibition of Lysosome Function with Bafilomycin A, E64d and Pepstatin A Prevented the Formation of TVAs -

Studies on canonical autophagy show that autophagosomes formed in response to starvation fuse with lysosomes resulting in degradation of LC3. Degradation of LC3 can be stopped with bafilomycin A1 which raises lysosomal pH by preventing acidification by inhibiting vacuolar-type H^+ ATPase (V-ATPases). In figure 4.10, HEK 293 cells expressing eGFP-LC3 were incubated with bafilomycin A1. In control cells LC3-positive autophagosomes were visible in the cytoplasm even in complete media. These most likely represented autophagosomes generated through basal autophagy. When the cells were starved in the presence of bafilomycin A1 large numbers of GFP-LC3 punctae were seen in the cytoplasm. Interestingly, when bafilomycin was added to cells incubated with Transfast the TVAs failed to form. Instead small GFP-positive vesicles accumulated in the cytoplasm, similar to cells which have been starved. Similarly, other compounds such as E64d and pepstatin which inhibit the degradative function of lysosomes had a similar effect. When added either alone or together they prevented the formation of TVAs (figure 4.10C). Taken together these results indicated that formation of the large TVAs in the perinuclear region required functional lysosomes that are able to degrade substrates.

Figure 4.11 shows CHO eGFP-LC3 incubated with Transfast in starvation media and also in the presence of torin-1. Torin-1 activates the autophagy pathway through inhibition of the mTORC1 complex. Autophagy stimulation can occur prior to incubation with liposomes in starvation media alone (A – left panel), or during incubation in starvation

media and liposomes (A – right panel) and both the TVAs and the punctate autophagosomes formed and indicated that no competition between the formation of the structures. This was also true with torin-1, in control cells punctate autophagosomes formed (B-left panel). Incubation with Transfast and torin-1 in OptiMEM (B – right panel) also formed TVAs and punctate structures.

4.3.5 Recruitment of LC3 in TVAs Requires LC3-II Processing Atg5 and Atg16

The previous results showed that LC3 is redistributed in response to incubation with transfection reagents. The next experiments were conducted to see if recruitment of LC3 to TVAs required LC3 processing and attachment of PE. To determine if LC3 processing from the LC3-I to LC3-II was required for the formation of TVAs, CHO cells stably expressing the mutant form of LC3 which cannot be lipidated, GFP-LC3G120A, were incubated with either calcium phosphate precipitate or Transfast. Figure 4.12 shows that the mutation prevented incorporation of GFP-LC3 into autophagosomes during starvation (HBSS) or following incubation with calcium phosphate or Transfast.

The requirement of Atg5 in TVA formation was assessed by silencing of Atg5 with a mix of three Atg5 specific siRNA oligonucleotides. Panel A of figure 4.13 shows that after day three of silencing, cells were unable to produce GFP-LC3 punctae in response to starvation or TVAs following incubation with Transfast. The level of knock-down was assessed through Western blots using Atg5 specific antibodies the level of Atg5 detected in the sample was reduced to 10% of the control (panels B and C). The experiment was repeated using MEF cells from Atg $5^{-/-}$ mice and again cells were unable to form TVAs (data not shown). This indicates that Atg5 is required for the formation of TVAs.

Similarly, as Atg5 forms a complex with Atg12 and Atg16L1, the localisation of Atg16L1 was investigated. In starvation condition, Atg16L1 formed distinct punctae throughout the cytoplasm, some of which were positive for LC3 (data not shown). In figure 4.14 panels A, Atg16L1 positive, LC3-positive puncta are formed at 30 minutes post-incubation with cationic liposomes, and at 60 minutes these have formed larger TVAs. There was not complete colocalisation of Atg16L1 with LC3, suggesting that although recruitment of Atg16L1 to TVAs is seen it was a transient association. Similarly, in panels B, the central structure of the TVA was positive for Atg16L1, but the tubular extension were not. There

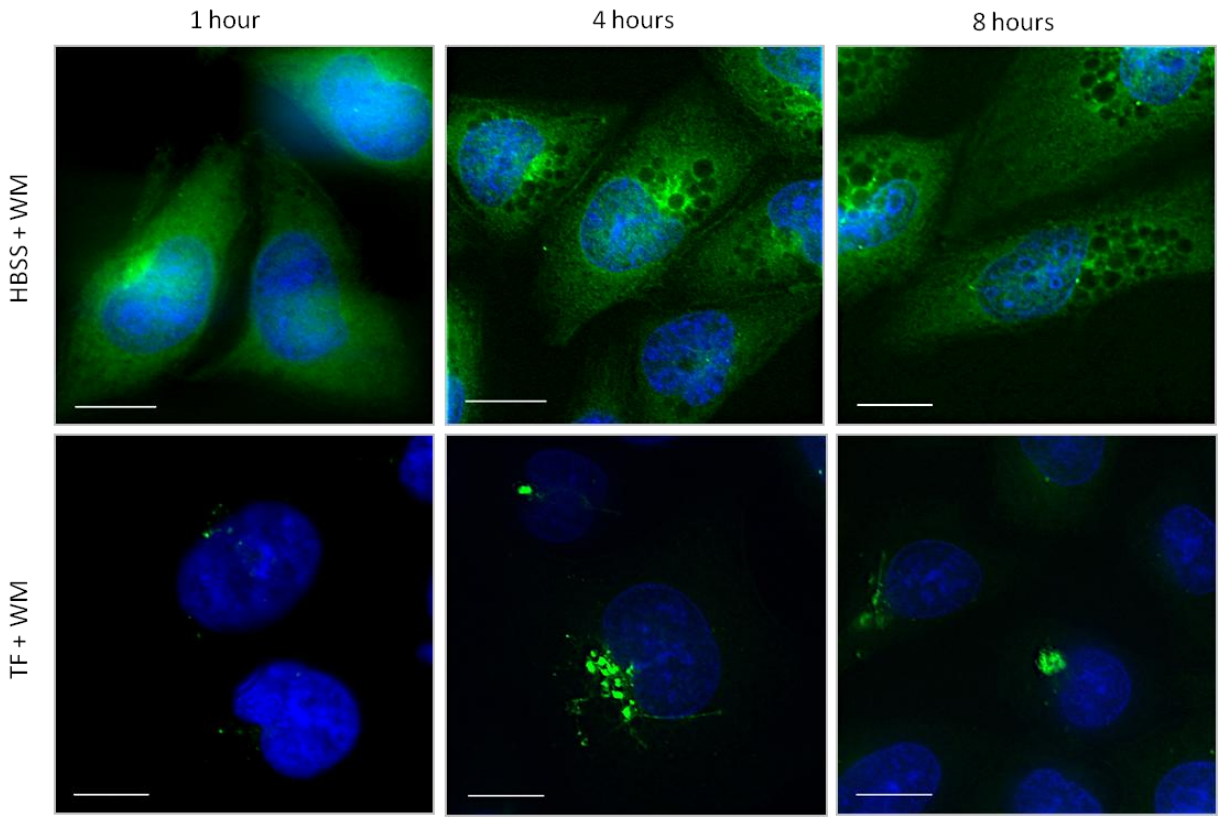

Figure 4.15 – Wortmannin Inhibits the Formation of Autophagosomes but Not Tubulo-Vesicular Autophagosomes (TVAs) - CHO cells stably expressing eGFP-LC3 (green) were grown on coverslips for 24 hours prior to incubation with 10 nM wortmannin in either HBSS or with Transfast in OptiMEM. Cells were fixed and nuclei stained with DAPI (blue) Bar is 10 µm.

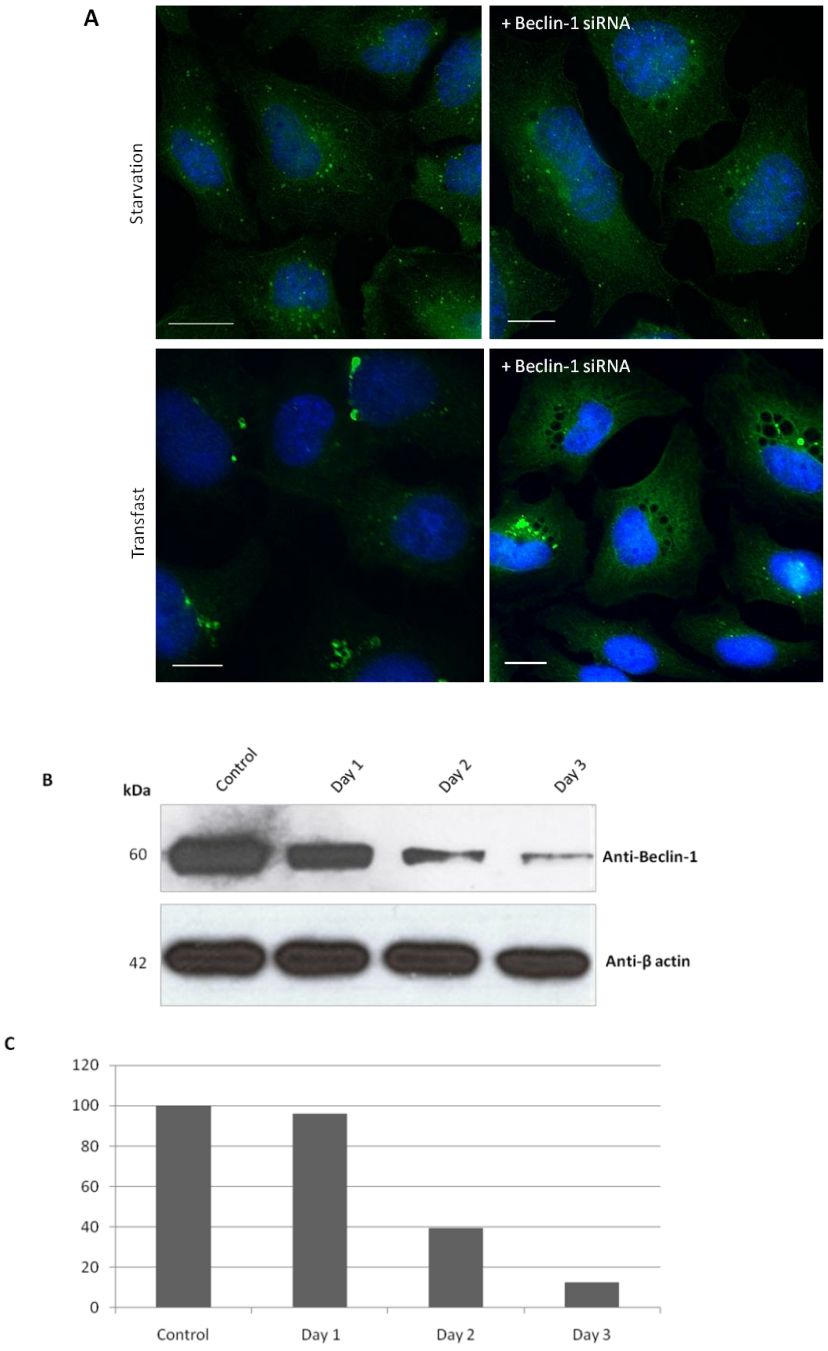

Figure 4.16 – siRNA Knock-Down of Beclin-1 Did Not Prevent the Formation Tubulo-Vesicular Autophagosomes (TVAs) – HeLa cells were transfected with siRNA oligos specific for beclin-1 using Lipofectamine 2000 and were further cultured and assayed at the time points stated to determine level of knock-down. (A) Coverslips were treated with siRNA for beclin-1 for 72 hours prior to fixation in 100% methanol and stained with anti-LC3 (green) and the nuclei with DAPI (blue). Bar is 10 µm. (B) Western blot of cell lysates from beclin-1 silencing, as show in A, were ran on a 12% gel and blotted for anti-beclin-1 followed by a chemiluminescent detection with a secondary HRP conjugate. (C) The percentage of protein knock-down after transfection with siRNA which has been normalised to actin.

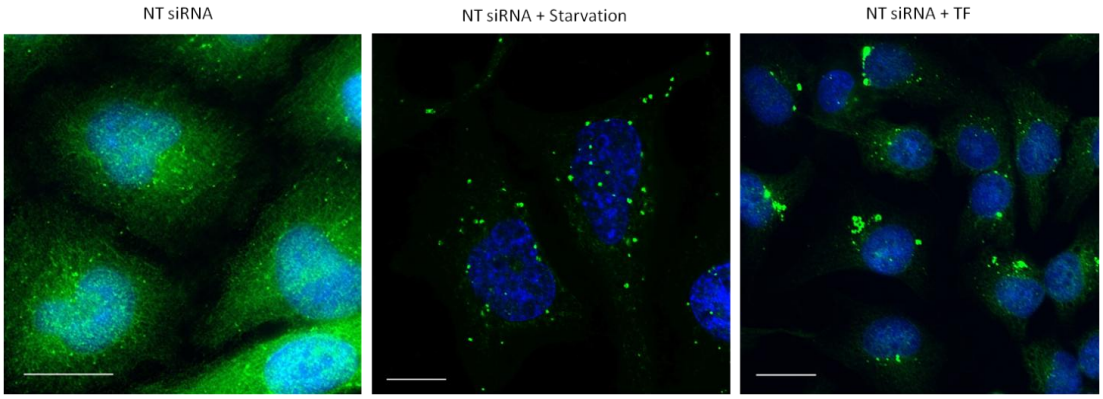

Figure 4.17 – Control siRNA Transfection with Non-Targeting (NT) Did Not Interfere with LC3 Localisation – HeLa cells were transfected with NT siRNA oligos Lipofectamine 2000 and were further cultured for 72 hours followed by fixation. Coverslips were stained with anti-LC3 (green) and the nuclei with DAPI (blue). Bar is 10 µm.

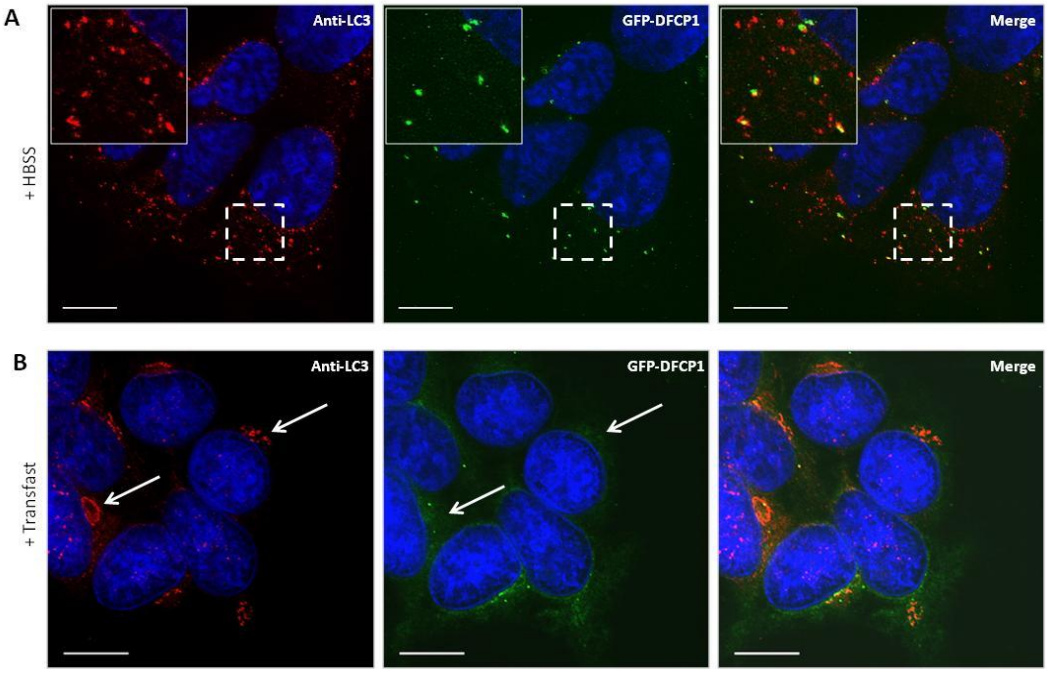

Figure 4.18 – DFCP1, a PI(3)P binding protein, Is Recruited During Autophagosome Formation But Not During Tubulo-Vesicular Autophagosomes (TVAs) Formation – HEK-293 stably expressing the plasmid containing GFP-DFCP1 (green) were cultured overnight on coverslips prior to 2 hours in HBSS (A) or with Tranfast transfection reagent in OptiMEM (B). Cells were subsequently fixed and stained with anti-LC3 antibody (red) and the nuclei with DAPI (blue). Bar is 10 µm.

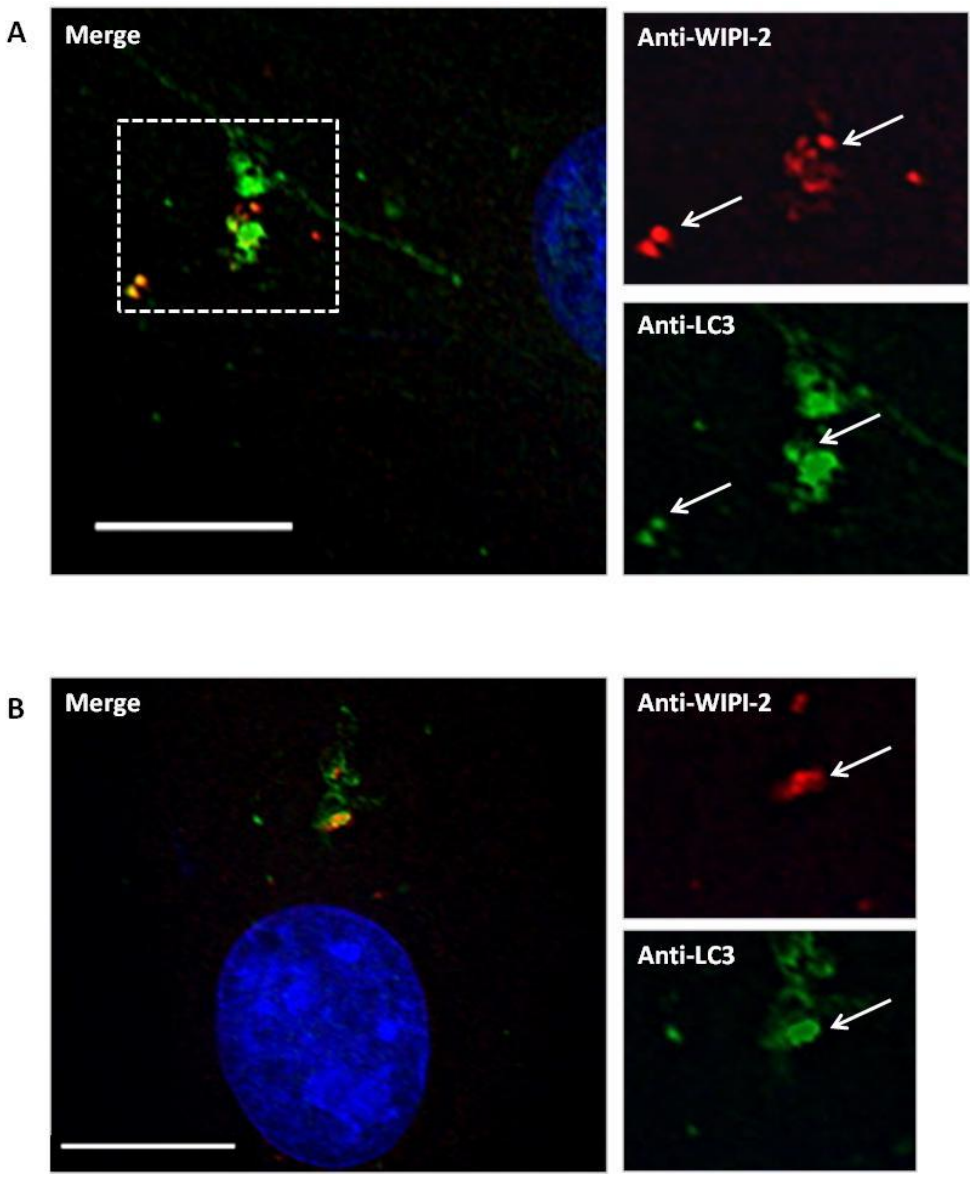

Figure 4.19 – WIPI-2 is Recruited During Tubulo-Vesicular Autophagosomes (TVAs) Formation and During Incubation with Wortmannin – Vero cells were cultured overnight on coverslips prior to 1 hour incubation with Tranfast cationic liposomes in OptiMEM (A). Vero cells in (B) were pre-treated for 30 minutes with 10 nM wortmannin, prior to 1 hour incubation with Transfast in OptiMEM. Cells were subsequently fixed and stained with anti-LC3 antibody (green) and anti-WIPI-2 (red) and the nuclei with DAPI (blue). Bar is 10 µm.

were, however, some Atg16L1 vesicles close to the LC3-positive tubule, as indicated by the arrow heads, indicating a possible role in their formation.

4.3.6 The Formation of TVAs Does Not Require PI-3 Kinase -

To determine if PI-3 kinase signalling was required for the generation of the TVAs, cells were incubated with wortmannin which is an inhibitor of PI-3 kinase signalling. Figure 4.15 compares the effect of wortmannin on the response of CHO eGFP-LC3 cells to starvation or cationic liposomes. The top panels show that wortmannin prevents formation of LC3 punctae in response to starvation. The bottom panels show that wortmannin does not prevent the formation of TVAs. TVAs were present in the cytoplasm at 1 hour after addition of liposomes and remained at 4 and 8 hours. This indicated that the formation of TVAs did not require PI-3 kinase signalling. To investigate if beclin-1, a component of the PI-3 kinase core machinery in autophagosome formation, was required for TVA formation, silencing of beclin-1 was performed with a mix of three specific siRNA oligos. The level of knock-down was assessed as described before, through Western blots, and the response of cells to starvation was used to determine if silencing prevented formation of eGFP-LC3 punctae. Figure 4.16C shows that protein levels were reduced to 20% after three days, and panel A shows that small number of eGFP-LC3 punctae still formed. The knock-down of beclin-1 reduced autophagosome formation but was not sufficient to completely prevent autophagy in response to starvation. Knock-down of beclin-1 did not have any noticeable effects on TVA formation. As a control to confirm that the process of siRNA transfection was not redistributing LC3 or prevented it from its normal function, the process of siRNA transfection was repeated with non-targeted (NT) siRNA, which had no homology to any mammalian mRNA was used, as shown in figure 4.17. The panels showed a normal cytoplasmic distribution under normal growth media, redistribution to punctate structures in HBSS and the formation of TVAs when incubated with liposomes. This indicated that the process was not interfering with LC3 localisation or redistribution.

Figure 4.18 investigated if generation of PI(3)P occurring during TVA formation. A HEK 293 cell line stably expressing a marker for PI(3)P generation known a double-FYVE (Fab1, YOTB, Vac 1 and EEA1) containing protein-1 (GFP-DFCP1) was used. Panel A shows cells starved with HBSS and counterstained in red for endogenous LC3 positive punctae

formed after one hour and some colocalise with GFP-DFCP1, as highlighted by the white square region of interest. Studies by Axe *et al* (2008) have shown that the population of green only punctae (GFP-DFCP1) represent omegasomes formed from the ER following activation of PI 3-kinase activity. Double positive structures represent omegasomes that have recruited LC3 while red only vesicles (endogenous LC3) are mature autophagosomes that have left the site of formation after phagophore closure. Panel B shows cells 1 hour after incubation with Transfast. The TVAs formed as seen by the rearrangement of endogenous LC3 (red) in the perinuclear region, however there was no localisation of GFP-DFCP1 to these structures. Some DFCP1 vesicles were formed in the cells however the majority remained spread through the cytoplasm and were not recruited to perinuclear structures. Given this, and the previous data with wortmannin, it can be concluded that TVA formation was PI 3-kinase independent.

Similarly, another protein that is recruited to the site of autophagosome formation in a PI(3)P dependent manner is WD repeat domain phosphoinositide-interacting protein 2 (WIPI-2). During autophagy induction, this formed distinct punctae in the cytoplasm, some of which colocalised with LC3 (data not shown). The inhibition of PI-3 kinase Vps34 with wortmannin prevented either WIPI-2 or LC3 positive punctae from forming (data not shown). An approach was taken to see if WIPI-2 is recruited to TVA formation, and if this can be prevented by incubation with wortmannin. As indicated by figure 4.19 panels A, WIPI-2 is recruited to the central structure of TVAs, but not the tubules. In the presence of wortmannin, panels B, WIPI-2 is still present on TVAs, indicating that generation of PI(3)P is not necessary for its attachment to LC3-positive structures generated in response to cationic liposomes.

4.3.7 p62 is Recruited to TVAs

An alternative marker to LC3 used to identify autophagy is p62 and this binds LC3 and becomes localised to the autophagosomes during starvation as shown in chapter 3 figure 3.3. The next experiment investigated if p62 redistributed to TVAs formed in the presence of cationic liposomes (Figure 14.20). Panel A follows immunostaining of endogenous p62 in MEF cells over time following the addition of Transfast. Panel B compares the distribution of endogenous LC3 and p62 in the TVAs. Cationic liposomes

caused p62 to be recruited to TVAs labelled with LC3. Recruitment of p62 to autophagosomes in response to starvation resulted in the degradation of p62. Western blots were therefore performed to see if recruitment of p62 to TVAs in response to cationic liposomes also caused degradation of p62. Figure 4.20C shows that the levels of p62 increased after one hour of starvation but then decreased over 8 hours. Levels of p62 increased following incubation with Transfast and remained high suggesting that incorporation into TVAs does not result in degradation through autophagy. p62 is known to interact with ubiquitin and can be incorporated into autophagosomes. The presence of ubiquitin in TVAs was examined and the distribution of ubiquitin is shown in figure 4.21 in both control cells in complete media, and those incubated with Transfast. It was not possible to see a signal for ubiquitin or TVA in cells in normal growth conditions figure 4.21A). Interestingly, during incubation with Transfast (4.21B), the central structure of the TVA was positive for ubiquitin, however ubiquitin was excluded from the tubular elements.

4.3.8 Increase in the Size of Lysosomes During Incubation with Liposomes

Autophagosomes fuse with lysosomes and the content is degraded. eGFP is not stable in acidic conditions and the GFP signal is lost when autophagosomes and/or lysosomes acidify. The relationship between TVAs and lysosomes was investigated by immunostaining for LAMP1. At 24 hours post incubation with Transfast (figure 4.22A), a large TVA structure formed in the perinuclear region of the cell. This cell also had a number of larger LAMP1-positive lysosomes, as indicated by the white arrows. These lysosomes were larger than lysosomes in the neighbouring cells which did not have TVAs. Panel B shows 48 hours post-incubation. At this time TVAs are reduced in number and fragments indicated by LC3-positive vesicles were seen associated with LAMP positive structures. Interestingly, all the cells with TVA LC3 positive fragments showed pronounced swelling of lysosomes.

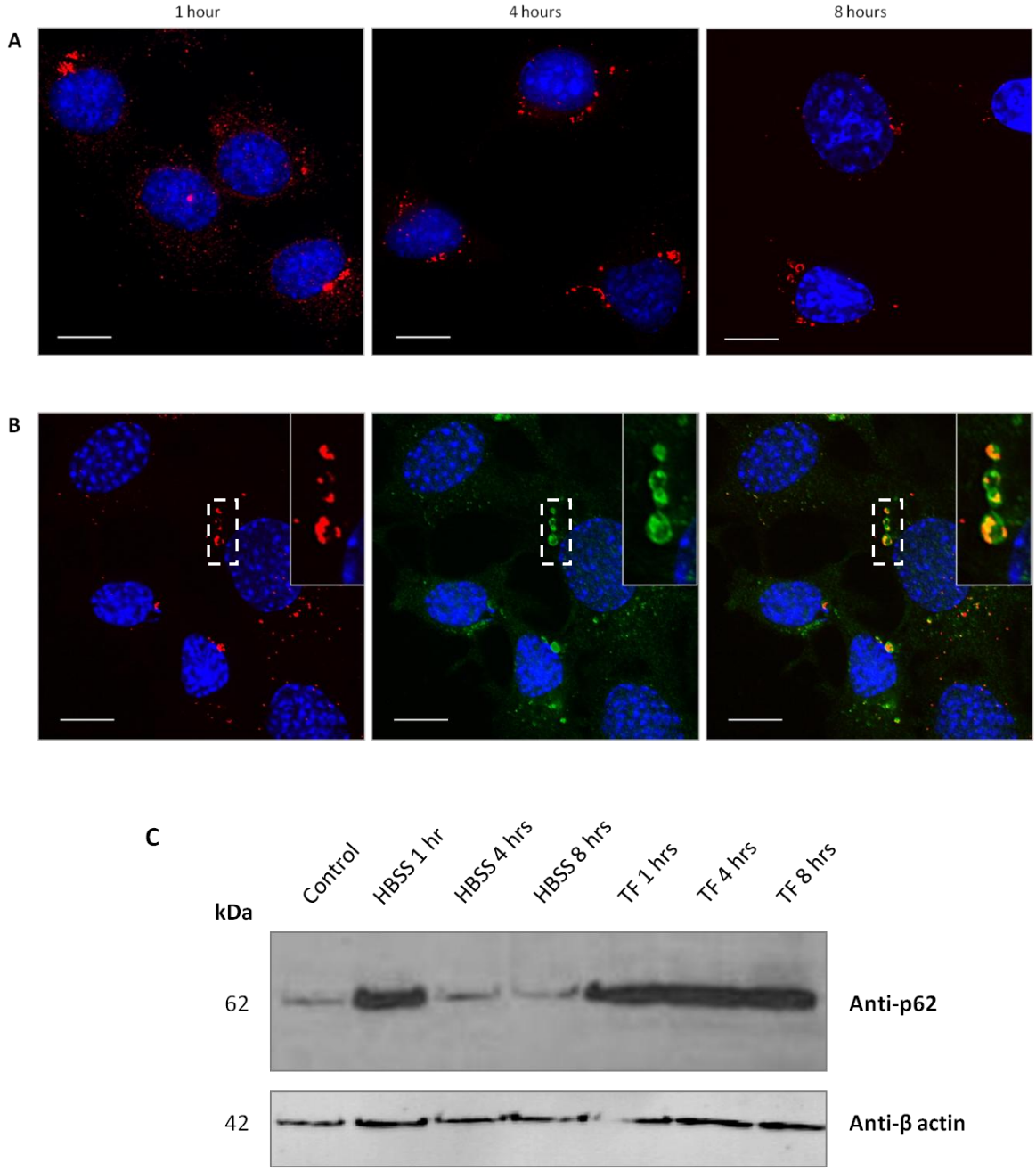

Figure 4.20 – Recruitment of p62 to Tubulo-Vesicular Autophagosomes (TVAs) During Incubation with Liposomes and Colocalisation with LC3 - MEF cells were cultured overnight on glass coverslips. Cells were incubated with Transfast for the time points stated before fixation (A), and stained using an anti-p62 antibody (red) and the nuclei with DAPI (blue). MEF cells were treated as above, and fixed at 4 hours (B) and stained using an anti-LC3 (green) and anti-p62 (red). Bar is 10 µm. 293 eGFP-LC3 cells were incubated with Transfast for the time points stated before lysis (C) ran on a 12% gel and blotted for anti-p62 followed by a chemiluminescent detection with a secondary HRP conjugate. Blots were stripped and subsequently reblotted for β-actin.

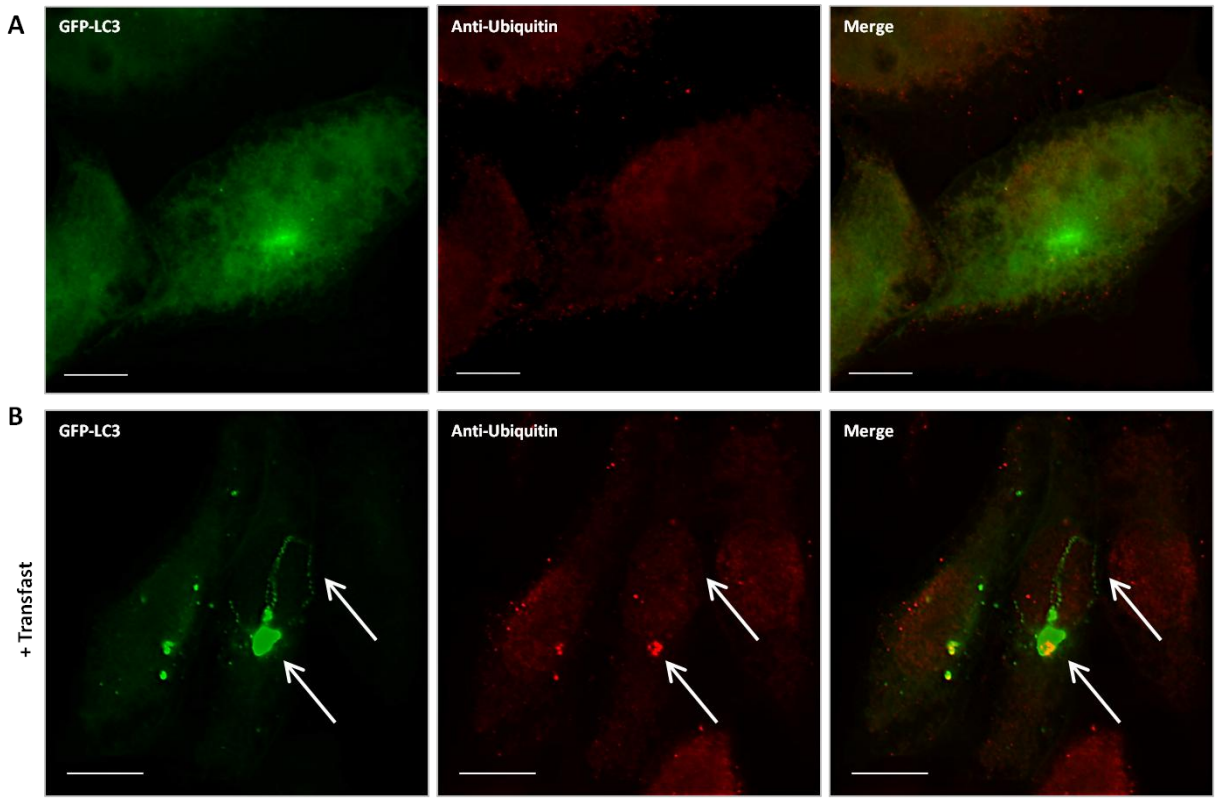

Figure 4.21 – The Centres of Tubulo-Vesicular Autophagosomes (TVAs) Contain Ubiquitin but Ubiquitin is Excluded from the Tubules - CHO cells stably expressing eGFP-LC3 (green) were in full media (A) or treated Transfast (B) for 4 hours before fixation. Cells were stained using an anti-ubiquitin (red). Bar is 10 µm.

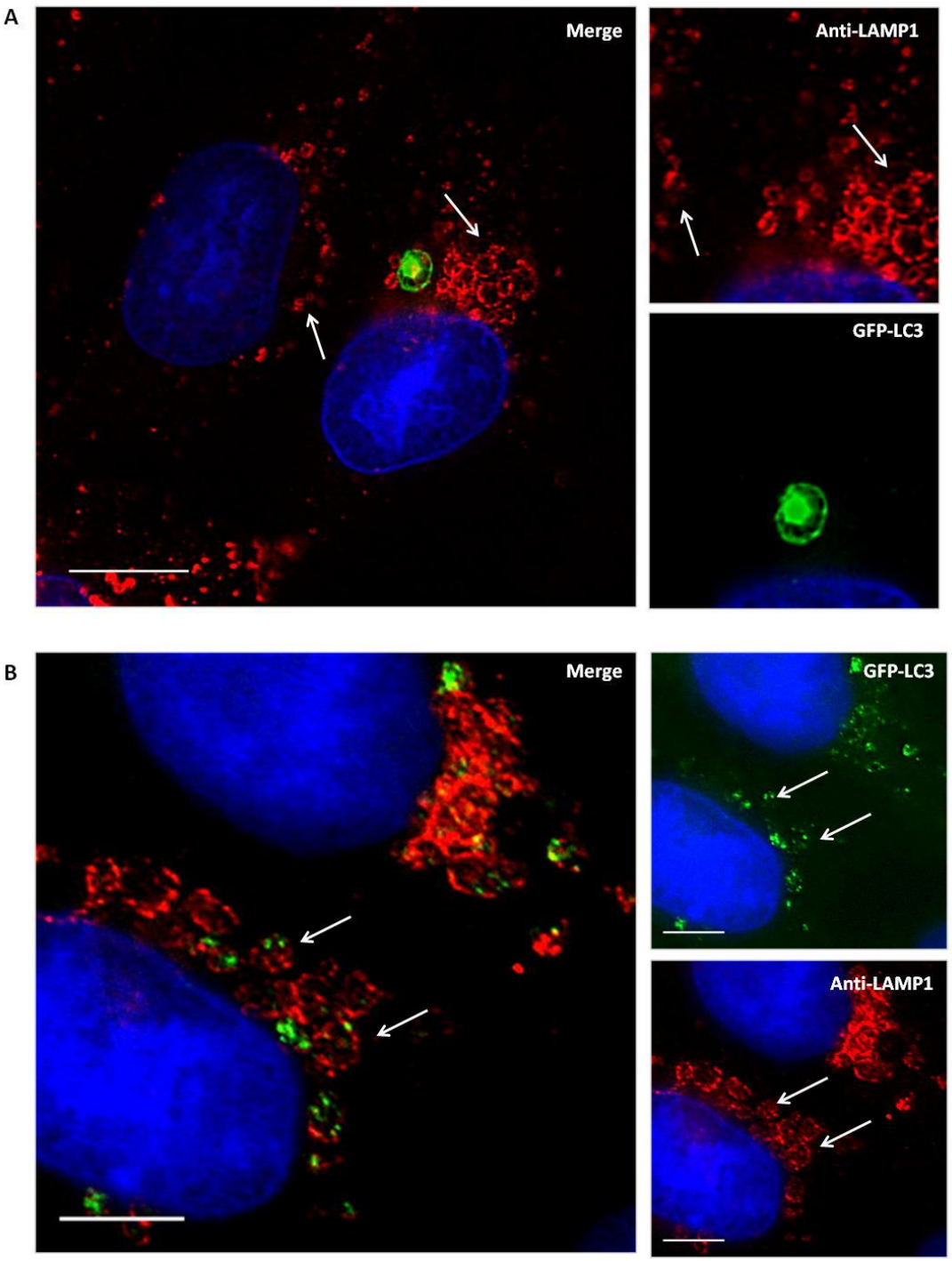

Figure 4.22 – Delayed Degradation of Tubulo-Vesicular Autophagosomes (TVAs) in Lysosomes Results in Swelling of Lysosomes - CHO cells stably expressing eGFP-LC3 (green) were grown on coverslips for 24 hours prior to incubation with Transfast in OptiMEM for 8 hours. Cells were washed and the media replaced with complete media at 8 hours. Cells were fixed at 24 hours (A) and 48 hours (B) post-incubation with Transfast and stained with an anti-LAMP1 antibody (red) and the nuclei stained with DAPI (blue) Bar is 10 µm.

4.4 Discussion

This chapter has demonstrated that incubation of cells with non-viral DNA delivery vectors such as cationic liposomes induced the redistribution of LC3 into large tubular-vesicular autophagosomes (TVAs). Initial visualisation of the morphology of the TVAs indicated they are much larger than the punctate autophagosomes seen during starvation, and also the TVAs rapidly changed shape over time. Observations at early times after addition of cationic liposomes showed that these large tubulo-vesicular structures formed from small punctate vesicles that resembled canonical autophagosomes. However, we also identified a network of tubular structures that were not usually seen during autophagosome formation in response to starvation. TVAs were induced by a number of different transfection reagents indicating perhaps an innate response to non-viral DNA vectors.

The TVAs are dynamic and contained tubular elements which extended and retracted from central structures. The formation of TVAs was not affected by cycloheximide, and TVAs can form from pre-existing pools of LC3. Large structures could be observed to form by fusion of smaller structures, possibly involving connections involving tubules. Interestingly, the recruitment of GFP-LC3 to small early TVAs was unaffected by treatment with nocodazole and did not require intact microtubules. However, the tubular elements and accumulation at the perinuclear region was blocked by nocodazole indicating a role for microtubule transport and microtubule motor proteins such as dynein and kinesin. LC3 was originally identified as a protein that co-precipitates with the microtubule-associated proteins 1A and 1B (MAPs) which associate with microtubules and facilitate stability (Kabeya *et al* 2000). Autophagosome movement and the fusion with lysosomes is dependent on an intact microtubule network (Kimura *et al* 2008). It is possible that TVAs used the same mechanism of transport to move inside cells.

The TVAs recruited LC3 but they were not rapidly degraded by autophagy as they remained in the cytoplasm for up to 48 hours after formation. Generally the number of autophagosomes formed in response to starvation peaks between three to four hours and then numbers decrease as they fuse with lysosomes, and disappear (Mitchener *et al* 1976). The number of large TVAs in each cell was generally much lower than the number of autophagosomes generated by starvation, and at the later stages this is reduced to one

large perinuclear TVA. The reason for the large size is due to any new LC3 positive structures are incorporated into the pre-existing TVAs, and this might be a cellular response to sequester excessive aggregation of proteins into one region to do less damage to the cell. Recent studies into the nature and behaviour of liposomes in different environments has revealed a number of different morphologies the liposomes can take. Zidovska *et al* look at the differences in shape liposomes take in different pH and salt conditions, at pH 4 tubulation and multilamellar vesicles can form (Zidovska *et al* 2009). The change in pH during the trafficking of liposomes through the endocytic and/or the autophagy pathway might possibly result in the formation of the tubulo-vesicular structures that are positive for LC3 due to fusion of autophagosomes with endosome components to form amphisomes.

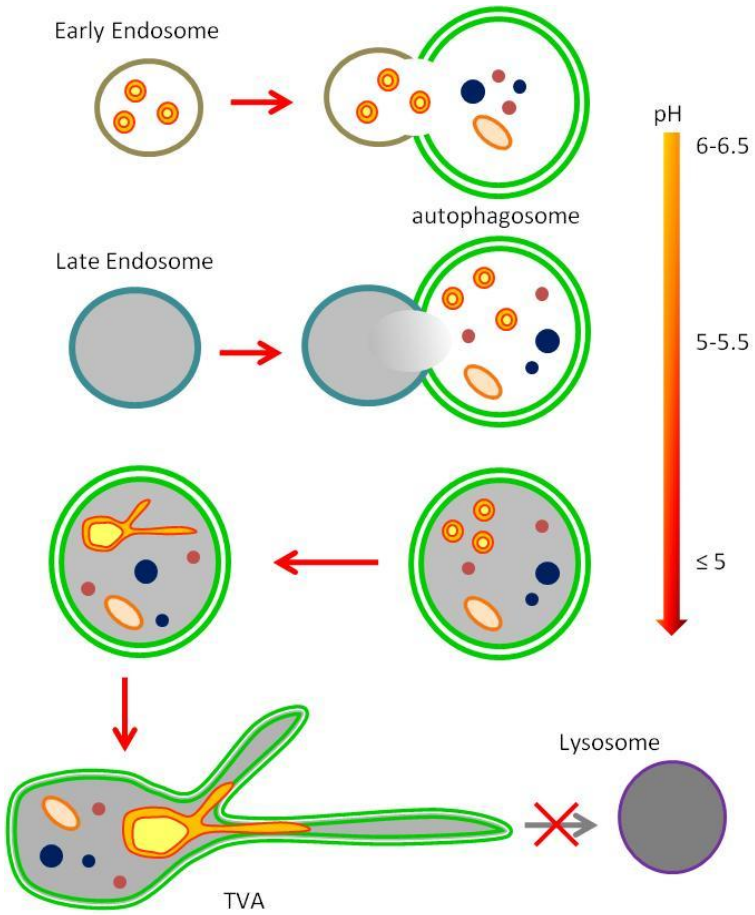

Figure 4.23 – Model of Increasing Acidification of Endolysosomal Vesicles Results in Cationic Liposome Tubulation

It is possible that the fusion of autophagosomes with late endosomes would lower the pH of the vesicle containing the liposomes and result in their tubulation. These tubulated structures could alter the morphology of autophagosomes and result in their

tubulation, and hinder attempts at degradation, as shown in figure 4.23. This would also account for the recruitment of LC3 to the TVAs.

Canonical autophagy is regulated by the class III PI-3 kinase, Vps34 and beclin-1. This complex phosphorylates phosphoinositol (PI) to form phosphoinositol 3-phosphate (PI(3)P) to nucleate the components required for autophagosome formation. Beclin-1 is an important regulator of this complex and plays an important role in the induction of autophagy. Experiments tested if beclin-1 and class III PI 3-kinase activity was required for the formation of TVAs. Interestingly, reduction of beclin-1 levels by siRNA silencing, and the use of wortmannin to block class III PI 3-kinase activity inhibited the formation of starvation-induced autophagosomes, but was unable to inhibit TVA formation. Recent studies show recruitment of Vps34-beclin-1 complex to the ER at the start of autophagosome formation (Axe *et al* 2008, Hayashi-Nishino *et al* 2009). Localised production of PI(3)P in the ER recruits DFCP1 and WIPI-2 which binds PI(3)P through FYVE domains. This means that sites of PI(3)P production can be visualised by redistribution of GFP-DFCP1 and WIPI-2 to punctae after starvation. However, when cells expressing GFP-DFCP1 were incubated with cationic liposomes the GFP-DFCP1 remained largely cytoplasmic. WIPI-2 did redistribute to punctae and to the larger TVAs in response to cationic liposomes. However, in the presence of wortmannin WIPI-2 was still localised to TVAs. This suggests again that TVAs do not require PI(3)P. It is, however, possible that generation of the PI(3)P for the development of TVAs may have a very rapid turnover and may not have been captured at the time point the cells were fixed. However, given the previous data set with the beclin-1 silencing and the wortmannin treatment it is likely that the TVAs do not use beclin-1 or the PI-3 kinase complex in the formation of the TVAs. Interestingly, it is thought the pool of PI(3)P recruits WIPI-2 to the forming membrane, but another protein is responsible for anchoring it there (Polson *et al* 2010). There is also evidence that WIPI-2 has a role in the lipidation of LC3 during autophagosome formation. During incubation with wortmannin where PI(3)P production cannot occur, WIPI-2 is still localised to TVAs. The data presented here reveals that perhaps an interaction with LC3 during the lipidation step may be responsible for the incorporation of WIPI-2 into TVAs.

There is recent evidence that there are PI(3)P independent routes to generate autophagosomes. VopQ is a type III secreted effector protein that is secreted into cells

during *Vibrio parahaemolytics* infection and induces a PI-3 kinase independent rearrangement of LC3 to the perinuclear region of cells (Burdette *et al* 2009). Similar results were reported in MCF-7 cells in response to resveratrol, where neither beclin-1 nor Vps34 were required for generation of autophagosomes (Scarlatti *et al* 2008). Both illustrate emerging roles for non-canonical autophagy in higher eukaryotes.

Activation of PI-3 kinase during starvation leads to the recruitment of the Atg5-Atg12-Atg16 complex to the pre-autophagosomal membrane and processing of LC3-I to LC3-II. During autophagosome formation the autophagy components Atg5, Atg12, Atg16L form a complex which is important for the location of LC3 to the membrane and also the maturation of the autophagosome (Hanada *et al* 2007). The lipidated LC3 (LC3-II) localises to a growing cup-shaped isolation membrane which closes to form a double membrane vesicle that fuses with lysosomes. The role played by Atg5 and LC3 lipidation in TVA formation was investigated using Atg5 silencing, Atg5-/- knock-out MEF cells and cells expressing eGFP-LC3G120A a mutant form of LC3 which cannot be lipidated. Silencing resulted in 90% knock-down of Atg5 in cells and this was sufficient to stop formation of autophagosomes during starvation. The loss of Atg5 also prevented the formation of TVAs. TVAs were also unable to recruit the G120A mutant of LC3. Taken together the results suggest that the recruitment of LC3 to TVAs is independent of PI-3 kinase activation but nevertheless required Atg5, most likely as part of the Atg5-Atg12-Atg16 complex and lipidation of the C-terminus of LC3.

The TVAs were much larger and longer-lived than autophagosomes induced by starvation. This could be explained if LC3-positive autophagosomes generated by cationic liposomes were resistant to degradation in lysosomes. LC3-positive autophagosomes would be drawn into close proximity with lysosomes by microtubule motor proteins and since they are not consumed by lysosomes they would be able to fuse with one another. The synthesis and recycling of lysosomes after fusion with autophagosomes is fundamental to autophagy. This is evident following incubation with bafilomycin A1 which inhibits lysosomal proteolysis and causes accumulation of autophagosomes in the cytoplasm. The effect of disrupting lysosome function on TVAs was therefore investigated. Surprisingly, TVAs did not form in cells incubated with bafilomycin A1, instead LC3 punctae were seen, much like autophagosomes generated during starvation. Bafilomycin A1 blocks the vacuolar ATPases that lead to the acidification of lysosomes. The result suggests that TVA formation needs

lysosomal acidification and/or active proteases within the organelle. Interestingly, both E64d and pepstatin A also prevented the formation of TVAs suggesting that formation of TVAs requires lysosomal proteolysis. The swelling of lysosomes observed following incubation with cationic liposomes also suggested that the transfection reagents may impede lysosome function.

A recent study by Yu *et al* (2010) has studied the mechanism of recycling of lysosome and autophagosome components after fusion of autophagosomes with lysosomes. Many lysosomes are consumed during autophagy because they form autolysosomes. Yu *et al* (2010) show that the lysosomal membrane tubulates in response to protein degradation in the lumen of the lysosome, as highlighted by figure 4.24. The tubules pinch off to form new vesicles called proto-lysosomes, which mature to form lysosomes. This process, which is termed autophagic lysosome reformation (ALR), is regulated by the mTOR kinase. It is thought that the TOR kinase can sense amino acids leaving the lysosome and activation of mTOR inhibits autophagy and promotes tubule formation to restore a full complement of lysosomes.

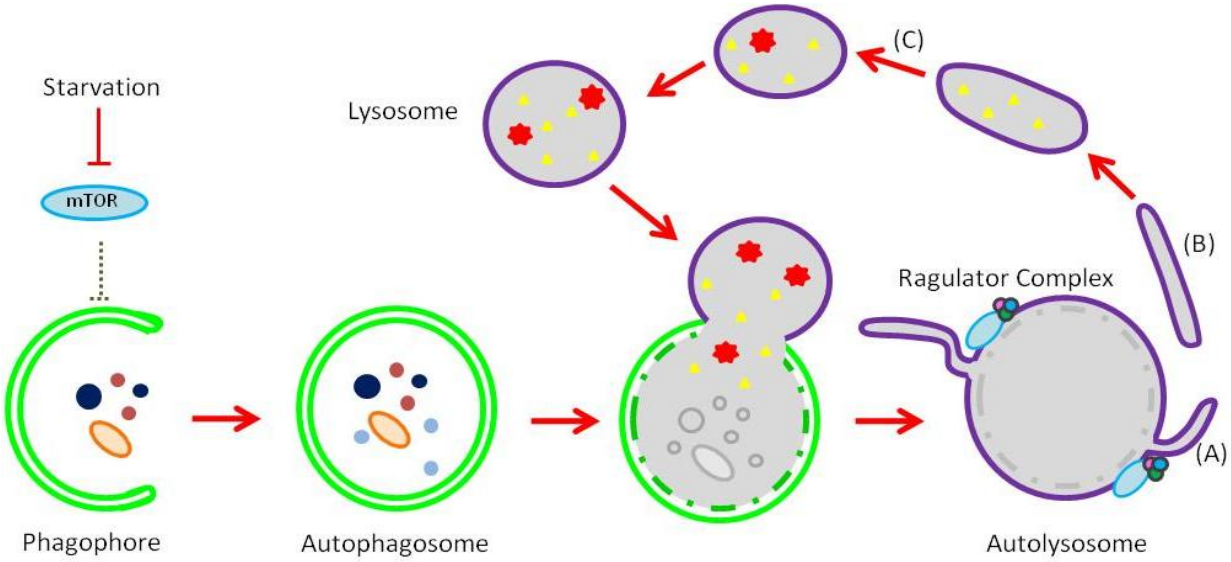

Figure 4.24 – Autophagic Lysosome Reformation (ALR) – during autophagy when autophagosomes fuse with lysosomes to form autolysosomes, the lysosomes must regenerate in order to degrade further material. Lysosome reformation occurs when mTOR which is initially inhibited during activation of autophagy and is relocalised to the lysosome by the Ragulator complex, senses the release of nutrients from lysosomes and becomes reactivated. This causes the tubulation of the autolysosome membrane (A) which pinch off (B) and mature (C) to become functional lysosomes, adapted from Yu *et al* (2010).

Yu *et al* (2010) show that at 4 hours post-starvation lysosomes and autophagosomes fuse to generate large LAMP1 and LC3 positive autolysosomes. At 8 hours post-starvation the large lysosomes generate LAMP1 positive tubules, whilst the LC3 signal remains with the vesicles and eventually returns to the cytoplasm. Our results showed that formation of TVAs also required degradation of protein in lysosomes making it possible that TVA formation is in some way linked to ALS and TOR signalling. Cationic liposomes also generated swollen lysosomes suggesting disruption of lysosome homeostasis with possibly a block in the formation of tubules. The role of TOR signalling was tested by adding torin1 to cells incubated with cationic liposomes however this did not prevent formation of TVAs. This results suggested mTOR independent mechanism for the tubulation. Further studies would be required to determine the location and activation of mTOR during TVA formation. It is possible the cationic liposomes are activating mTOR and causing a premature tubulation event. However, this does not explain the result from using torin-1 which inhibited the mTORC1 complex. During incubation with torin-1 and Transfast the TVAs still formed in the cytoplasm.

In this study the formation of tubulo-vesicular autophagosomes (TVAs) was investigated during the incubation of cells with a range of transfection available. The characterisation of these structures with respect to standard autophagosomes was also demonstrated some difficulty arose during the silencing of beclin-1 yet other techniques were used to verify the results. Similarly, silencing of Atg5 illustrated these structures are dependent on Atg5 for their formation. The investigation was largely based on using LC3 and p62 as markers for the structure, further investigation is required to see if other components are incorporated in the formation of TVAs.

Chapter 5:

Comparison of Tubulo-Vesicular Autophagosomes to Other Perinuclear Structures

Chapter 5 – Comparison of TVAs to Other Perinuclear Structures

5.1 Aims –

Tubulo-vesicular autophagosomes (TVAs) are clearly different from autophagosomes formed in response to starvation. The aim of this chapter is to compare the TVAs to other cellular structures induced by different types of stress that have been associated with LC3 and/or autophagy such as protein aggregates, dendritic cell aggresome-like structures/aggresome-like structures (DALIS/ALIS), lipid droplets and stress granules (SGs).

5.2 Introduction –

5.2.1 Lipid Droplets -

Autophagy is known to play a role in lipid metabolism and recent data indicate LC3 is associated with the formation of lipid droplets in cells during proliferation (Ohsaki *et al* 2006, Shibata *et al* 2009, 2010). Lipid droplets (LDs) are sites of lipid storage which are formed when lipids are in excess and can be used later as an energy store. Generally, excess fatty acids and cholesterol are stored as triacylglycerol and cholesterol esters, and can be released in a regulated manner as free fatty acids the fate of which depends on the cell energy requirements (Ducharme and Bickel 2008). LDs are the main cellular pool of lipids for energy storage and membrane synthesis. Specialised adipose tissue and adipocytes predominantly use this type of storage; however, non-specialised cell types can also store lipids in this way. LDs are composed of neutral lipid cores with a phospholipid monolayer, and are thought to emerge from a site in the ER, as depicted in figure 5.1 below. Research shows that knock-down of Atg7 or LC3 results in a reduction of triacylglycerol, and hence the formation of lipid droplets. LC3 forms large perinuclear structures in adipocytes during lipid droplet formation (Shibata *et al* 2010). Cationic liposomes are made from lipids making it possible that the additional uptake of lipid following fusion with liposomes could be promoting increased lipid storage and in the process recruiting LC3 to the site.

5.2.2 Aggresomes -

Aggresomes are formed when mis-folded or damaged proteins are not removed from the cell and begin to accumulate due to the degradative machinery being overwhelmed. As a part of a cytoprotective mechanism, the cell directs the protein aggregates to the perinuclear region of the cell via microtubules where they accumulate and increase in size if degradation does not occur, see figure 5.1 (Kopito 2000). Aggresomes contain proteins tagged with ubiquitin for degradation in the proteasome. Protein aggregates are, however, difficult to degrade and can overload the proteasomes and therefore remain in the cytoplasm. Vimentin is an intermediate filament which forms part of the cytoskeleton. During aggresome formation vimentin has been known to collapse and form a cage around the aggresome, to sequester protein aggregates and protect the cell from further damage (Garcia-Mata *et al* 1999). Ubiquitinated proteins are recognised by p62/seqestersome 1 which binds LC3, and these can be incorporated into autophagosomes, for degradation inside lysosomes.

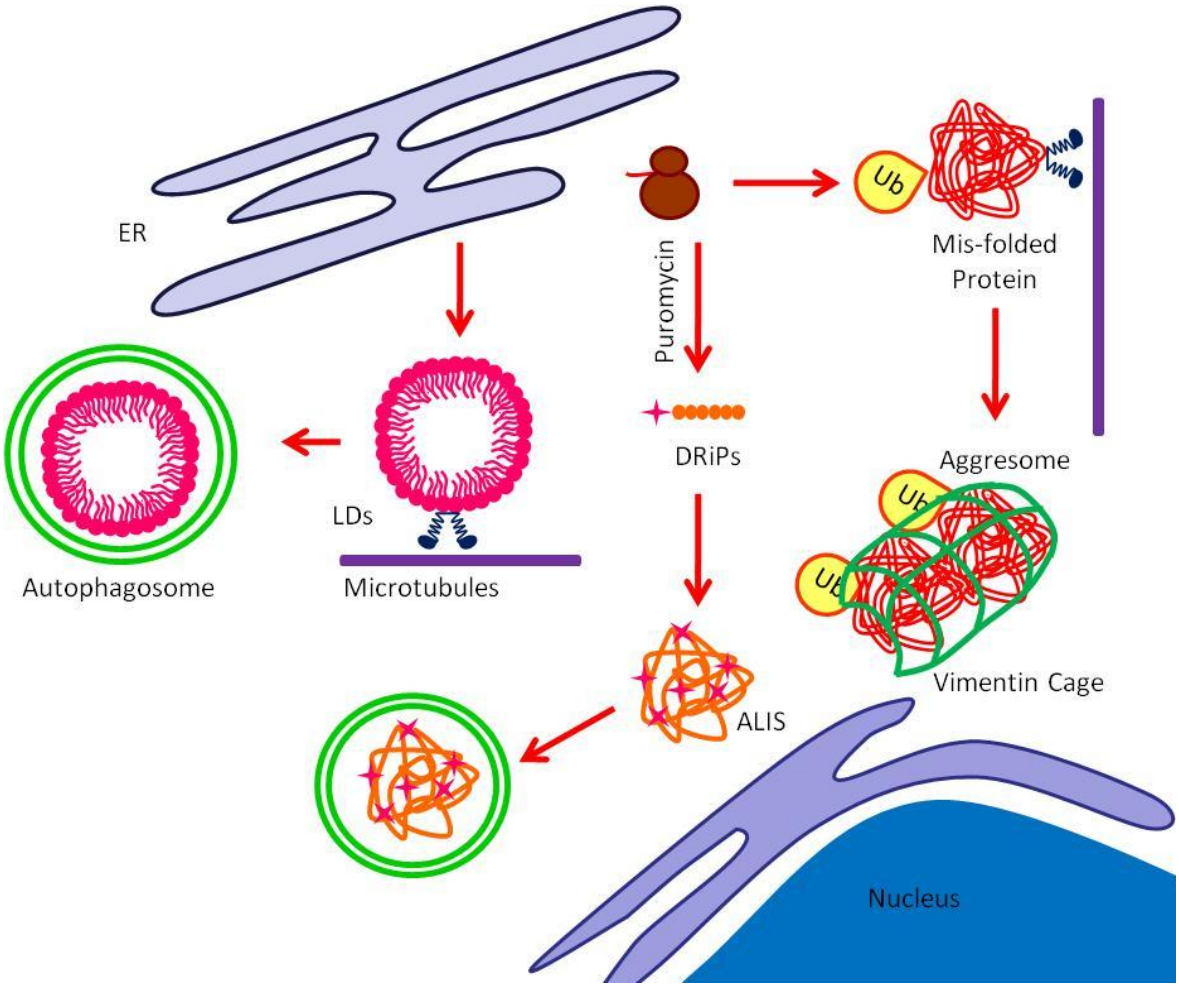

Figure 5.0 – Formation of LDs, ALIS and aggresomes in the perinuclear region of the cell – LDs derived from the ER use microtubules for transport within the cell and can be removed by autophagy. Puromycin-induced formation of DRiPs results in ALIS formation which are removed by autophagy (Szeto *et al* 2006). Aggresomes form as a result of improper protein translation and an accumulation of mis-folded proteins, the large perinuclear structures will have vimentin collapse around them.

5.2.3 DALIS/ALIS -

A similar structure which was first identified in dendritic cells (DC) is termed DC aggresome-like structure (DALIS) which forms during DC maturation. DALIS stores defective ribosomal products (DRiPs) that are formed during times of cellular stress. DRiPs are non-functional proteins which contain errors due to premature termination during translation, wrong or deletion of amino acids, and/or they could be formed due to mis-folding of the protein. Therefore DRiPs are removed from the cell by tagging with ubiquitin and directed to the proteasome (Pierre 2005). DALIS can be induced by incubation with puromycin which causes premature chain termination during translation. Szeto *et al* (2006) showed that puromycin can induce DALIS-like inclusions in non-professional APC and called these structures ALIS. DALIS and ALIS are not dependent on either microtubules or actin cytoskeleton for formation. However, autophagy plays a role in their degradation, and GFP-LC3 can be recruited to ALIS independently of autophagy. This was demonstrated through use of Atg5-/- MEFs and the mutant LC3 G120A, and in both conditions LC3 was recruited to ALIS (Herter *et al* 2005).

5.2.4 Stress Granules (SGs) -

Similarly, conditions which trigger a stress response in cells can also arrest translation and synthesis of new proteins. As a result the mRNA and proteins involved in translation are triaged in to a region known as stress granules (SGs), and the fate of the mRNA, whether to continue with translation or degradation, is decided (Kimball *et al* 2003, Anderson and Kedersha 2008). The cell halts unnecessary translation of proteins, and SGs form and can play a role in altering cell metabolism for survival. SGs are comprised mainly of aggregated mRNA molecules, and also the initiation factors for translation as well as mRNA binding proteins for stability, and silencing proteins which includes T cell internal antigen-1 (TIA-1). TIA-1 and TIAR (TIA-related) are responsible for stress-induced translational arrest and aggregate to form SGs (Anderson and Kedersha 2008). Phosphorylation of eIF2α is

required for SG formation, and also results in LC3-II formation during the ER unfolded protein response (UPR) (Kouroku *et al* 2007). It is possible that the use of cationic lipids could initiate a stress response and/or induce the formation of SGs. The TVAs may represent attempts to use autophagy in their removal.

This chapter investigates the relationship between the perinuclear structures mentioned above, and TVAs. Lipid droplets are studied using Nile red which is a lipophilic dye that binds intracellular lipids and LDs. Both aggresomes and DALIS/ALIS contain ubiquitinated proteins and can be detected using ubiquitin immunostaining. DALIS/ALIS can be induced by adding puromycin to cells to cause premature termination of a protein translation. Similarly stress granules can be formed in response to sodium arsenate or puromycin and detected by following TIA-1 which is a protein that is incorporated into SGs.

5.3 Results –

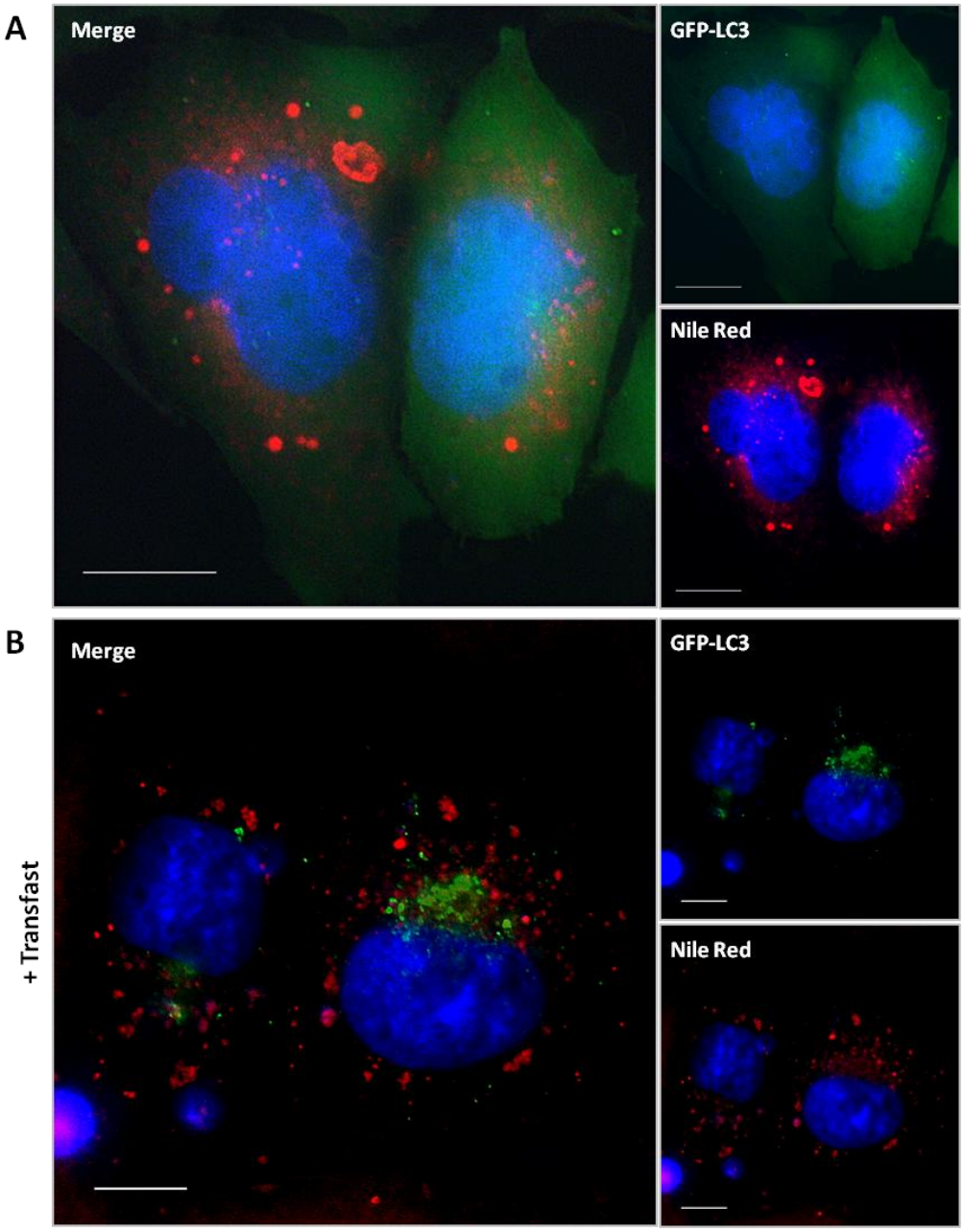

Figure 5.1 – Distribution of LC3 and Lipid Droplets in Cells Incubated with Cationic Liposomes - CHO cells stably expressing eGFP-LC3 (green) were cultured on coverslips for 24 hours with complete nutrient media and oleic acid. Cells were remained in complete nutrient media for 4 hours (A) or cells were incubated with Transfast in OptiMEM (B) for 4 hours. Cells were then fixed and lipid droplets were stained using Nile Red (red) and nuclei stained with DAPI (blue). Bar is 10 µm.

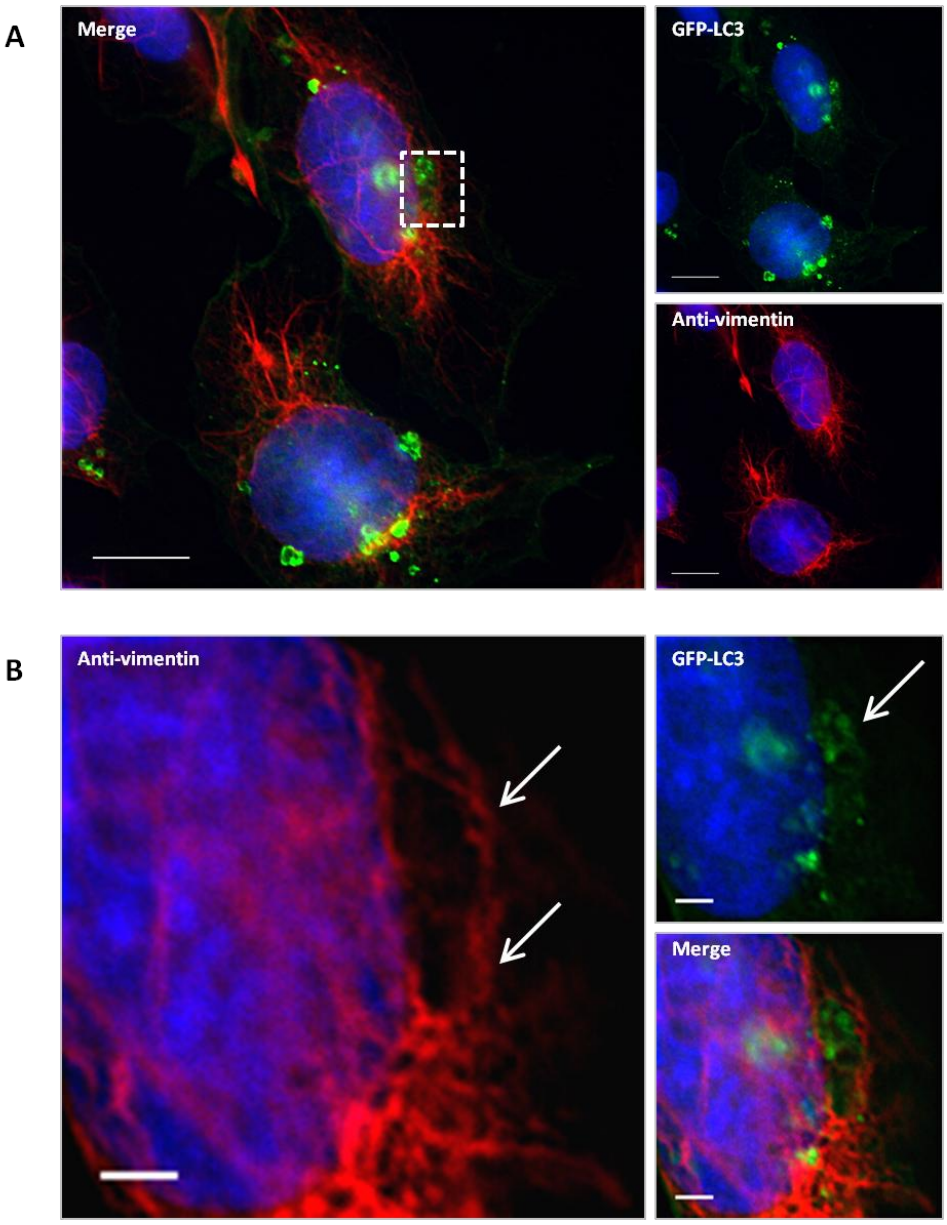

Figure 5.2 – The Intermediate Filament Vimentin Does Not Form a Cage Around Tubulo-Vesicular Autophagosomes (TVAs) - CHO cells stably expressing eGFP-LC3 (green) were cultured overnight on coverslips and then incubated with Transfast in OptiMEM for 4 hours before fixation in methanol/MES solution (A). Cells were stained using an anti bodies against vimentin (red) and nuclei with DAPI (blue). Bar is 10 µm. Panel B shows high magnification image of the region of interest outlined by the white square in A, the white arrows indicate vimentin filaments and the TVA. Bar is 2 µm.

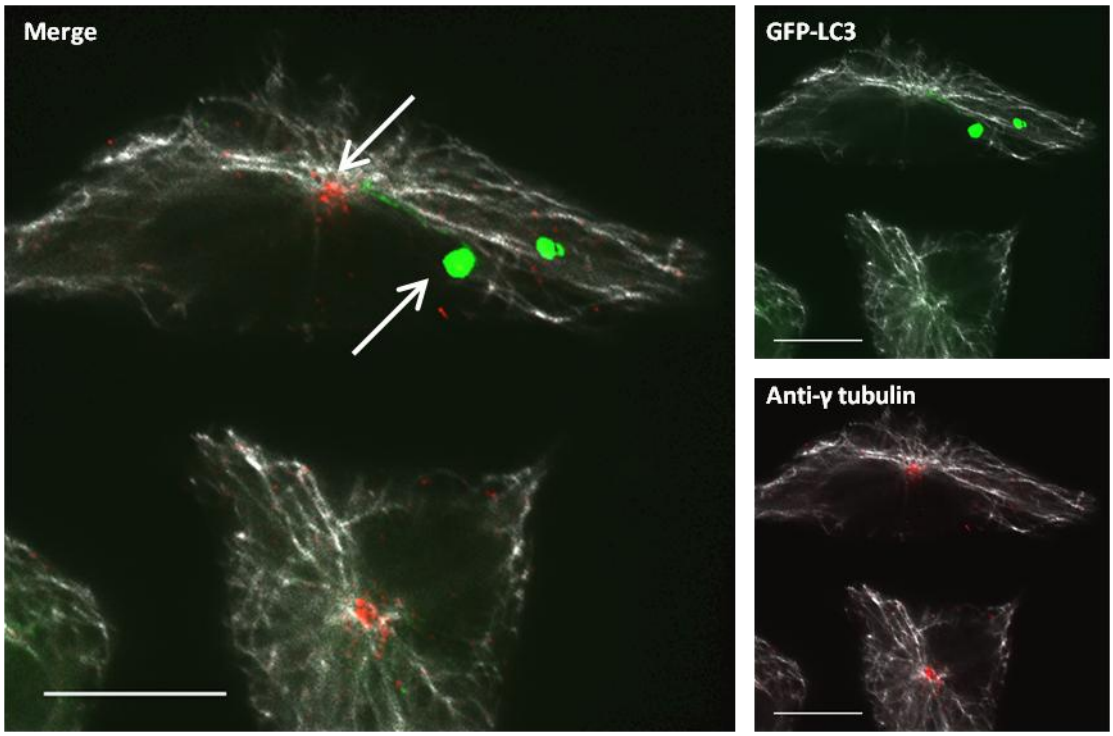

Figure 5.3 –Tubulo-Vesicular Autophagosomes (TVAs) Do Not Localise to the MTOC - CHO cells stably expressing eGFP-LC3 (green) were cultured overnight on coverslips and then incubated with Transfast in OptiMEM for 4 hours before fixation in methanol/MES solution (A). Cells were stained using an anti-γ tubulin (red) and anti-α tubulin antibody (pseudo-coloured white). Bar is 10 µm.

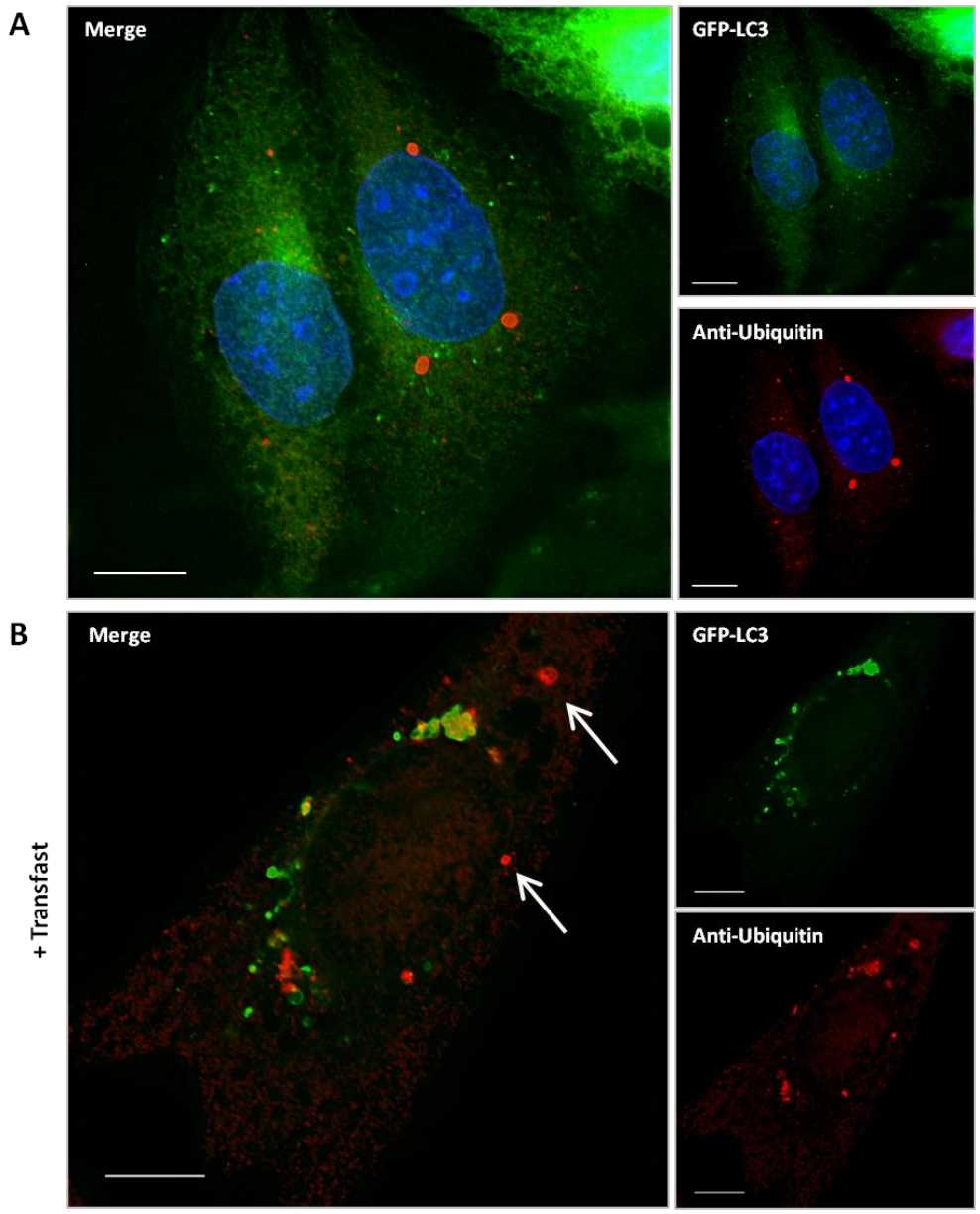

Figure 5.4 – Distribution of aggresome-like intracellular structures (ALIS) and Tubulo-Vesicular Autophagosomes (TVAs) – CHO cells stably expressing eGFP-LC3 (green) were cultured overnight on coverslips and then incubated with puromycin (15 µg/ml) to induce DRiPs (Panel A) cells incubated in nutrient media (Panel B) cells incubated with Transfast for 4 hours. Cells were stained using an antibodies against ubiquitin (red) and nuclei with DAPI (blue). Bar is 10 µm.

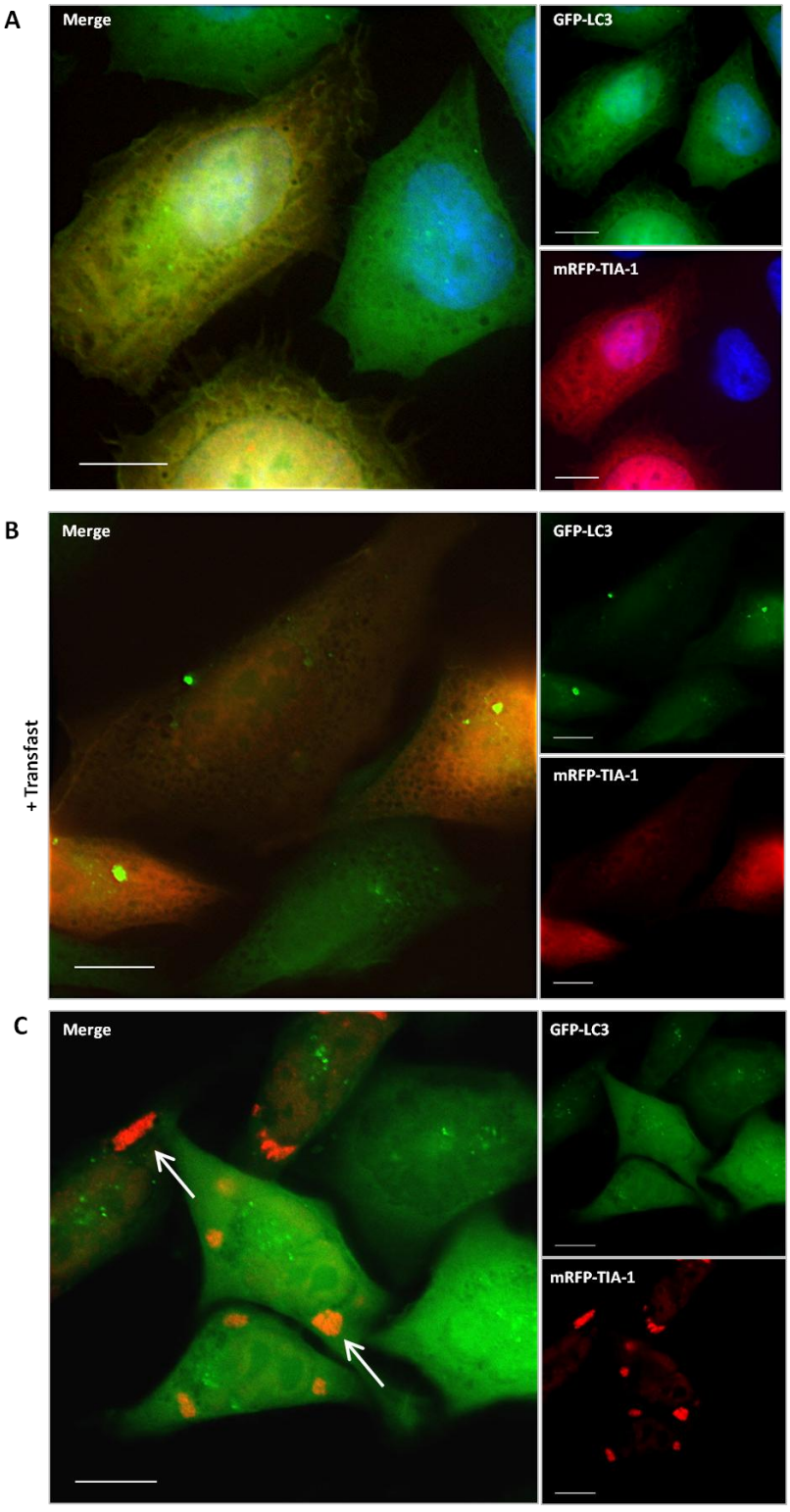

Figure 5.5 – Distribution of Stress Granule Marker TIA-1 and Tubulo-Vesicular Autophagosomes (TVAs) - CHO cells stably expressing eGFP-LC3 (green) were transfected with a plasmid expressing mRFP-TIA-1 using calcium phosphate. 36 hours post-transfection, cells were incubated in full media. (A), with Transfast (B) or with sodium arsenate (C) for 2 hours prior to fixation. Bar is 10 µm

5.3.1 TVAs induced by Cationic Lipids are not Incorporated into LD Storage Sites –

Lipid droplets are sites of lipid storage and formed in cells incubated with oleic acid. In figure 5.1A CHO cells expressing GFP-LC3 were incubated with oleic acid to induce lipid droplets. Lipid droplets stained with Nile Red (figure 5.1A) were heterogeneous in size with some large droplets located close to the nucleus. The GFP-LC3 signal remained cytoplasmic. Oleic acid lipid droplet induction did not therefore induce autophagosome formation and LC3 was not recruited to lipid droplets. In figure 5.1B, cells were incubated with oleic acid and cationic liposomes. The lipid droplets were scattered through the cytoplasm and TVAs formed in the perinuclear region of the cell, however there was no colocalisation between the signals from GFP and Nile Red. The result showed that TVAs do not recruit lipids detected by Nile Red and are not therefore closely related to lipid droplets.

5.3.2 TVAs Contain Ubiquintated Proteins but are not Related to Aggresomes. –

Aggresomes containing ubiquitinated mis-folded proteins are formed at the MTOC and can recruit p62. To investigate if TVAs share characteristics with aggresomes, CHO cells stably expressing eGFP-LC3 were co-stained with markers for aggresomes which include vimentin, location to the MTOC and ubiquitin. In figures 5.2 CHO cells expressing GFP-tagged LC3 showed the perinuclear rearrangement of LC3 following incubation with Transfast. When stained using an antibodies against vimentin, it was difficult to determine if there was a cage surrounding the TVAs (figure 5.2). On closer inspection of a region of interest (5.2B), the vimentin was displaced and surrounded the TVA, however, it was not clear if vimentin had collapsed around the TVA. Aggresomes are transported and localised to the microtubule organising centre (MTOC). In figure 5.3, the MTOC is highlighted by the white arrow. TVAs were localised to the perinuclear region, but unlike aggresomes they were separate from the MTOC. In a small population of cells the TVA appeared to be in close proximity to the MTOC (data not shown).

5.3.3 TVAs are Distinct from ALIS containing DRiPs and Stress Granules –

Defective ribosomal products (DRiPs) are formed in response to puromycin which causes premature termination of translation by ribosomes. The resulting DRiPs are ubiquitinated for degradation in the proteasome. Accumulation of DRiPs results in the

formation of ALIS. Figure 5.4 shows that cells incubated in puromycin formed large ubiquitinated structures in the cytoplasm similar to the ALIS described by Szeto *et al* (2006). These structures did not recruit LC3. Incubation with both puromycin and Transfast resulted in an increase in the number of ubiquitinated structures, some of which recruited GFP-LC3 (figure 5.4B). It is likely that the $LC3^{+}$ Ub^{+} structures were TVAs. However it was not possible to exclude the notion that DRiPs could also be incorporated into TVAs during their formation as these were also ubiquitinated.

Figure 5.5 shows cells incubated with sodium arsenate to induce stress granules. Stress granules were identified from the accumulation of mRFP-TIA-1 expressed in the cells as a marker. Sodium arsenate induces cellular stress by uncoupling the electron transport chain in the production of ATP which results in oxidative stress. Transient transfection of mRFP-TIA-1 showed that during normal growth conditions, both TIA-1 and LC3 had a cytoplasmic distribution, as in figure 5.5A. During incubation with liposomes, LC3 redistributed to TVAs, whereas TIA-1 remained cytoplasmic (figure 5.5B). During arsenate stress (figure 5.5C), TIA-1 redistributed to stress granules in the perinuclear region of the cell, however LC3 remained cytoplasmic. The results show that TVAs do not recruit stress granule marker TIA-1 and formed at sites separate from stress granules.

5.4 Discussion -

The aim of this chapter was to see if TVAs shared properties with other perinuclear structures known to recruit LC3 in response to stress. LC3 has been reported to be incorporated into LDs (Shibata *et al* 2010). There was, however, no evidence for colocalisation of LC3 with Nile Red staining following incubation of cells with oleic acid, suggesting that TVAs are not associated with lipid droplets. LC3 recruitment to LDs reported by Shibata *et al* appeared to be an additional function of the LC3 protein not previously observed, and was not involved in the formation of TVAs investigated in this chapter (Shibata *et al* 2010). The methods and time points used to visualise LC3 recruitment to LDs was different to those used in this chapter, which could be the reason LC3 did not localise to LDs produced using oleic acid.

TVAs contained ubiquitinated proteins and p62 and in this way resembled aggresomes, however it was not clear if a vimentin cage, which is known to collapse around aggresomes, also enclosed the TVAs. Close examination of vimentin showed a ring around the TVA, but the remaining vimentin was undisturbed. The results may represent displacement of vimentin rather than the collapse towards the centrosome seen during aggresome formation. In early work on aggresomes, Johnston *et al* discuss the rearrangement of vimetin into bundles in the perinuclear region, rather than the complete collapse of vimentin around the aggresome. However, aggresomes mainly form at the MTOC and in most cases TVAs were not localised to the MTOC. In summary it is not possible to rule out an association between TVAs and aggresomes, but they are not identical structures. It is known that p62 can accumulate in ubiquitin-positive protein aggregates, and it interacts with a FYVE domain protein known as Alfy to degrade them via autophagy (Clausen *et al* 2010). From the data presented in this chapter, it is possible that cationic liposomes can induce aggresomes formation as a stress response that are degraded via autophagy. However, the formation of the tubular extensions indicated these are dynamic structures, and these tubular structures are not documented for aggresome formation.

Autophagy can be activated through a number of stress stimuli and this led the investigation to look at two structures which are form during time of stress called defective ribosomal products (DRiPs,), aggresome-like structures (ALIS) and stress granules (SGs). These structures can form following invasion of pathogens into cells. Cationic liposome entry may follow the pathway of pathogen entry and therefore activate the same cellular response. When DRiPs were induced by puromycin cells formed inclusions containing ubiquitinated proteins as reported for the formation of ALIS (Szeto *et al* 2006). Cationic liposomes generated TVA in cells incubated with puromycin and some of these co-localised with ubiquitin suggesting association with ALIS. TVAs can associate with ubiquitinated inclusion induced by puromycin but several lines of evidence suggested they were not ALIS. In common with TVAs, ALIS are mobile and can fuse with each other but unlike TVAs they are rapidly degraded. (Pierre 2005). TVA formation was unaffected by cycloheximide whereas the formation of the DRiPs which accumulate to form ALIS is dependent on protein synthesis, in contrast TVAs do not require protein synthesis because they are unaffected by cycloheximide. ALIS form from DRiPs, and interestingly, they are removed by autophagy,

and LC3 can localise to ALIS regardless of Atg5 or lipidation. As discussed in chapter 4, knock-down of Atg5 inhibited TVA formation, and LC3-II processing must occur for it to localise to TVAs. Taking all the data into consideration from this and the previous chapter, it is therefore unlikely that TVAs are formed from DRiPs or that they are ALIS. Lastly, like DRiPs, stress granules (SGs) can form during pathogen invasion. Comparison of the TIA-1 marker which localised to SGs revealed that TVAs did not recruit this marker. Whilst it is true that SGs contain many different components, and only one was used in this study, TIA-1 is an RNA binding protein. The exclusion of TIA-1 from TVAs suggested they do not contain RNA. This further confirmed the DRiPs data and TVAs are not associated with SGs, and are unique structures.

In this study the characterisation of tubulo-vesicular autophagosomes (TVAs) was investigated with respect to other perinuclear structures. It is possible from the data presented that TVAs could be aggresomes; however the tubular extensions of TVAs make this seem an unlikely conclusion. The evidence also suggests TVAs are novel structures that form in response to cationic liposomes and do not have the characteristic of LDs, DRiPs, ALIS or SGs.

Chapter 6:

Role for the Endocytic Pathway in the Formation of Tubulo-Vesicular Autophagosomes

Chapter 6 – Role of the Endocytic Pathway in Formation of TVAs

6.1 Aims –

The aims of this chapter are to determine the role of endocytosis in the formation of TVAs by inhibiting this pathway, and also following the fusion of TVAs with endocytic vesicles using endocytic Rab GTPases as markers.

6.2 Introduction –

The entry of molecules in into cells via endocytosis can occur through a number of different mechanisms. The most widely understood is clathrin-mediated endocytosis (CME), whereby a region of the plasma membrane is deformed to form a pit, which can bud inwards and is pinched off from the membrane forming an independent vesicle. This vesicle will then traffic through the cell, the contents will either be degraded in lysosomes or it can be recycled to the plasma membrane. CME requires a number of different proteins which work to provide structure for forming the pit and vesicle. Self assembly of clathrin within coated pits facilitates vesicle formation and proteins such as dynamin (Doherty and McMahon 2010) pinch vesicles off from the plasma membrane to form early endosomes. The trafficking of the vesicle through the cell can also result in the fusion with other vesicles such as autophagosomes. Fusion with early/late endosomes and lysosomes is mediated by Rab GTPases, and also the ESCRT machinery for autophagosome-multivesicular body (MVBs) fusion, (figure 6.0). Rab5 plays an important role in the fusion of early endosomes with other endosomes as well as a function in enhance degradation of protein aggregates (Ravikumar *et al* 2008). Rab7 is important for the fusion of late endosomes and autophagosomes with lysosomes,

Endocytic vesicles can also fuse with autophagosomes and the convergence of autophagy and the endocytic pathways can occur at different stages and appears to be crucial for the maturation of the autophagosomes. Inhibition or over-expression of dominant negative Rab7 result in the accumulation of autophagosomes (Gutierrez *et al* 2004). Rab5 may play a role in autophagy because dominant negative Rab5 slows

degradation of proteins aggregates. Knock-down of β-COP which is involved in Golgi stability and early endosome function; also result in the accumulation of autophagosomes (Razi *et al* 2009). Clathrin-mediated endocytosis may also play a role during autophagy. A recent study by Ravikumar *et al* (2010) indicates that inhibitors of CME decrease the number of autophagosomes formed in the cytoplasm and it is suggested that endocytosis delivers membrane from the plasma membrane to autophagosomes and this study also revealed that Atg16L1 plays a role in clathrin-mediated endocytosis, and when dynamin is inhibited by the drug dynasore, the colocalisation between clathrin and Atg16L1 is increased. The proposal is that Atg16L1 function during the formation of very early endosomes, which are EEA1-negative, which mature to form early endosomes.

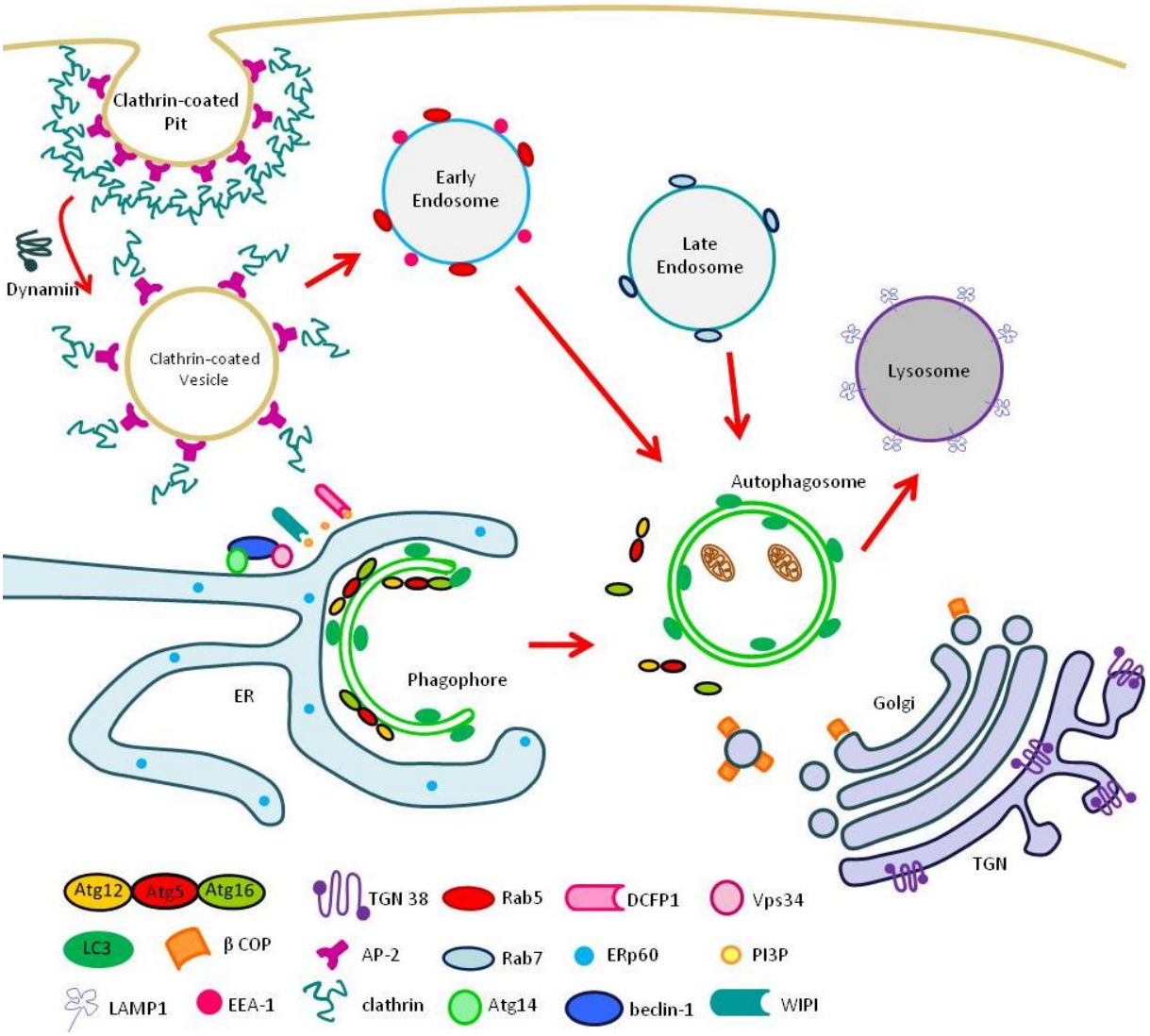

Figure 6.0 - Convergence of the autophagic and endocytic pathways – (adapted from Orsi *et al* 2010) the formation of autophagosomes from the ER through to degradation to the lysosomes requires input from other endocytic vesicles.

Previous chapters have shown that cationic liposomes induce TVAs. Since liposomes enter cells using clathrin-mediated endocytosis it is possible that the overlap between endocytosis and autophagy may play a role in the formation of TVAs. This chapter seeks to determine whether the endocytic pathway plays a role in the formation of TVAs. This will involve testing for the presence of endosome marker proteins in TVAs, inhibition of clathrin-mediated endocytosis with chlorpromazine and dynasore and documenting the effects of dominant negative Rab5 and Rab7 GTPases on TVA formation and trafficking. Following the trafficking through endosomal compartments marked with ERp60 to detect the ER, β-COP and anti-mannosidase II to detect the Golgi apparatus, and also the use of wild-type of TVAs.

6.3 Results –

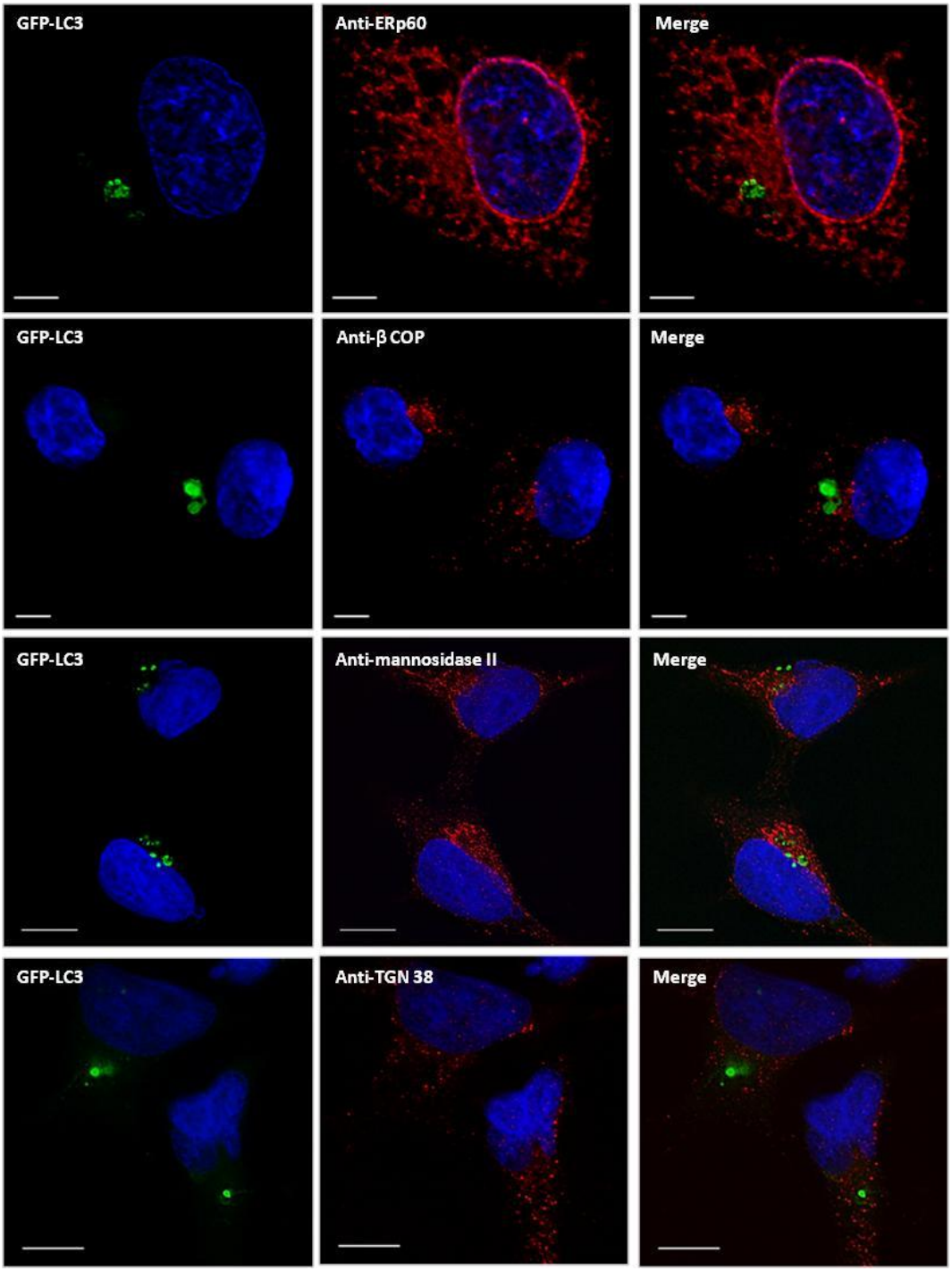

Figure 6.1 – TVAs Do Not Colocalise with Markers for the ER or the Golgi Complex – CHO cells stably expressing eGFP-LC3 (green, top two rows), or HEK 293 stably expressing eGFP-LC3 (bottom two rows)were cultured overnight on coverslips. Following this, cells were incubated with Transfast for 4 hours prior to fixation. Cells were stained using either an anti-β COP or anti-ERp60 antibody (top 2 rows, red), or for anti-mannosidase II or anti-TGN38 (bottom 2 rows, red) and nuclei with DAPI (blue). Bar is 5 µm.

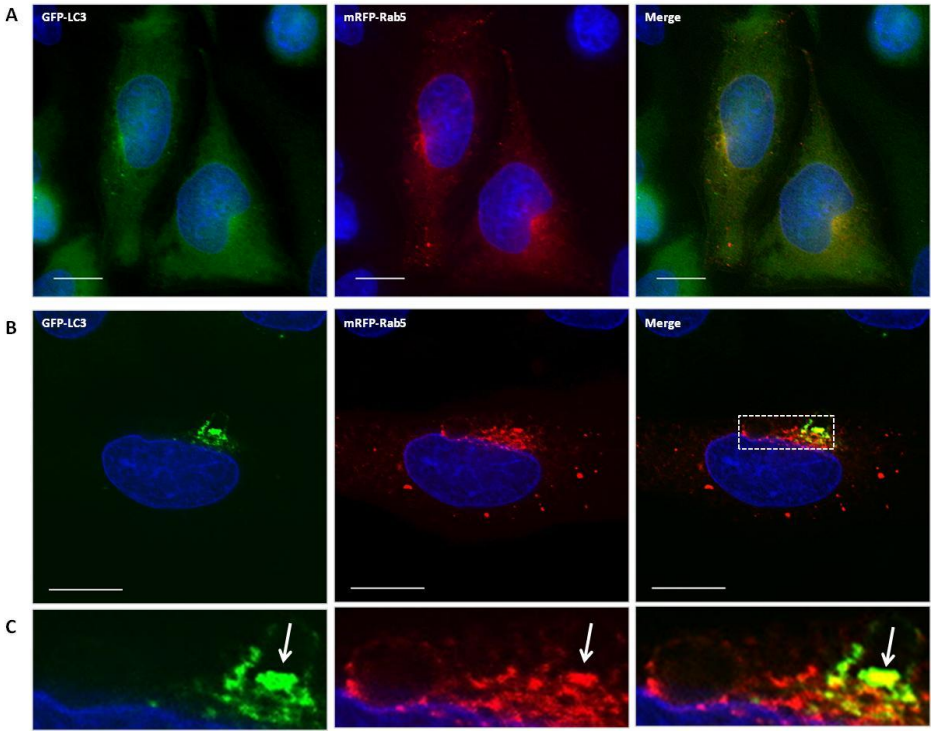

Figure 6.2 – Rab5 WT Partially Colocalised with TVAs - CHO cells stably expressing eGFP-LC3 (green) were transfected with a plasmid containing mRFP-Rab5 WT in complete media. 36 hours post-transfection cells were either left in full media (A) or incubated in Transfast for 4 hours (B). Region of interest is highlighted by the white square (C). Bar is 10 µm.

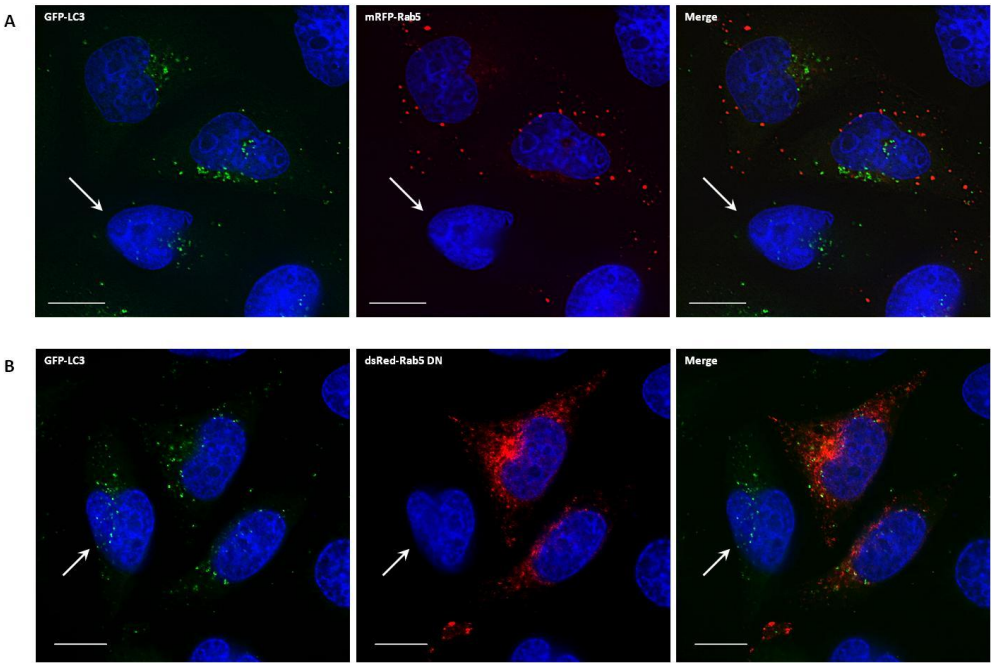

Figure 6.3 – Rab5 Dominant Negative Mutant Does Not Prevent Formation of Autophagosomes - CHO cells stably expressing eGFP-LC3 (green) were transfected with a plasmid containing mRFP-Rab5 WT (A) or dsRed-Rab5 DN (B) in complete media. 36 hours post-transfection cells were then starved in HBSS for 4 hours (B). The white arrows highlight cells not expressing the Rab5 construct. Bar is 10 µm.

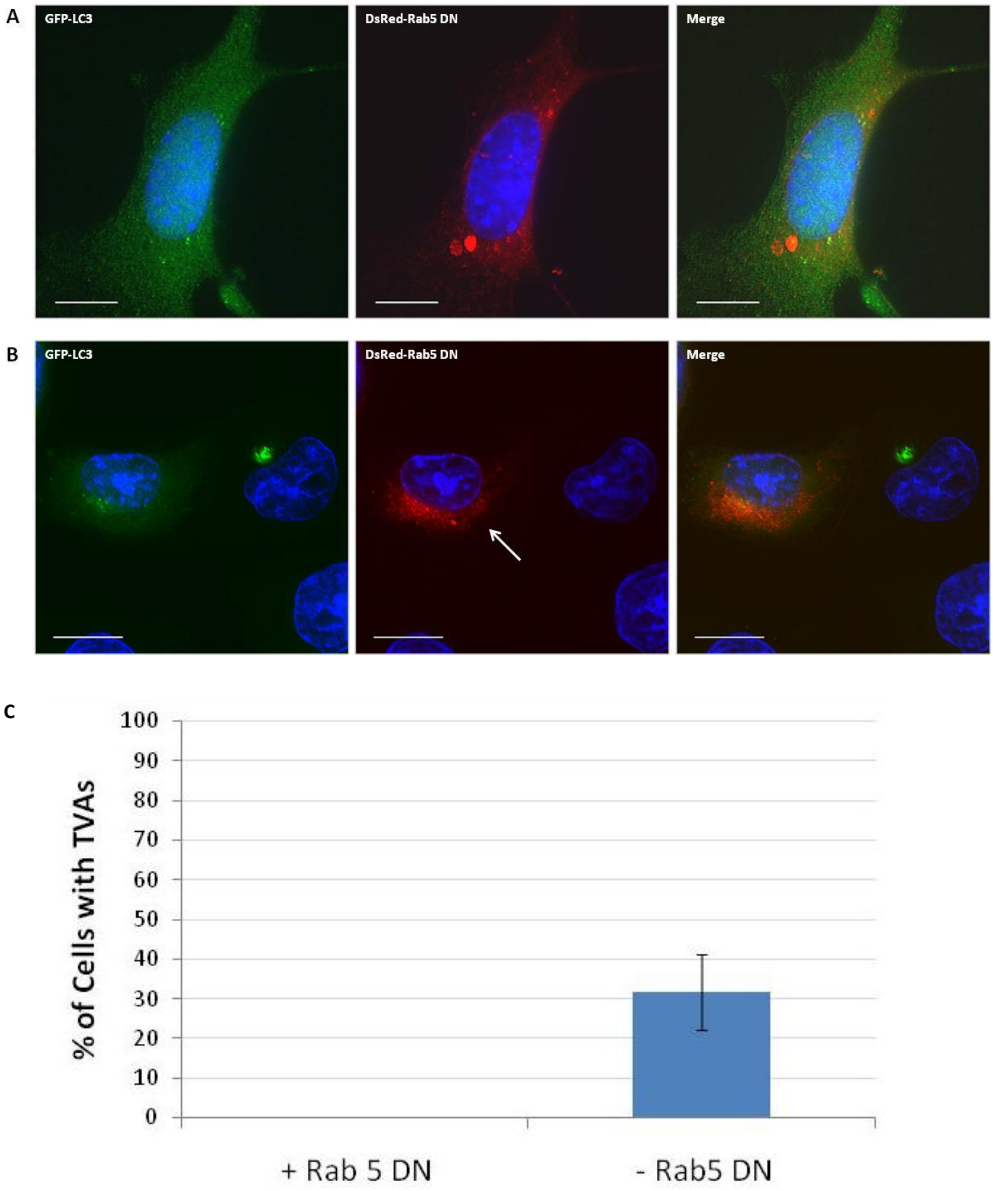

Figure 6.4 – Rab5 DN Prevents the Formation of TVAs – CHO cells stably expressing eGFP-LC3 (green) were transfected with a plasmid containing DsRed-Rab5 DN. 36 hours post-transfection cells were either left in full media (A) or incubated in Transfast for 4 hours (B). DAPI was used for the nuclei stain (blue). Bar is 10 µm. The white arrow indicates a cell expressing the Ds-Red-Rab5 DN. (C) Frequency (%) of TVA formation in cells with or without expression of Rab5 DN construct; values are the mean +/- standard error bar.

6.3.1 Endomembrane System -

To determine if other organelles in the endomembrane system contributed to the formation of TVAs, cell stably expressing eGFP-LC3 were stained with markers for the ER, Golgi and trans-Golgi network (TGN). The ER had a fine network throughout the cytoplasm and was found to be undisturbed by the large formations (figure 6.1). There was no colocalisation with the ER luminal marker ERp57 and LC3-positive TVA. Similarly, the mannosidase II and β-COP localised to the luminal space and outside the Golgi respectively and revealed the Golgi is not disturbed in the formation of TVAs. In some cases, the TVA appeared to be localised above the Golgi as in figure 6.1 yet this did not disrupt its location. Lastly, figure 6.1 (bottom panels) showed a normal distribution of TGN which did not colocalise with LC3 in the formation of TVAs.

6.3.2 Role of Rab 5 in formation of TVAs –

Endocytic trafficking through the cell requires a number of Rab proteins which are important in distinct steps. Rab5 is a marker for early endosomes and may also be required for formation of autophagosomes. Figure 6.2 shows CHO cells expressing GFP-LC3 and wild type Rab5 fused to red fluorescent protein (mRFP) (A) or GFP-LC3 and dominant negative Rab5 (DN) as a dsRed fusion (B). Cells were starved in HBSS to induce autophagy and wild type Rab5 and DN Rab5 were located to vesicles throughout the cytoplasm. Induction of autophagy induced LC3 punctae but these did not colocalise with the Rab5. Similarly Rab5 DN did not prevent the formation of autophagosomes. During incubation with Transfast (figure 6.3) induced TVAs in the perinuclear region of the cell, there was also an accumulation of Rab5 in the perinuclear region, some of which partially colocalised with the LC3. The region of interest is shown (C); the white arrow highlights the colocalisation of LC3 and Rab5. Similarly the cytoplasmic distribution of Rab5 was noticeably more vacuolar in places but the vacuoles were negative for LC3. The experiment was repeated in the presence of DN Rab5. Cells expressing DN Rab5 were unable to generate TVAs in response to cationic liposomes but many small GFP-positive vesicles were in the cytoplasm. This was quantified by looking at a number of cells which had TVA formation; of the total number of cells counted this was 30% of the population. From this, none of those were expressing the Rab5 DN construct, indicating this prevented the TVA formation.

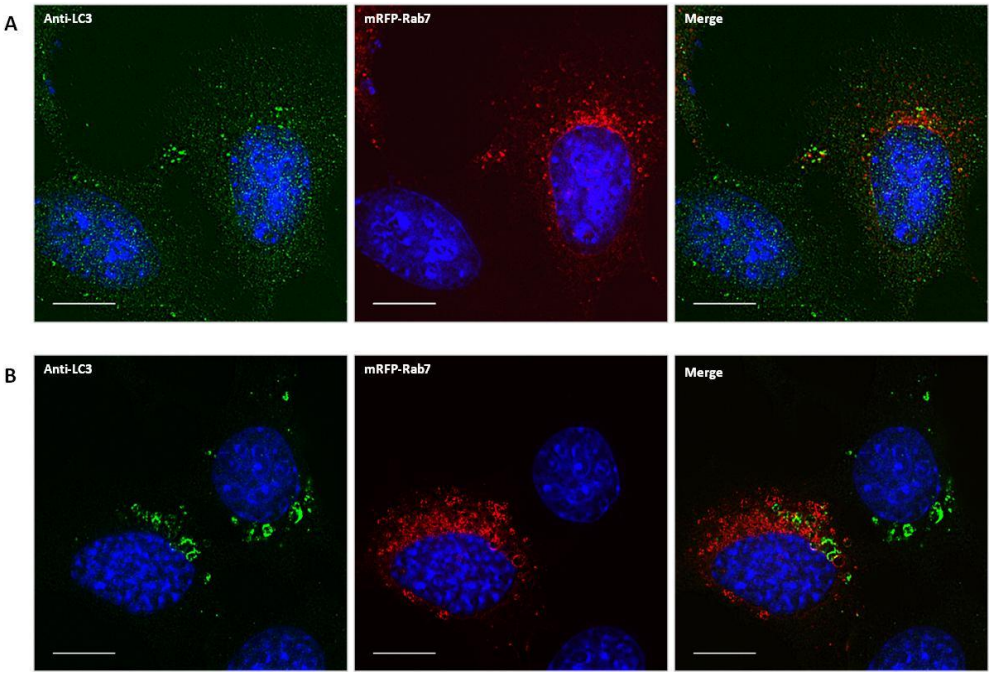

Figure 6.5 – Rab7 WT Did Not Colocalise to TVAs – MEF cells were transfected with a plasmid containing mRFP-Rab7 WT. 36 hours post-transfection cells were further incubated in complete media (A) or in OptiMEM containing Transfast for 4 hours before fixation (B). Cells were subsequently stained using an anti-LC3 antibody (green) and DAPI was used for the nuclei stain (blue). Bar is 10 µm.

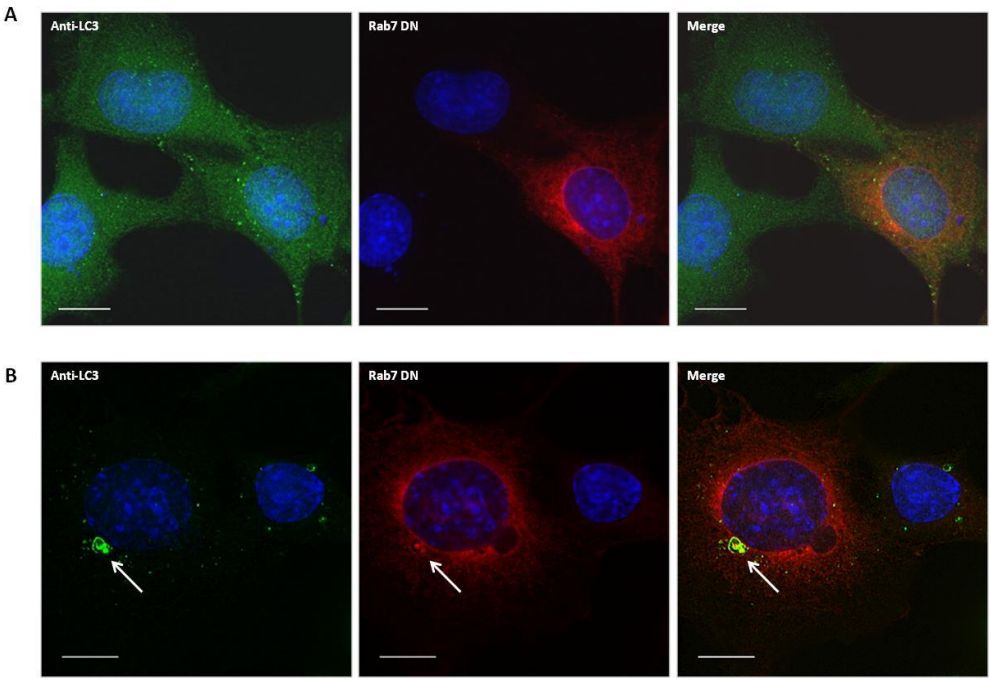

Figure 6.6 - Rab7 DN Did Not Prevents the Formation of TVAs – MEF cells were transfected with a plasmid containing GFP-Rab7 DN (pseudo-coloured red). 36 hours post-transfection cells were further incubated in full media (A) or in OptiMEM containing Transfast for 4 hours before fixation (B). Cells were subsequently stained using an anti-LC3 antibody (green) and DAPI was used for the nuclei stain (blue). Bar is 10 µm. White arrows points to a TVA in the perinuclear region of the cell.

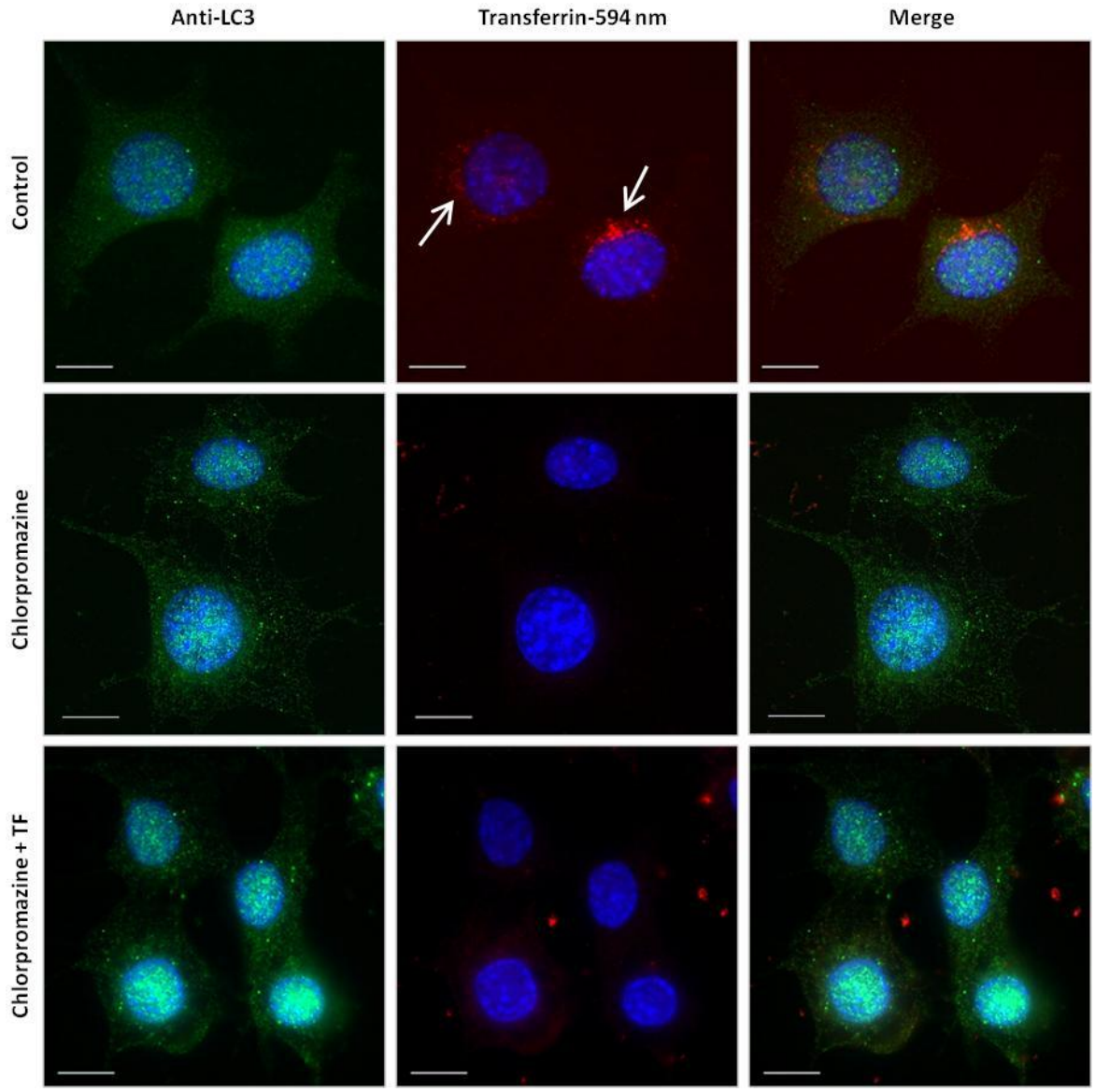

Figure 6.7 – Chlorpromazine Prevents Internalisation of Transferrin and the Formation of TVAs – MEFs were incubated in either complete media (control), with 50 µM chlorpromazine (chlorpromazine) or with Transfast and 50µM chlorpromazine (chlorpromazine + TF) for 1 hour prior to fixation. All sample also contained 5 µg/ml transferrin for the duration of the experiment. Cell nuclei were stained with DAPI (blue). Bar is 10 µm. White arrows highlight the distribution of transferrin inside the cell.

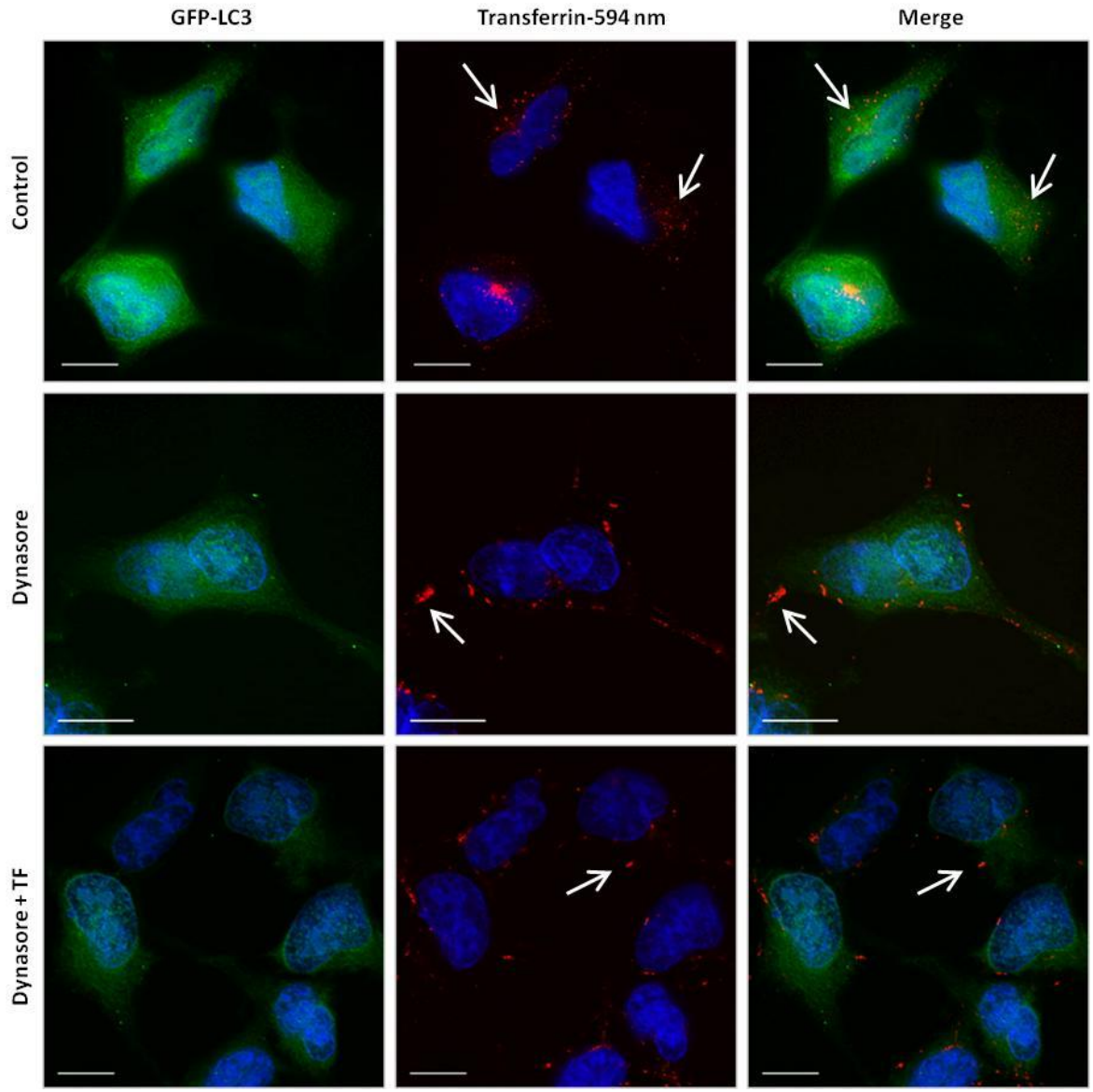

Figure 6.8 – Dynasore Prevents Internalisation of Transferrin and the Formation of TVAs – HEK 293 cells stably expressing eGFP-LC3 were incubated in either complete media (control), with 80 µM dynasore (dynasore) or with Transfast and 80 µM dynasore (dynasore + TF) for 1 hour prior to fixation. All sample also contained 5 µg/ml transferrin for the duration of the experiment. Cell nuclei were stained with DAPI (blue). Bar is 10 µm. White arrows highlight the distribution of transferrin inside the cell.

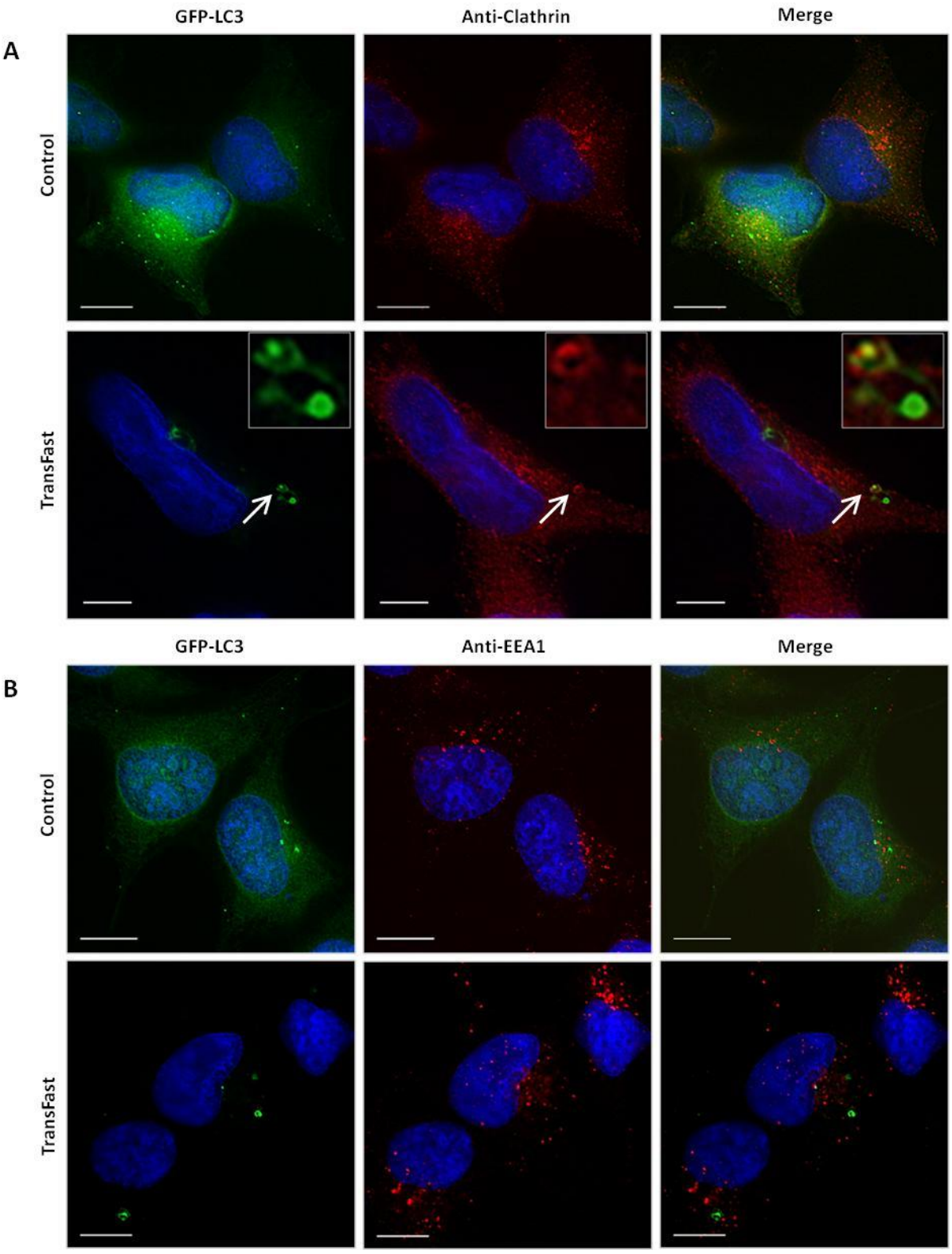

Figure 6.9 – Partial Colocalisation of Clathrin with Peripheral TVAs and No Colocalisation with EEA1 – HEK 293 cells stably expressing eGFP-LC3 were incubated in with for 4 hours prior to fixation. Cells were stained for anti-clathrin (A) or anti-EEA1 (B) and the nuclei were stained with DAPI (blue). Bar is 10 µm (A and B).

6.3.3 Role of Rab7 in the Formation of TVAs –

CHO cells expressing GFP-LC3 and Rab7 fused to RFP are shown in figure 6.5. Cells were either starved to induce autophagy (panel A) or incubated with cationic liposomes (panel B). Following this, expression of a plasmid contain mRFP-Rab7 in cells showed a cytoplasmic distribution and Rab7 concentrated in the perinuclear region (figure 6.5), and a cytoplasmic LC3 localisation. Incubation with Transfast induced TVAs. The majority of the Rab7 was in the perinuclear region, however the TVAs did not colocalise with Rab7. The experiment was repeated using DN Rab, the Rab7 DN protein was concentrated around the nucleus and distributed thorough the cytoplasm distribution (figure 6.6A) but did not prevent the formation of TVAs (figure 6.6B). The experiments were carried out in both MEF and CHO eGFP-LC3 cell lines and confirmed that a functional Rab5 is required for the formation of TVAs, however Rab7 does not play a role.

6.3.4 Role played by Clathrin-Mediated Endocytosis during the Formation of TVAs

Chlorpromazine inhibits the formation of clathrin-coated pits (CCPs) at the plasma membrane (Wang *et al* 1993). Dynasore inhibits dynamin, a GTPase that is responsible for the scission of CCPs to form clathrin-coated vesicles (CCVs) and thus transport into the cell is halted (Macia *et al* 2006). The effects of chlorpromazine on endocytosis of fluorescent transferrin (red) are shown in figure 6.7. Under control, conditions, transferrin is taken up by endocytosis and accumulates in the perinuclear region, as highlighted by the white arrows. Chlorpromazine prevented the uptake of transferrin and the cells are negative for red fluorescence (middle panels of figure 6.8). The effects of chlorpromazine on TVA formation in response to Transfast is shown in the lower panels. Chlorpromazine prevented redistribution of LC3 which remained distributed through the cytoplasm. Membrane blebs containing fluorescent transferrin were seen outside the cells, the nature of these structures is unknown. The experiments were repeated using dynasore to inhibit dynamin. Figure 6.9 showed that dynasore prevented perinuclear accumulation of transferring and caused the accumulation of the transferrin at the surface of the cell, highlighted by the white arrow. The nature of these localised concentrations of transferring are unknown. Importantly, incubation of cells with cationic liposomes in the presence of dynasore also prevented the formation of TVAs. These experiments indicate that CME is required for the formation of TVAs.

To investigate if clathrin played a role in the formation of TVAs, HEK 293 cells stably expressing eGFP-LC3 were incubated with Transfast and stained for clathrin (Figure 6.9A). In the majority of the cells the perinuclear TVAs were not colocalised with clathrin, however, in TVAs that were closer to the cell periphery (arrow) there was a partial colocalisation with clathrin. To determine if peripheral TVAs fuse with early endosomes, cells were stained for an early endosome antigen (EEA1). However the EEA1 and TVAs were separate structures and there was no colocalisation between LC3 and EEA1.

6.4 Discussion -

Rab GTPase function was used in order to investigate the role of the endocytic pathway in the formation of the TVAs; both the inhibition of CME and the Rab GTPases was used to dissect which compartments would contribute. Liposomes are known to enter cells through clathrin-mediated endocytosis as shown in this chapter which correlates with the data presented by Rejman *et al* 2005. The results of this chapter show that formation of TVAs required clathrin mediated endocytosis and Rab5. In addition peripheral TVAs recruited clathrin and Rab5 was located to some areas within the TVA. In the study by Rejman *et al,* transfection efficiency was used as a measure of liposome entry into cells. They show that inhibition of CME by both chlorpromazine and potassium depletion decreased the rate of transfection efficiency, suggesting that CME s the major route of entry of cationic liposomes. This appears specific because incubation with a inhibitors of caveolae-mediated endocytosis inhibitor did not further decrease transfection efficiency. The route for cationic liposomes into cells is largely through CME, however, it is not clear if the liposomes remain inside endosome or are delivered to the cytoplasm. In this chapter it was shown that TVAs formation is dependent on CME and TVAs partially colocalised with clathrin. This suggests that TVA formation may be a consequence of endocytosis of cationic liposomes. Even so there was no colocalisation with EEA1. It is possible the cationic liposomes escape the endosomes before fusion with early endosomes. The role of EEA1 is to tether vesicles and aid in the fusion with early endosomes, and it is a Rab5 effector protein. EEA1 has a FYVE domain in which it binds to endosomes in a PI (3)P dependent manner, and interact with GTP-bound Rab5 (Simonsen *et al* 1998). Since Rab5 was shown to be important in the formation of TVAs, it is surprising that EEA1 is not also recruited. The data presented here shows that although TVA formation is Rab5-dependent it does not recruit

the effector protein EEA1, as shown in figure 6.9. One possibility is that liposomes are released into the cytoplasm before or during fusion with early endosomes, and are then engulfed by autophagosomes.

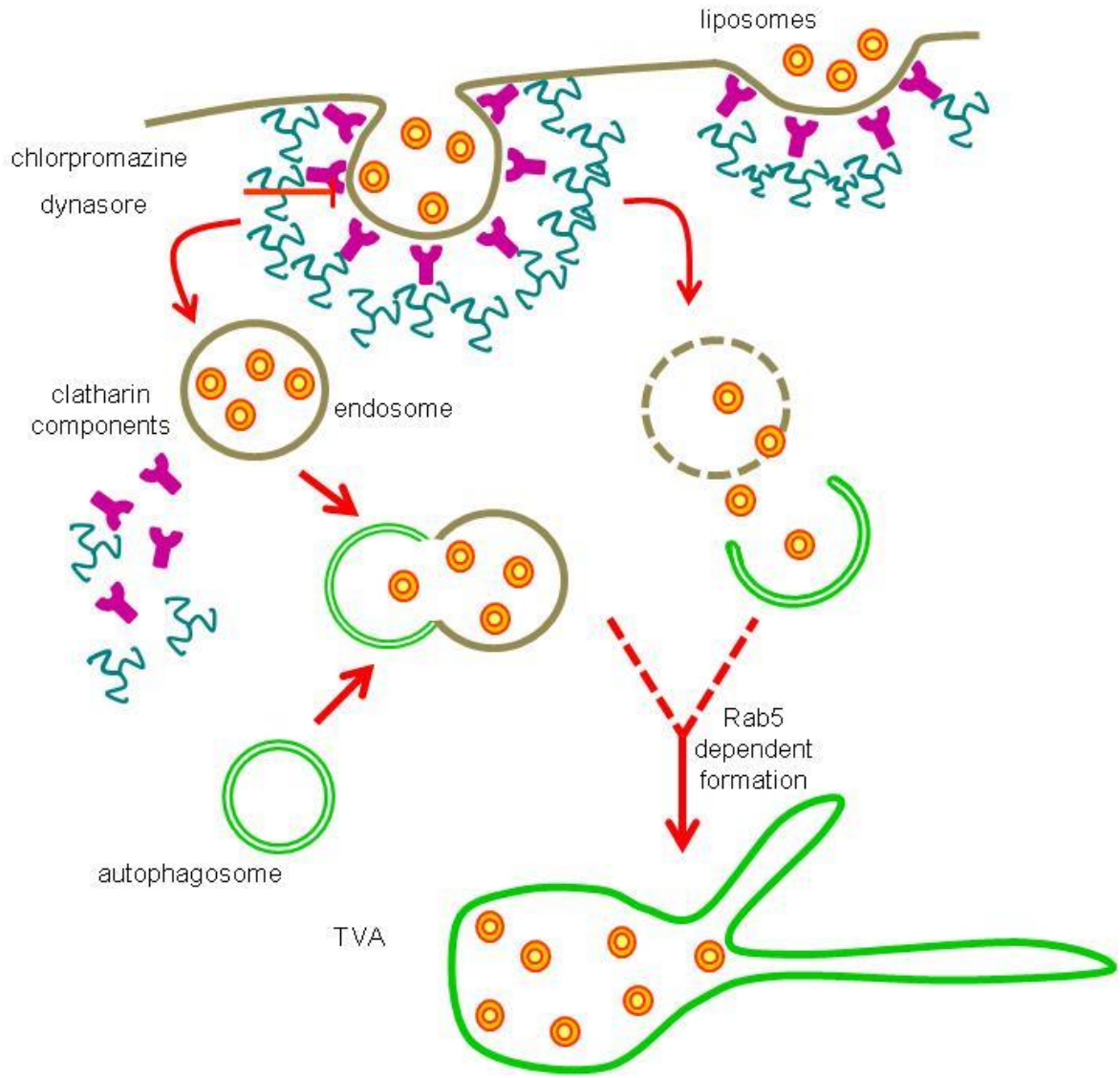

Figure 6.10 – The formation of TVA following clathrin-mediated endocytosis

Data present in this chapter also show that TVA formation does not require Rab7 and Rab 7 is not recruited to TVAs. Rab7 is required for endosome fusion with lysosomes and for autophagosome:lysosome fusion (Gutierrez *et al* 2004). This result correlates with the data in the previous chapter showing lack or severe delay of fusion of TVAs with lysosomes.

Interestingly, previous work has shown that Rab5 participates in the early steps of autophagy coordinating the conjugation of Atg5 to Atg12 (Ravikumar *et al* 2008). It was possible that the DN Rab5 may have inhibited TVA formation through a direct effect on Atg5-12 conjugation. However in the cell system used in this current study, it was not possible to demonstrate inhibition of autophagosome formation in response to starvation by DN Rab5. In the same cells DN Rab5 inhibited TVA formation and it is concluded that this is because DN Rab5 is inhibiting endocytosis. In summary, the data presented in this chapter reveal a role for clathrin-mediated endocytosis in the formation of TVAs. This could be the delivery of liposomes into the cytoplasm, or endosomes containing liposomes which fuse with autophagosomes, further research on this would be required. Also demonstrated was a role for clathrin in the peripheral TVAs, and a role for Rab5 in their formation.

Chapter 7:

Final Discussion

Chapter 7 – General Discussion –

7.1 Summary -

This thesis has studied the formation of tubulo-vesicular autophagosomes (TVAs) in response to the cationic liposomes commonly used as non-viral DNA delivery vectors. Experiments also showed that TVAs were formed in response to calcium phosphate precipitates and cationic liposomes which are used routinely as transfection reagents to deliver plasmids into cells for protein expression. Parallel work in the Pirbright Laboratories (see appendix) has shown that TVAs are produced when cells are incubated with Foot and Mouth Disease virus (FMDV) empty capsids, or UV-inactivated FMDV. It is possible that TVAs form following activation of a common cell signalling pathway and this will be discussed later (figure 7.1). TVAs are classed as autophagosomes because they show several similarities to autophagosomes generated in response to starvation. TVA formation is dependent on Atg5, involves conjugation of LC3 to PE and redistribution of LC3 from the cytoplasm to membranes. TVAs induced by cationic liposomes were, however, different from autophagosomes in several ways. They formed independently of starvation, and did not appear to require class III PI 3-kinase or beclin-1. TVAs were highly heterogeneous structures containing vesicles and tubules enriched with LC3 which concentrated close to the nucleus, and compared with autophagosomes, they were relatively long-lived. TVA formation was also highly dependent on endocytic pathways, and required on-going proteolysis in lysosomes. TVAs were also separate and distinct from other perinuclear stress-induced structures such as aggresomes or ALIS that recruit LC3.

7.2 Model for Formation of Tubulo-Vesicular Autophagosomes –

Cationic liposomes are known to enter cells through clathrin-mediated endocytosis (CME). The results show that TVAs required endocytosis and that there was a transient association with early endosome marker rab5. This suggests that endocytosis is an important step in the formation of TVAs (figure 7.1). Time lapse images show that the first vesicles containing LC3 formed in response to the liposomes resemble the LC3 punctae generated by starvation. This suggests that endocytosis of liposomes, or liposomes released

into the cytoplasm, may activate autophagy (steps 1-2a and 2b). Activation of autophagy by liposomes was however independent of both class III PI 3-kinase activity and starvation so the signalling mechanism remains unknown. The small LC3-punctae, generated by liposomes could then engulf liposomes (step 2b), or fuse with endosomes containing liposomes (step 3), and then fuse together to form large heterogeneous vesicles. This requires intact microtubules suggesting that LC3 punctae induced by liposomes are drawn together by microtubule motor proteins (steps 4 and 5).

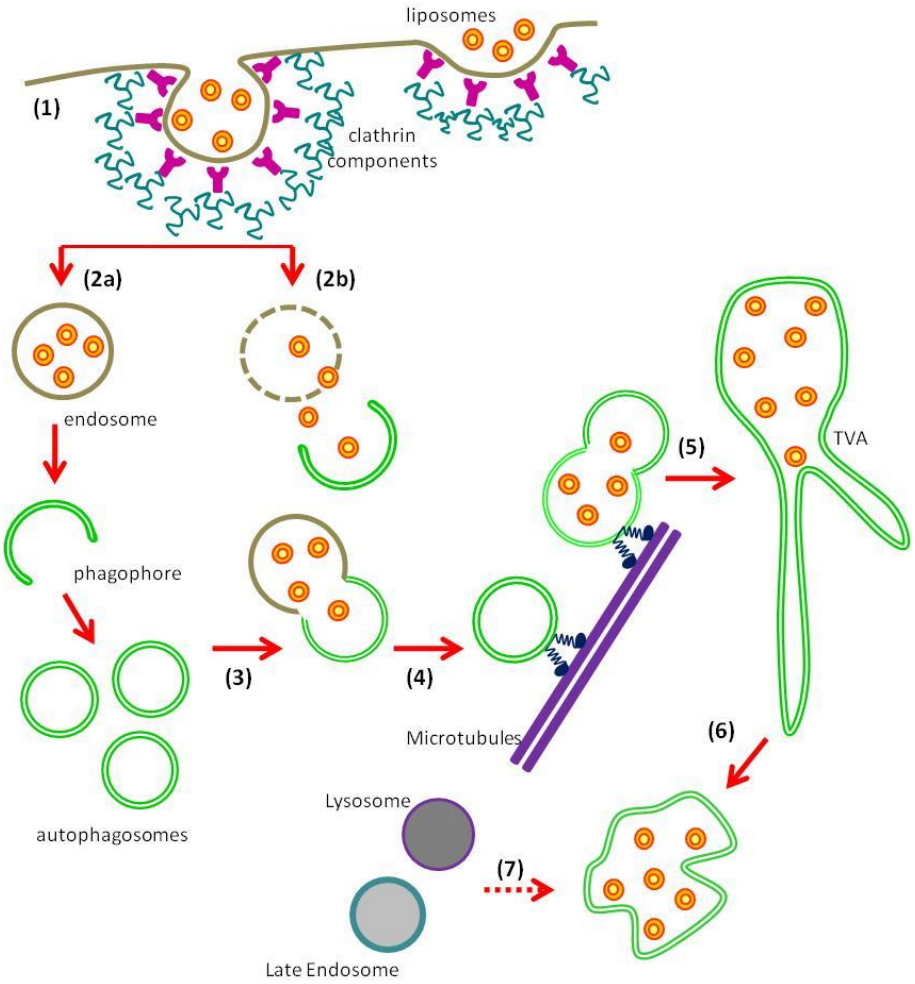

Figure 7.1 - Model for Formation of TVAs Following Incubation with Liposomes

Large heterogeneous vesicles then generate tubular extensions and networks (step 5) and these again required intact microtubules. The TVAs accumulate close to the nucleus and remained in cells for up to 48 hours (step 6). The lack of degradation of LC3 during this time suggested a block in fusion with lysosomes. This was supported by studies showing slowed degradation of p62 and accumulation of ubiquitinated proteins. Interestingly,

inhibition of lysosome acidification using bafilomycin A1 or the protease inhibitor E64d prevented formation of TVAs, suggesting that acidified late endosomes and/or lysosomes play a role in TVA formation and stability (step 7). At the later stages, 8 hours post formation onwards, less tubule-like extensions were generated from the central structures, and the lysosomes swell, some of the TVAs colocalise with LAMP1-positive structures indicating a slow delivery of LC3 to lysosomes.

7.2.1 - Overlap between Endocytosis and Autophagy -

Recent studies show that Atg16L1 may play a role at the very early stages of endocytosis at the plasma membrane (Ravikumar *et al* 2010). Atg16L1 binds clathrin, and inhibition of dynamin to stabilise clathrin-coated pits during endocytosis increases colocalisation between Atg16L1 and clathrin. Furthermore, knock-down of clathrin heavy chain, AP2 and epsin-1 slow endocytosis and decrease the number of autophagosomes formed in response to starvation (Ravikumar *et al* 2010). The data presented in this thesis show that TVA formation requires endocytosis and activation of autophagy via Atg5. Recruitment of Atg16 to sites of liposome endocytosis could seed autophagosome formation.

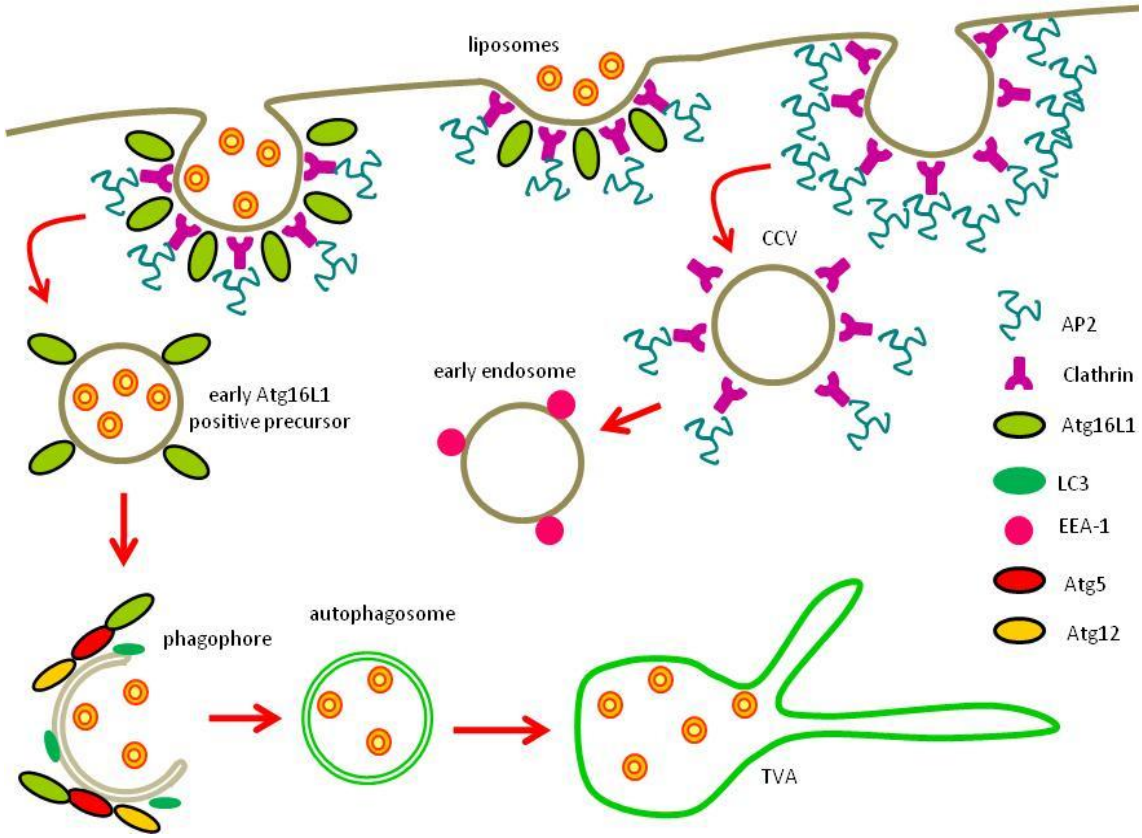

Figure 7.2 – The Involvement of Atg16L1 in Endocytosis of Liposomes During TVA Formation – (adapted from Ravikumar *et al* 2010) - Atg16L1 binds clathrin and forms early Atg16L1 positive precursors during endocytosis of cationic liposomes. Clathrin coated vesicles (CCV) form from the plasma membrane which mature into EEA-1-positive endosomes. Atg16L1-positive precursors may aid in autophagosome formation, and recruits LC3 to the phagosome which matures to form autophagosome. These autophagosome, as described in figure 7.1, fuse and become larger TVAs.

7.2.2 - Alternative pathways for tubule formation -

The tubulation of TVAs is a dynamic and novel characteristic which sets them apart from typical autophagosomes. Tubule formation required intact microtubules suggesting they may be formed from vesicles by microtubule motor proteins (figure 7.1). There are however a number of proteins that are involved in membrane tubulation during endocytosis. These proteins contain BAR, F-BAR, ENTH or ANTH domains (Kutateladze 2010) which bind to different phosphoinositol intermediates and/or integral proteins in membranes to induce membrane curvature and tubulation. An example includes the epsin-1 protein which contains an ENTH domain, is required for cationic liposome endocytosis, (Zuhorn et al 2002) and plays a role in CME (McMahon and Gallop 2005). The role of epsin-1 in CME is to stabilise and aid in the formation of clathrin-coated pits which bud off from the plasma membrane (Ford *et al* 2002). Epsin-1 can bind to $PI(4,5)P_2$ in the plasma membrane through the ENTH domain which inserts into the membrane to induce membrane curvature during pit formation. The binding of the ENTH domain is dependent on acidic pH. It is clear that prevention of acidification of lysosomes with bafilomycin presents TVA formation, it is possible that bafilomycin prevents tubule formation by inhibiting binding of the Epsin-1 ENTH domain. TVAs contain ubiquitinated material and the presence of an ubiquitin-interacting motif (UIM) in epsin-1 would allow it to recognise ubiquitinated cargoes (Hom *et al* 2007). In the presence of $PI(4,5)P_2$ in the membrane to bind the ENTH domain could again cause membrane deformation and tubulation during TVA acidification.

7.3 Comparison of Thesis with Published Data on TVAs –

7.3.1 Formation of TVAs in Response to Cationic Liposomes

The data presented by Man *et al* argues that cationic lipids induce genuine autophagy through a PI-3 kinase independent mechanism. The paper studies DOTAP alone,

and not the helper lipid DOPE, and DOTAP induces autophagy in cells through LC3 aggregation and conversion to LC3-II. These aggregates colocalise with Lysotracker, and partially with Mitotracker, indicating functional autophagosomes (Man *et al* 2010). Given recent data on the origin of the autophagosome membrane it is possible that both organelles contribute to the formation. Man *et al* also show the formation of autophagosomes by DOTAP in the presence of 3-methyladenine (3-MA). This thesis shows that TVAs induced by cationic lipids are PI-3 kinase and beclin-1 independent, as they form in the presence of wortmannin and beclin-1 knock-down respectively. Similarly, in concurrence with Man *et al*, the data from the thesis also demonstrates that TVAs form through an mTOR independent pathway, as they still form in the presence of the inhibitor torin-1. Man *et al* did not explore the formation of TVAs from small punctae to large heterogenous structures containing vesicles and tubules as explored in this thesis using live cell imaging. This data presented in this thesis has illustrated a role for microtubules in trafficking punctae to the larger structures that accumulate in the perinuclear region of the cell.

7.3.2 - The Formation of TVAs in Response to Calcium Phosphate Precipitates (CPP) -

At the start of this thesis work by Gao *et al* demonstrated that calcium phosphate precipitates (CPP) will produce large LC3-positive aggregates in a dose-dependent manner (Gao *et al* 2008). Calcium phosphate is a classical method for transfection but TVA formation does not require DNA to be incorporated into the precipitate, incubation with calcium phosphate precipitate in the absence of DNA will rearrange LC3 indicating an increase in the production of autophagosomes. Autophagosome formation by CPP was verified by electron microscopy showing formation of increased numbers of double-membraned vesicles. Moreover, recruitment of LC3 required processing by Atg4 and exposure of Gly 120 at the terminus of LC3 for addition of PE, and activation by CPP was inhibited by wortmannin and silencing of beclin-1. CPP also induced degradation of GFP-LC3 and p62 indicating fusion with lysosomes resulting in a decline in autophagosomes numbers to control levels at 24 hours. Increased autophagic flux in response to CPP was verified using the tandem mRFP-GFP-LC3 probe which generated large numbers of red punctae (indicating autolysosomes) in response to CPP. The formation of LC3 punctae was blocked when calcium was chelated suggesting that autophagy was activated by calcium entering the cell.

Sakar *et al* (2009) followed up on this work and confirmed that CPP increases the number of autophagosomes at the early time points. However, continuous exposure to CPP for 24 hours caused a block in autophagosome:lysosome fusion. This was indicated by reduced degradation of p62 or mutant Huntington aggregates, less conversion of mRFP-GFP-LC3 to red punctae and accumulation of large autophagosomes. It was also confirmed that CPP induced autophagy was dependent on Atg5 and lipidation of LC3, which again agrees with the data presented in this thesis.

In the most recent paper by Gao *et al* (2010) TVAs were immunopurified from lysates taken from cells starved to induce autophagy or incubated with CPP. The authors demonstrate the formation of TVAs during starvation; however CPP induced a stronger response. This is the first paper to describe the formation of tubulovesicular autophagosomes in response to starvation, yet the majority of the data presented used CPP as the stimulus. The immunopurified vesicles were examined by electron microscopy and revealed heterogeneous ultrastructure with individual vesicles, and vesicles with tubules attached. This was consistent with their fluorescence images showing that 60-70% of LC3 positive structures were individual vesicles, 20-30% were vesicles with tubules attached and the remainder were tubules. Proteomic analysis showed the presence of Atg5, Atg16L1 and Atg5-Atg12 involved in early processes of isolation membrane and phagophore formation. The presence of LC3-II, Atg9 and p62 confirmed the relationship with mature autophagosomes. Levels of beclin-1 and Vps34 were low but UVRAG was present. Autophagosomes formed by CPP also contained endocytic markers Rab4, Rab5 and Rab7, however, clathrin and Rab5 effector proteins EEA-1 and Rabaptin-5 were absent. Analysis of the entire TVA proteome showed a further 100 proteins, with 40% originating from Golgi, ER and mitochondrial membranes, but a clear link between these proteins and known autophagy pathways was not clear.

7.3.3 Comparison of TVAs Formed by CPP with Those Formed by Cationic Liposomes -

The TVAs generated by CPP were broadly similar in morphology to those induced by cationic liposomes. As reported in this thesis TVAs generated by CPP were transient structures and survived for 8 hours but were short lived compared with the 24 hours seen for TVAs induced by cationic liposomes. A role for clathrin-mediated endocytosis and

endocytic Rab proteins in the formation of TVAs by CPP has not been tested but the presence of endocytic markers such as Rab4, Rab5 and Rab7 suggests that endosomes may provide membranes for TVAs. One difference for CPP TVAs is the presence of Rab7, which was absent from TVAs induced by cationic liposomes. In agreement with work in this thesis p62 was concentrated in the interior of the vesicular component of the TVA, but was also found in tubular extensions. The signalling mechanism by which CPP induced autophagy was not investigated however, it appears from preliminary experiments using inhibitors cited in the paper (Gao *et al* 2008) that it is independent of the calcium activate kinase CaMKKβ.

A combination of fluorescence images, time lapse microscopy and electron micrographs allowed Gao *et al* (2010) to construct a model for the formation of TVAs. Most pathways involve the bending of tubule-like membranes to enclose cytoplasm that could bud from the tubules to generate double-membraned vesicles (figure), alternatively, membranes could invaginate inwards into the swollen head of TVAs. Gao *et al* did not study the role of microtubules or lysosome acidification and proteolysis in TVA formation in response to CPP, and did not explain how these processes would be essential for formation of tubules and/or conversion to double membrane vesicles.

7.3.4 Possible Cell Signalling Pathways Activated by Cationic Liposomes -

Interestingly, the formation of autophagosomes during starvation is dependent on the generation of PI(3)P by Vsp34 which localises to ER membranes in the beclin-1 complex with Atg14, and results in the recruitment of FYVE-domain containing protein such as WIPI to induce the formation of the autophagosome (Hayashi-Nishino 2009). The TVAs in this thesis formed in the presence of wortmannin, a class III PI 3-kinase inhibitor, suggesting PI 3-kinase independent mechanism. A recent report by Nishida *et al* illustrates that in $Atg5^{-/-}$ and $Atg7^{-/-}$ cells there is an alternative form of autophagy where the Golgi and the TGN play a role in forming double-membrane vesicles. Although independent of Atg5 or Atg7, these vesicles are still dependent on PI 3-kinases and Rab9 which also play a role in canonical autophagy (Nishida *et al* 2009). Other examples include the PI 3-kinase and beclin-1 independent pathway involved during *Vibrio parahaemolytics* infection, and also following resveratrol treatment (Scarlatti *et al* 2008, Burdette *et al* 2009). The incubation with cationic liposomes may trigger one of the alternative routes and result in the formation of TVAs.

Data presented by Ouali *et al* (2007) show that cationic liposomes containing DiC14-amidine, DOTAP, DDAB and lipofectamine raise intracellular calcium during the first hour of being added to cells. The calcium appeared to be released from the ER Ca^{2+} store since the rise in calcium can be inhibited by thapsigargin which inhibits the ER Ca^{2+} ATPase and U73122 an inhibitor of phopholipase C and prevents production of inositol 1,4,5-triphosphate. Release of calcium was dependent on the positive charge of the cationic lipid head group. Data from work with cationic liposomes in this thesis show that the cationic liposomes used did not produce a change in intracellular calcium (see appendix). Cationic lipids show large structural diversity and can activate a range of cellular pathways. Cationic lipids, such as DiC14-amidine, that resemble bacterial lipopolysaccharide activate Toll-like receptor 4 and can signal through MyD88 and NF-kB (Lonez et al 2009). Most cationic lipids including DOTAP and lipofectamine are not recognised by TLR4 but activate MAPK pathways involving ERK1/2, JNK and p38, and this can lead to a diagnostic up-regulation of CD80/CD86. These lipids may bind CD14 and lipopolysaccharide binding protein (LBP). By using inhibitors of the ERK1/2, JNK and p38 is would be possible to determine if these signalling components play a role in the formation of TVAs.

Cell entry of cationic liposomes may also be mediated by β1 integrins (Zuhorn et al 2007) since uptake of liposomes containing DOPE can be reduced by antibodies that block β1 integrins and β1 integrin silencing, but is not reduced by antibodies blocking E-cadherin or an RGD peptide that blocks αv integrin. Integrin binding followed by clustering interactions normally involved in cell adhesion, would activate protein kinase C and trigger release of Ca^{2+} from the ER Ca^{2+} store and/or activate MAP kinase pathways such as ERK1/2. It has been proposed that the □1 integrin adhesion receptors may be a 'natural' receptor for cationic liposomes. Their ability to cluster would allow negatively charged domains in the β1 integrin to bind repeatedly to positive head groups on the liposome in a manner analogous to the binding and uptake of viral particles with repeating structures generated by the assembly of capsid proteins. FMDV is known to enter cells using integrin receptors, and collaboration with Pirbright has indicated that empty capsids also form TVAs. It is possible that cationic liposomes use a similar entry mechanism as viruses, and these early upstream events are key in TVA formation.

7.4 Other Nano-materials which Activate Autophagy -

Small molecules such as liposomes, are included in the nanoparticle family, are not the only molecules to be reported to induce autophagy. Autophagy is activated during incubation with nanoparticles such as quantum dots (QDs), which are increasingly used to label cells due to their improved fluorescence intensity and stability inside a cellular environments. As shown in figure 7.3, QDs are composed of a semi-conductor core usually of cadmium selenite or indium phosphide, and for biological imaging consist of a shell of zinc sulphate. The shell can also have other biocompatible molecules conjugated to it such as small ligands and antibodies for cell surface interactions and also peptides for intracellular localisation (Zhou and Ghosh 2007). However, Seleverstov *et al* (2006) reported that it is the size of the nanoparticles, not the composition which induces autophagy. The data suggests that the larger QDs activates autophagy, and results in a large perinuclear aggregate of LC3 during incubation with QDs (Seleverstov *et al* 2006).

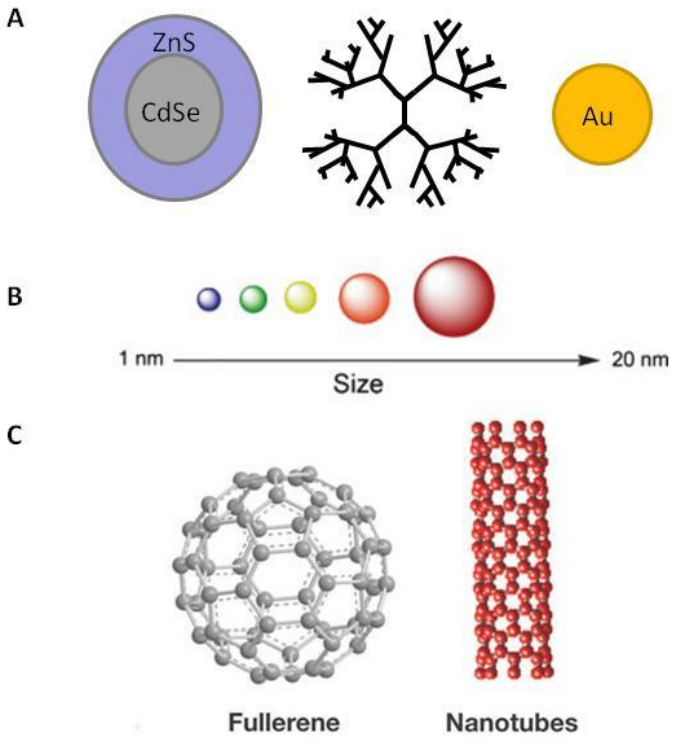

Figure 7.3 – Different nanoparticles that activate autophagy – (A) QDs, dendrimers and gold nanoparticles (Au) (B) QDs fluorescence depends on size (C) fullerene and carbon nanotubes.

There have also been other reports of carbon nanotubes, dendrimers and gold nanoparticles activating autophagy, monitored by increased production in LC3-II (Li *et al*

2010, Li *et al* 2009, Yamawaki and Iwai 2006). There is a possibility that there is a generic cellular response to the nanoparticles which are delivered into the cytoplasm, and autophagy is activated as part of an innate defence mechanism much like when pathogens such as bacteria and viruses invade. The overlaps between the endocytic pathway and autophagy allows for thorough monitoring of all pathways delivering contents into the cytoplasm.

With the development nanotheranostics, the use of nanomaterials in therapeutics and as diagnostic tools, there is an increasing use of liposomes aiding in treatments and delivery of drugs. Many of the current therapeutic agents for cancer which are intravenously delivered have poor pharmacokinetics and unsuitable distribution in the body (Lammers *et al* 2010). Liposomes can also be used in MRI diagnostics with a magnetic molecule conjugated to their surface or encapsulated during formation, in addition with specific ligand conjugation to the liposome surface to target specific tissues (Strijkers *et al* 2010). The *in vivo* application of lipsosomes in anti-cancer therapies, as well as diagnostic tool for MRI scans illustrates a wider application than cell culture as DNA delivery vector. However, given the data presented in this thesis and emerging evidence from the literature it is clear that liposomes, as well as other nanoparticles are activating other cellular pathways that may have beneficial or potentially harmful effects. Further investigation into the activation and biological processing of nanoparticles, particularly *in vivo*, are required to determine the eventual cellular effects and outcomes.

Appendix

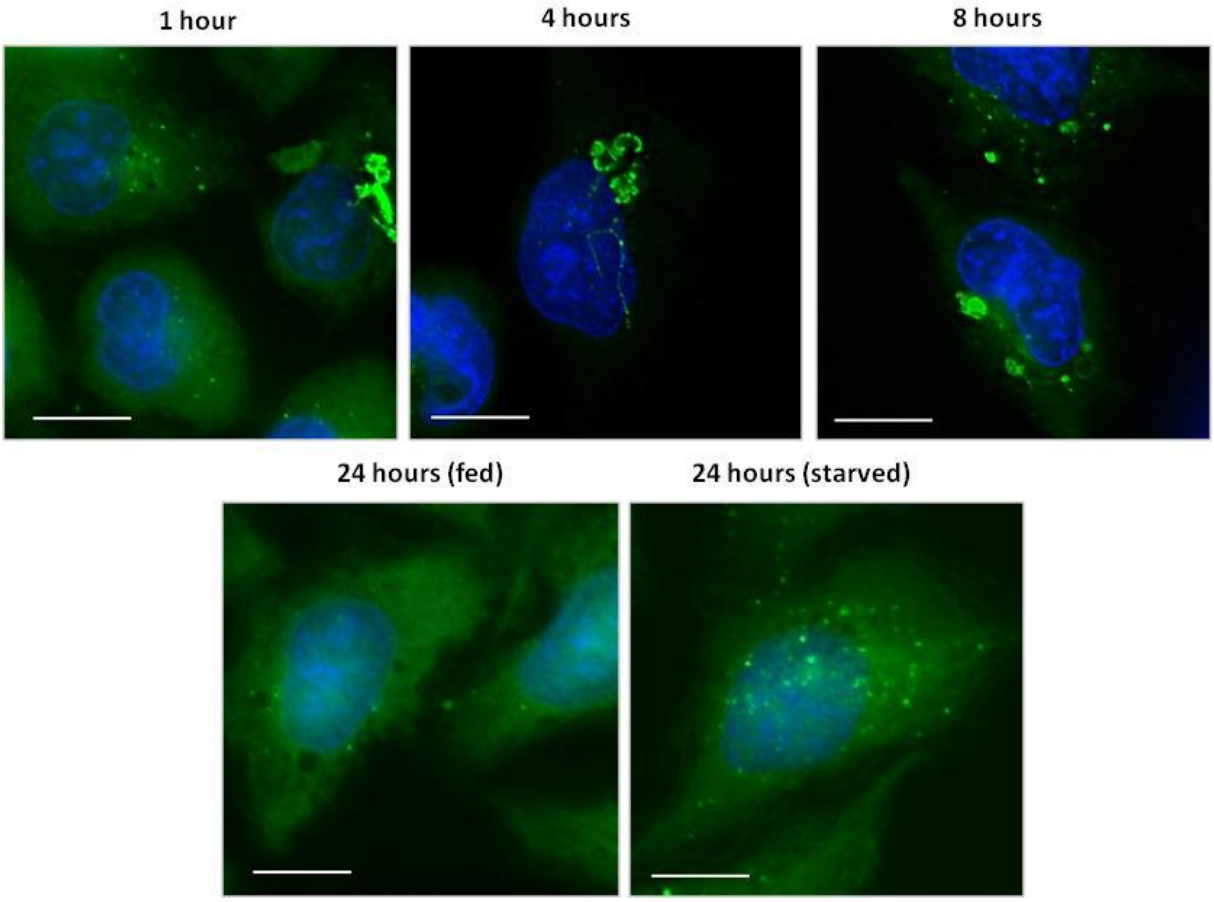

Figure A – Calcium Phosphate Induced Formation of TVAs - CHO cells stably expressing eGFP-LC3 were incubated with calcium phosphate transfection reagent for 1 hour, 4 hours and 8 hours prior to fixation (top panels). Calcium phosphate was removed at 8 hours and the cells were allowed to recover (24 hours fed), additionally following this recovery, cells were also starved (24 hours starved). Cells were fixed and nuclei stained with DAPI (blue). Bar is 5 µm.

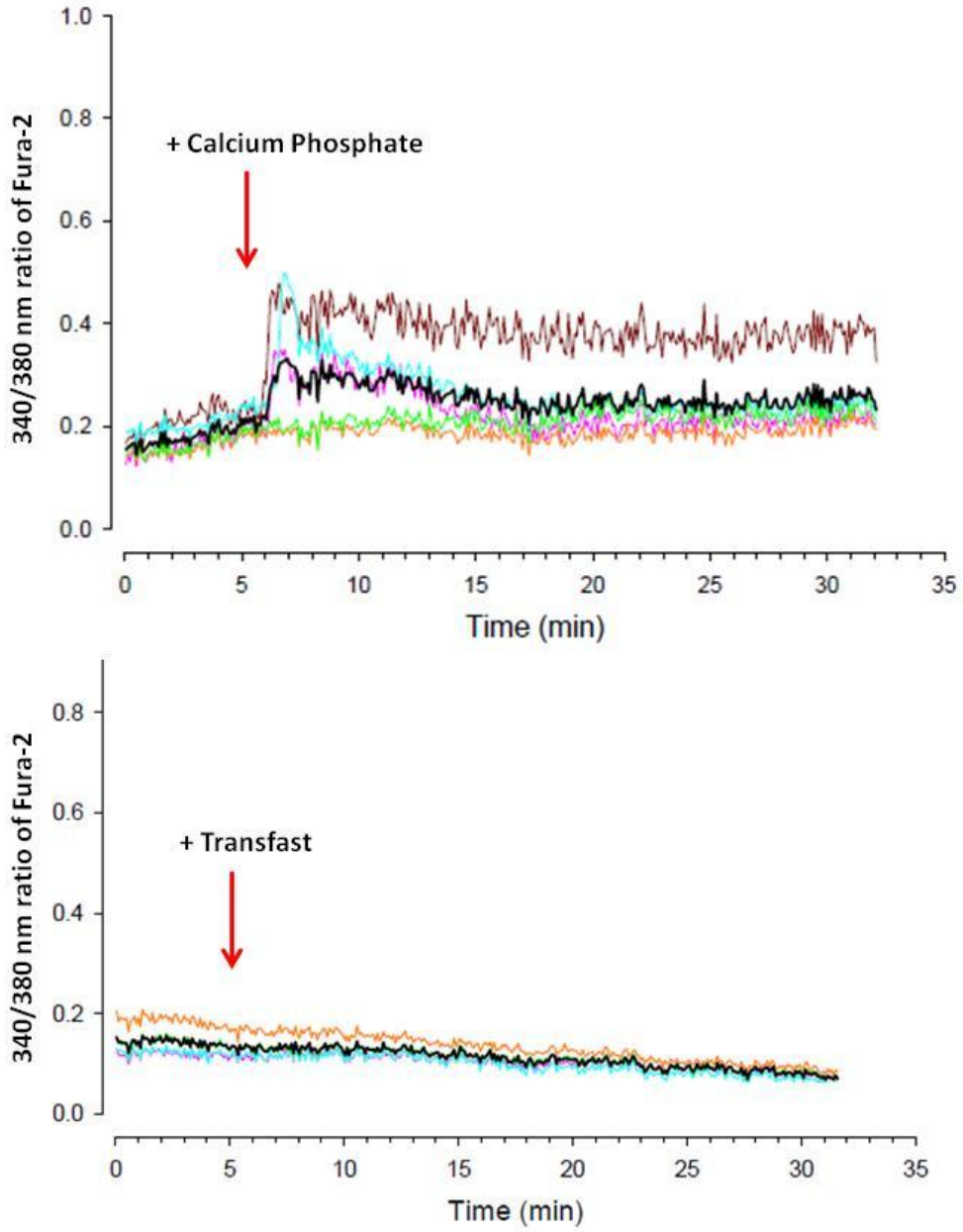

Figure B – Measuring Calcium Signalling During Formation of TVAs - For measurement of $[Ca^{2+}]_i$, CHO cells were loaded with 2·5 µM fura-2/AM for 60 min at 37 °C, and then washed free of extracellular dye. Experiments were carried out at 37°C using a heated stage (Medical Systems, USA) while perfusing (~1 mL/min) using a peristaltic pump. Pairs of fluorescence images at 340 nm and 380 nm were obtained using a fast-scanning monochromator (Kinetic Imaging, UK) every 5 secs on a Nikon Diaphot 200 microscope at x40. At indicated times the perfusion medium was changed by using a two-way, switchable valve adding the transfection reagent. For analysis, cells were outlined and the background-subtracted, mean fluorescence intensity was measured at each wavelength. The ratio of the 340-nm-excited fluorescence divided by the 380-nm-excited fluorescence was calculated for each time-point and plotted against time.

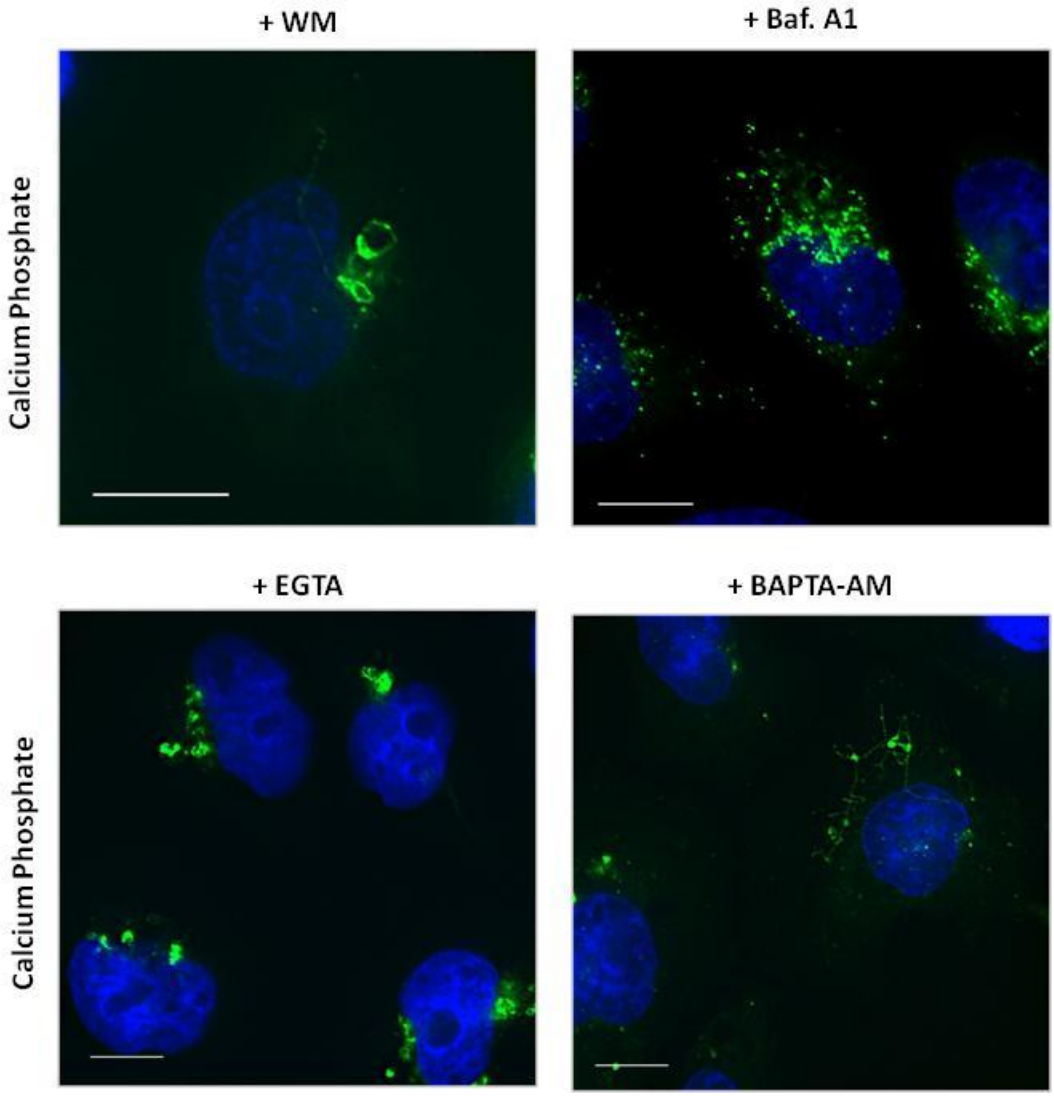

Figure C – Calcium Phosphate Induced Formation of TVAs in the Presence of Autophagy Inhibitors and Calcium Chelators - CHO cells stably expressing eGFP-LC3 were pre-incubated with either 100 nM wortmannin or 100 nM bafilomycin A1 (top panels) for 30 minutes, or with 3 mM EGTA for 15 minutes or 40 µM BAPTA-AM for 40 minutes (bottom panels). Cells were subsequently incubated with calcium phosphate transfection reagent for 4 hours prior to fixation). Cells were fixed and nuclei stained with DAPI (blue). Bar is 5 µm.

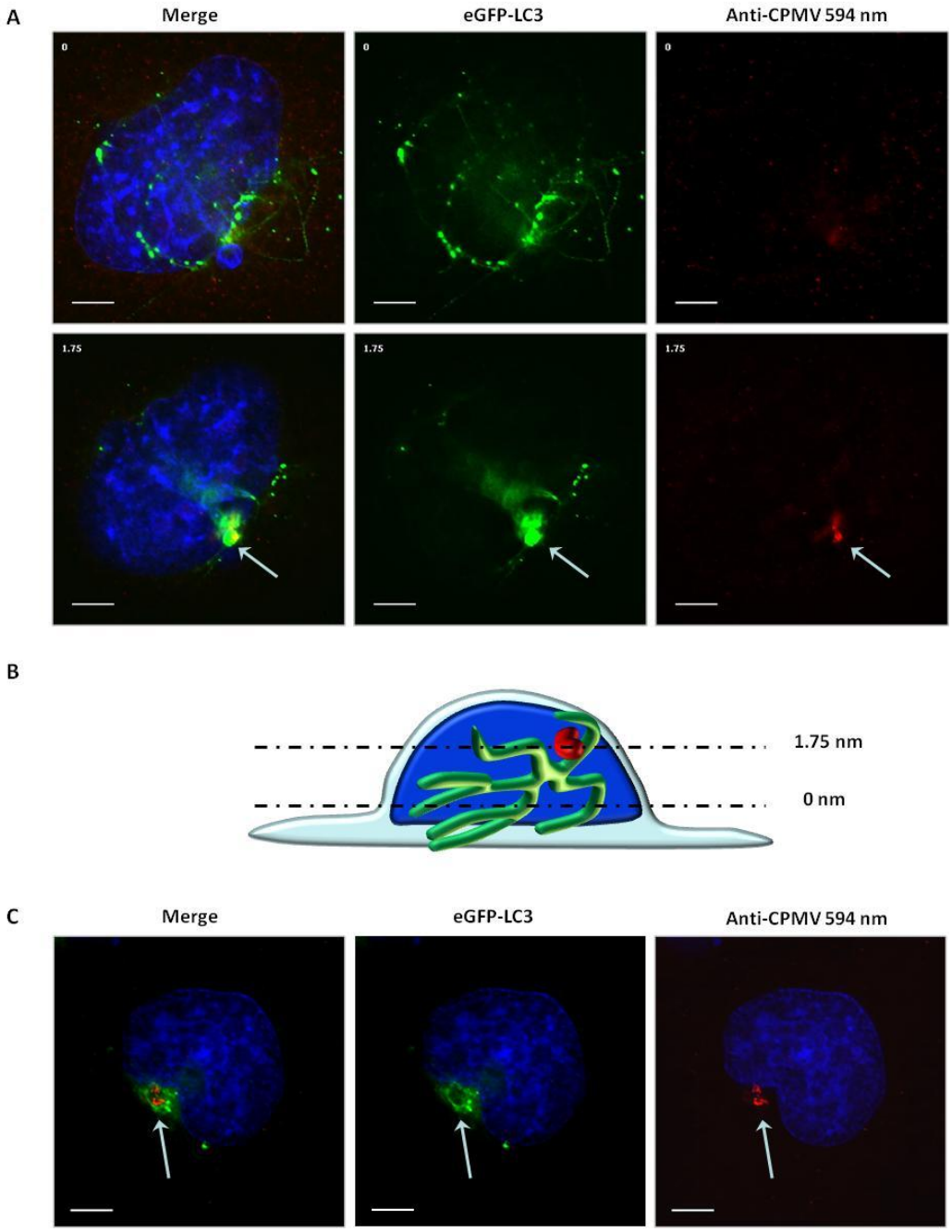

Figure D – Cowpea Mosaic Virus (CPMV) Induced Formation of TVAs - CHO cells stably expressing eGFP-LC3 were incubated with CMPV for 8 hours prior to fixation. Cells were subsequently fixed and CPMV was visualised by staining for the capsid protein (red). Bar is 5 µm. A Z-stack through the cell (panels A) shows a TVA in the top bottom focus plane (indicated in B) and the immunofluorescence from the capsid in a higher focal plane. The white arrow (panels A) indicates the central TVA structure colocalised with the capsid for CPMV.

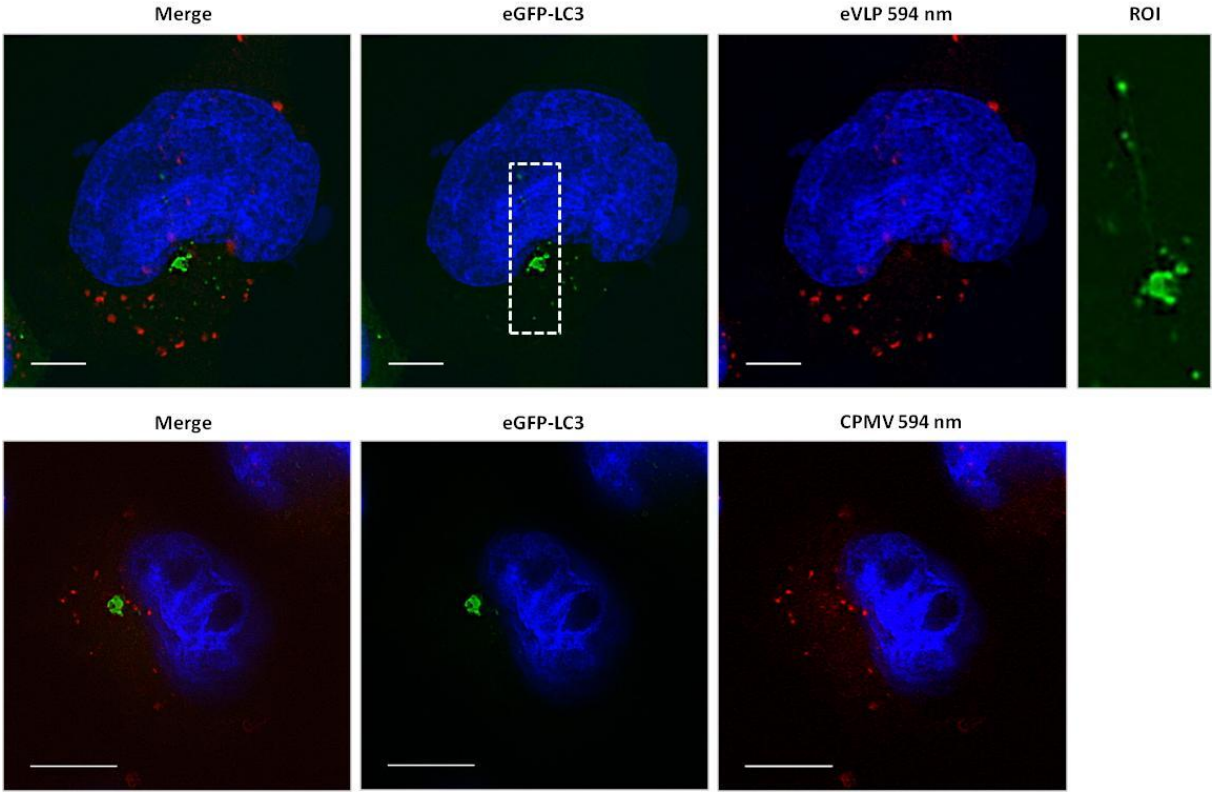

Figure E – Fluorescently Conjugated Cowpea Mosaic Virus (CPMV) and Empty Virus-like Particles (eVLP) Induced Formation of TVAs - CHO cells stably expressing eGFP-LC3 were incubated with the fluorescently labelled Dyelight-conjugated (red) CPMV and eVLP for 2 hours prior to fixation. Cells were subsequently fixed and nuclei stained with DAPI (blue). The ROI shows a TVA formed in the perinuclear region of the cell. Bar is 5 µm.

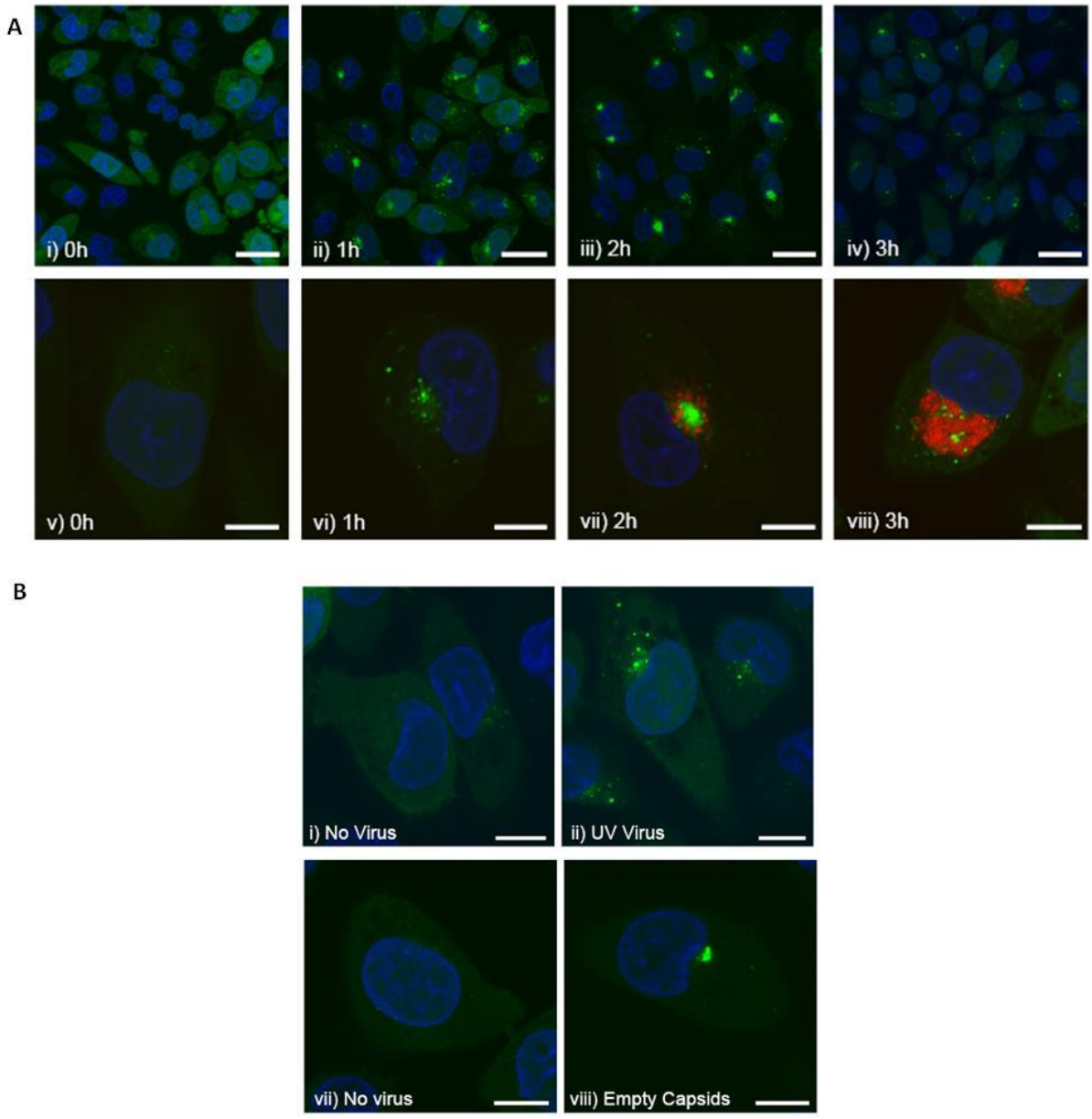

Figure E – Redistribution of GFP-LC3 in response to FMDV Infection, UV inactivated virus and Empty Capsids – (adapted from Berryman *et al* 2011) – Cho cells stably expressing GFP-LC3 were incubated for increasing times with FMDV virus (panels A i-iv). Higher magnification images (v-viii) show LC3 redistribution (green) and FMDV non-structural protein 3A (red) detected using antibody 2C2. Nuclei are stained with DAPI (blue). Bar is 30 µm (i-iv) and 10 µm (v-viii). LC3 redistribution is also seen when CHO cells stably expressing GFP-LC3 are incubated with UV-inactivated virus and empty FMDV type capsids (panel B) for 2 hours. Bar is 10 µm.

Generic Name	Chemical Name	Helper Lipid	Company	Notes
Transfast	N,N [bis (2-hydroxyethyl)-N-methyl-N-[2,3-di(tetradecanoyloxy) propyl] ammonium iodide	DOPE	Promega	Cationic lipid
Lipofectamine	2,3-dioleyloxy-N-[2(sperminecarboxamido)ethyl]-N,N-dimethyl-1-propanaminium trifluoroacetate (DOSPA)	DOPE	Invitrogen	Cationic lipid
HiPerfect	based on dioctadecyl glycyl spermine (DOGS)	-	Qiagen	Cationic lipid
Fugene HD	-	-	Roche	Non-liposomal transfection reagent based on a proprietary blend of lipids and other components
Turbofect	based on PEI - “Proton-sponge” buffers endosomal pH	-	Fermentas	Proprietary non-immunogenic cationic polymer
Nanojuice	based on dendrimers	-	Merck	Mixture uses Priostar® dendrimers with a proven polycationic liposomal formulation
JetPRIME	based on PEI and cationic lipids	-	PolyPlus Transfection	Mixture using the best lipids followed by proton sponge mediated endosomal escape
INTERFERin	-	-	PolyPlus Transfection	-
NBD-DOTAP	1-oleoyl-2-[6-[(7-nitro-2-1,3-benzoxadiazol-4-yl)amino]hexanoyl]-3-trimethylammonium propane	DOPE	Avanti Lipids	Cationic lipid conjugate to nitrobenzoxadiazole (NBD) fluorophore

Table F – Chemical Name (if known) and Description of the Commercially Available Cationic Liposomes for Transfection Used to Study the Formation of TVAs

References

References

Alberts B., Johnson A., Lewis J., Raff M., Roberts K. and Walter P. (2002) *Molecular Biology of the Cell* (4th Ed.) Garland Science, New York.

Anderson P. and Kedersha N. (2008) *Stress Granules: the Tao of Triage*. Trends Biochem Sci. 33:141-150

Axe E.,Walker S., Manifava M., Chandra P., Roderick H., Habermann A., Griffith G. and Ktistakis N. (2008) *Autophagosome Formation from Membrane Compartments Enriched in Phosphotidylinositol 3-phosphate and Dynamically Connected to the Endoplasmic Reticulum*. J Cell Biol. 182:685 – 701.

Bandyopadhyay U., Kaushik S., Varticovski L. and Cuervo A. (2009) *The Chaperone-mediated Autophagy Receptor Organises in Dynamic Protein Complexes at the Lysosomal Membrane.* Mol Cell Biol 28:5747-5763

Bayer N., Schober D., Prchla E., Murphy R., Blaas D. and Fuchs R. (1998) *Effects of Bafilomycin A1 and Nocodazole on Endocytic Transport in HeLa Cells: Implications for Viral Uncoating and Infection*. J Virol. 72:9645-9655

Bjorkoy G., Lamark T., Brech A. Outzen H., Perander M., Stenmark H. and Johansen T. (2007) p62/SQSTM 1 Forms Protein Aggregates Degraded by Autophagy and has a Protective Effect on Huntingtin-Induced Cell Death. J Cell Biol 171, 4, p 603 – 614

Burdette D., Seemann J. and Orth K. (2009) *Vibrio VopQ Induces PI3-kinase Independent Autophagy and Antagonizes Phagocytosis*. Mol Microbiol. 73:639-649

Chan E. and Tooze S. (2009) *Evolution of Atg1 Function and Regulation*. Autophagy 5:758-765

Chang Y. and Neufeld T. (2009) *An Atg1/Atg13 Complex with Multiple Roles in TOR-mediated Autophagy Regulation*. Mol Cell Biol 20:2004-2014

Clausen T., Lamark T., Isakson P., Finley K., Larsen K., Brech A., Øvervatn A., Stenmark H., Bjørkøy G., Simonsen A. and Johansen T. (2010) *p62/SQSTM1 and ALFY Interact to Facilitate the Formation of p62/ALIS and their Degradation by Autophagy*. Autophagy 6:330-344

Corradetti M. and Guan K. (2006) *Upstream of Mammalian Target of Rapamycin: Do All Roads Pass Through mTOR?* Oncogene 25:6347-6360

Ding W., Ni H., Gao W., Yoshimori T., Stolz D., Ron D. and Yin X. (2007) *Linking of Autophagy to Ubiquitin-Proteasome System is Important for the Regulation of Endoplasmic Reticulum Stress and Cell Viability*. Am J Pathol 171:513-524

Doherty G. and McMahon M. (2009) *Mechanisms of Endocytosis*. Annu. Rev. Biochem. 78:857-902

Ducharme N. and Bickel P. (2008) *Minireview: Lipid Droplets in Lipogenesis and Lipolysis*. Endocrinology 149:942-949

Dunn W. (1990a) *Studies on the Mechanisms of Autophagy: Formation of the Autophagic Vacuole*. J Cell Biol. 110:1923–1933.

Dunn W (1990b) *Studies on the Mechanisms of Autophagy: Maturation of the Autophagic Vacuole*. J Cell Biol. 110:1935–1945.

Edeling M., Smith C. and Owen D. (2007) *Life of a Clathrin Coat: Insight from Clathrin and AP Structures*. Nat Mol Cell Biol. 7:32-44

Eisinger-Mathason T, Andrade J., Groehler A., Clark D., Muratore-Schroeder T., Pasic L., Smith J., Shabanowitz J., Hunt D., Macara I and Lanningan D. (2008) *Codependent Functions of RSK2 and the Apoptosis-Promoting Factor TIA-1 in Stress Granule Assembly and Cell Survival.* Mol Cell 31:722-736

Fass E., Shvets E., Degani I., Hirschberg K. and Elazar Z. (2006) *Microtubules Support Production of Starvation-induced Autophagosomes but not Their Targeting and Fusion*. J Biol. Chem. 281:36303-36313

Felgner P., Gadek T., Holm M., Roman R., Chan H., Wenz M., Northrop J., Ringold G. and Danielsen M. (1987) *Lipofection: A Highly Eddificient, Lipid-Mediated DNA-Transfection Procedure*. Proc. Natl. Acad. Sci 84, p7413 – 7417.

Flinn R., Yan Y., Goswami S., Parker P. and Backer J. (2010) *The Late Endosome is Essential for mTORC1 Signalling*. Mol Biol Cell 21:833-841

Ford M., Mills I., Peter B., Vallis Y., Praefcke G., Evans P. and McMahon H. (2002) *Curvature of Clathrin-Coated Pits Driven by Epsin* Nat 419:361-366

Fujita N., Hayashi-Nishino M., Fukumoto H., Omori H., Yamamoto A., Noda T. and Yoshimori T. (2008) *An Atg4B Mutant Hampers the Lipidation of LC3 Paralogues and Causes Defects in Autophagosome Closure*. Mol Biol Cell 19:4651-4659

Fujita N., Itoh T., Omori H., Fukuda M., Noda T. and Yoshimori T. (2007) *The Atg16L Complex Specifies the Site of LC3 Lipidation for Membrane Biogenesis in Autophagy*. Mol Biol Cell 19:2092-2100

Fushman D. and Walker O. (2010) *Exploring the Linkage Dependence of Polyubiquitin Conformations Using Molecular Modelling*. J Mol Biol 395:803-814

Ganley I., Lam D., Wang J., Ding X., Chen S. and Jiang X. (2009) *ULK1-Atg13-FIP200 Complex Mediates mTOR Signalling and is Essential for Autophagy*. J Biol Chem. 284:12297-12305

Gao W., Kang J., Liao Y., Ding W., Gambotto A., Watkins S., Liu Y., Stolz D. and Yin X. (2010) *Biochemical Isolation and Characterization of the Tubulovesicular LC3-positive Autophagosomal Compartments*. J Biol Chem 285:1371-1383

Gao W., Ding W., Stoltz D. and Yin X. (2008) *Induction of Macroautophagy by Exogenously Introduced Calcium*. Autophagy 4:754-761

Garcia-Mata R., Gao Y. and Sztul E. (2002) Hassles with Taking Out the Garbage: Aggravating Aggresomes. Traffic 3: 388-396

Greer E., Banko M. and Brunet A. (2009) *AMP-activated Protein Kinase and FoxO Transcription Factors in Dietary Restriction-induced Longevity*. Ann N Y Acad Sci 1170:688-692

Gutierrez M., Munafó D., Berón W. Colombo MI. (2004) *Rab7 is required for the normal progression of the autophagic pathway in mammalian cells*. J Cell Sci 117:2687-2697

Hailey D., Rambold A., Satpute-Krishnan P., Mitra K., Sougrat R., Kim P. and Lippincott-Schwartz J. (2010) *Mitochondria Supply Membranes for Autophagosome Biogenesis during Starvation*. Cell 141:656-667

Hafez I., Maurer N. and Cullis P. (2001) *On the Mechanism Whereby Cationic Lipids Promote Intracellular Delivery of Polynucleic Acids*. Gene Ther. 8:1188-1196

Hanada T., Noda N., Satomi Y., Fujioka Y., Takao T., Inagaki F. and Ohsumi Y. (2007) *The Atg12-Atg5 Conjugate has a Novel E3-like Activity for Protein Lipidation in Autophagy*. J Biol Chem. 282:37298-37302

Hara T., Takamura A., Kishi C., Iemura S., Natsume T., Guan J. and Mizushima N. (2008) FIP200, a UK-interacting Protein, is Required for Autophagosome Formation in Mammalian Cells. J Cell Biol. 181:497-510

Hayashi-Nishino M., Fuijia N., Noda T., Yamaguchi A., Yoshimori T. and Yamamoto A. (2009) *A Subdomain of the Endoplasmic Reticulum Forms a Cradle For Autophagosome Formation*. Nat Cell Biol 11:1433-1437

He C. and Levine B. (2010) *The Beclin 1 Interactome*. Curr Op Cell Biol. 22:1-10 (R)

He C., Baba M., Cao Y and Klionsky D. (2008) *Self-interaction is Critical for Atg9 Transport and Function at the Phagophore Assembly Site During Autophagy*. Mol Biol Cell 19:5506-5516

Hennig K., Colombani J. and Neufeld T. (2006) *TOR Coordinates Bulk and Targeted Endocytosis in the Drosophila melanogaster Fat Body to Regulate Cell Growth*. J Cell Biol 173:963-974

Herter S., Osterloh P., Hilf N., Rechtsteiner G., Hohfeld J., Rammensee H. and Schild H. (2005) Dendritic Cell Aggresome-Like-Induced Structure Formation and Delayd Antigen Presentation Coincides in Influenza Virus-Infected Dendritic Cells. J Immunol 175:891-898

Hom R., Voa M., Regner M., Subach O., Cho W., Verkhusham V., Stahelin R. and Kutateladze T. (2007) *pH-Dependent Binding of the Epsin ENTH Domain and the AP180 ANTH Domain to PI(4,5)P_2-containing Bilayer*. J Mol Biol 373:412-423

Hsu P., Kang S., Rameseder J., Zhang Y., Ottina K., Lim D., Peterson T., Choi Y., Gray N., Yaffe M., Marto J. and Sabatini D. (2011) The mTOR-regulated Phosphoproteome Reveals a Mechanism of mTORC1-mediated Inhibition of Growth Factor Signaling. Science 332:1317-1322

Huang W. and Klionsky D. (2002) *Autophagy in Yeast: A Review of the Molecular Machinery.* Cell Struc Funct 27:409 – 420

Itakura E., Kishi C., Inoue K. and Mizushima N. (2008) *Beclin 1 Forms Two Distinct Phosphatidylinositol 3-kinase Complexes with Mammalian Atg14 and UVRAG*. Mol Cell Biol 19:5360-5372

Jäger S., Bucci C., Tanida I., Ueno T., Kominami E., Saftig P. and Eskelinen E. (2004) *Role for Rab7 in Maturation of Late Autophagic Vacuoles*. J Cell Sci 117: 4837-4848

Jordan M. and Wurm F. (2003) *Transfection of Adherent and Suspended Cells by Calcium Phosphate*. Methods 33:136-143

Kabeya Y., Mizushima N., Ueno T., Yamamoto A., Kirisako T., Noda T., Kominami E., Ohsumi Y. and Yoshimori T. (2000). *LC3, a Mammalian Homologue of Yeast Atg8p, is Localised in Autophagosome Membranes After Processing*. EMBO J 19:5720 – 5728

Kim J., Kundu M., Viollet B. and Guan K. (2011) *AMPK and mTOR Regulate Autophagy Through Direct Phosphorylation of Ulk1*. Nat Cell Biol 13:132-141

Kim E., Goraksha-Hicks P., Li L., Neufeld T. and Guan K. (2009) *Regulation of TORC1 by Rag GTPases in Nutrient Response*. Nat Cell Biol. 10:935-945

Kimball S and Jefferson L. (2006) Signaling Pathways and Molecular Mechanisms Through Which Branched Amino Acids Mediate Translational Control of Protein Synthesis. J Nutr 136:227S-231S

Kimura S, Noda T. and Yoshimori T. (2008) *Dynein-dependent Movement of Autophagosomes Mediates Efficient Encounters with Lysosomes*. Cell Struct Func. 33:109-122

Kirchhausen T. (2009) *Imaging Endocytic Clathrin Structures in Living Cells.* Trends Cell Biol. 19:596-605

Kirchhausen T. (2000) *Clathrin*. Ann Rev Biochem 69:699-727

Kirkin V, Lamark T, Sou Y, Bjørkøy G, Nunn J, Bruun JA Shvets E, McEwan D, Clausen T, Wild P, Bilusic I, Theurillat J, Øvervatn A, Ishii T, Elazar Z, Komatsu M, Dikic I and Johansen T. (2009) *A Role for NBR1 in Autophagosomal Degradation of Ubiquitinated Substrates*. Mol Cell 33:505-516

Kirisako T., Ichimura Y., Okada H., Kabeya Y., Mizushima N., Yoshimori T., Ohsumi M., Takao T., Noda T. and Ohsumi Y. (2000) *The Reversible Modification Regulates the Membrane-Binding State of Apg8/Aut7 Essential for Autophagy and the Cytoplasm to Vacuole Targeting Pathway*. J Cell Biol 151:263-275

Kirisako T., Baba M., Ishihara N., Miyazawa K., Ohsumi M., Yoshimori T., Noda T. and Ohsumi Y. (1999) *Formation Process of Autophagosome Is Traced with Apg8/Aut7p in Yeast*. J Cell Biol 147:435-446

Klionsky D. (2005) *The Molecular Machinery of Autophagy; Unanswered Question*. J Cell Sci 118:7 – 18

Klionsky D., Cregg J., Dunn W., Emr S., Sakai Y., Sandoval I., Sirbirny A., Subramani S., Thumm M., Veenhuis M. and Ohsumi Y. (2003) *A Unified Nomenclature for Yeast Autophagy-Related Genes*. Dev Cell 5:539–545

Klionsky G. and Emr S. (2000) *Autophagy as a Regulated Pathway of Cellular Degradation*. Sci 290:1717 - 1721

Kochl R., Hu X., Chan E. And Tooze S. (2006) *Microtubules Facilitate Autophagosome Formation and Fusion of Autophagosomes with Endosomes.* Traffic 6, p 129-145

Kopito R (2000) Aggresomes, Inclusion Bodies and Protein Aggregations. Trends Cell Biol. 10, p 524 – 530

Korkhov V. (2009) *GPL-LC3 Labels Organised Smooth Endoplasmic Reticulum Membrane Independently of Autophagy*. J Cell Biochem 103:86-95

Korolchuk V., Menzies F. and Rubinsztein D. (2010) *Mechanisms of Cross-talk Between Ubiquitin-Proteasome and Autophagy-Lysosome Systems*. FEBS Lett. 584:1393-1398

Korolchuk V., Mansilla A., Menzies F., Rubenstein D. (2009) *Autophagy Inhibition Compromises Degradation of Ubiquitin-Proteasome Pathway Substrates*. Mol Cell 33:517-527

Kouroku Y., Fujita E., Tanida I., Ueno T., Isoai A., Kumagai H., Ogawa S., Kaufman R., Kominami E and Momoi T. (2007) ER Stress (PERK/eIF2α Phosphorylation) Mediates the Polyglutamine-induced LC3 conversion, an Essential Step for Autophagy Formation. Cell Death Differ 14 p 230 – 239

Kufe D., Pollock R., Weichselbaum R., Bast R., Gansler T., Holland J. and Frei E. (2003) *Cancer Medicine* (6th Ed.) pp759-775. Philadelphia PA, USA: BC Decker.

Kukowska-Latallo J., Bielinska A., Johnson J., Spindler R., Tomalia D., and Baker J. (1996) *Efficient Transfer of Genetic Material into Mammalian Cells Using Starburst Polyamidoamine Dendrimers*. Proc Natl Acad Sci 93:4897-4902

Kuma A., Matsui M. and Mizushima N. (2007) *LC3, an Autophagosome Marker, Can Be Incorporated into Protein Aggregates Independent of Autophagy*. Autophagy 3:323 – 328

Kunz J., Schwarz H. and Mayer A. (2004) *Determination of Four Sequential Stages During Microautophagy in Vitro*. J Biol Chem 279:9987-9996

Kutateladze T. (2010) *Translation of the Phosphoinositol Code by PI Effectors* Nat Chem Biol 6:507-513

LammersT., Kiessling F., Hennink W. and Storm G. (2010) *Nanotheranostics and Image-Guided Drug Delivery: Current Concepts and Future Directions*. Mol Pharm 7:1899-1912

Li J., Hartono D., On C., Bay B. and Yug L. (2010) *Autophagy and Oxidative Stress Associated with Gold Nanoparticles.* Biomaterials 31:5996-6003

Li C., Liu H., Sun Y., Wang H., Guo F., Rao S., Deng J., Zhang Y., Miao Y., Guo C., Meng J., Chen X., Li L., Li D., Xu H., Wang H., Li B. and Jiang C. (2009) *PAMAM Nanoparticles Promote Acute Lung Injury by Inducing Autophagic Cell Death through the Akt-TSC2-mTOR Signaling Pathway.* J Mol Cell Biol 1:37-45

Liu X. And Zheng X. (2007) *Endoplasmic Reticulum and Golgi Localization Sequences for Mammalian Target of Rapamycin*. Mol Biol Cell 18:1073-1082

Man N., Chen Y., Zheng F., Zhou W. and Wen L. (2010) *Induction of Genuine Autophagy by Cationic Lipids in Mammalian Cells.* Autophagy 6:1-6

Manning B. and Cantley L. (2003) *Rheb Fills the GAP between TSC and TOR.* Trends Biochem Sci 28:573-576

Matsunga K., Morita E., Saitoh T., Akira S., Ktistakis N., Izumi T., Noda T. and Yoshimori T. (2010) *Autophagy Requires Endoplasmic Reticulum Targeting of the PI3-kinase Complex via Atg14L*. J Cell Biol. 190:511-521

Matsunaga K., Saitoh T., Tabata K., Omori H., Satoh T., Kurotori N., Maejima I., Shirahama-Noda K., Ichimura T., Isobe T., Akira S., Noda T. and Yoshimori T. (2009) *Two Beclin 1-binding Proteins, Atg14-L and Rubicon, Reciprocally Regulate Autophagy at Different Stages.* Nat Cell Biol. 11:385-397

Medina-Kauwe L., Xie J. and Hamm-Alvarez S. (2005) *Intracellular Trafficking of Nonviral Vectors.* Gene Ther 12:1734-1751

Mitchener, J. S., Shelburne, J. D., Bradford, W. D. and Hawkins, H. K. (1976). *Cellular autophagocytosis induced by deprivation of serum and amino acids in HeLa cells*. Am. J. Pathol. 83:485-491

Mizushima N. (2007) *Autophagy: Process and Function*. Genes Dev 21:2861–2873.

Mizushima N. And Yoshimori T. (2007) *How to Interpret LC3 Immunoblotting*. Autophagy 3:542-545

Mizushima N., Yamamoto A., Matsui M., Yohimori T. and Ohsumi Y. (2004) *In Vivo Analysis of Autophagy in Response to Nutrient Starvation Using Transgenic Mice Expressing a Fluorescent Autophagosome Marker*. Mol Biol Cell 15:1101-1111

Mizushima N., Yamamoto A., Hatano M., Kobayashi Y, Kabeya Y., Suzuki K., Tokuhisa T., Ohsumi Y. and Yoshimori T. (2001) *Dissection of Autophagosome Formation Using Apg5-deficient Mouse Embryonic Stem Cells*. J Cell Biol 152 657-667

Mizushima N., Noda T., Yoshimori T., Tanaka Y., Ishii T., George M., Klionsky D., Ohsumi M. and Ohsumi Y. (1998) *A Protein Conjugation System Essential For Autophagy*. Nature 395:395-398

Munafo D. and Colombo M. (2001) *A Novel Assay to Study Autophagy: Regulation of Autophagosome Vacuole Size by Amino Acid Deprivation*. J Cell Sci 114:3691-3629

Myung J., Kim K. and Crews C. (2001) *The Ubiquitin-Proteasome Pathway and Proteasome Inhibitors*. Med Res Rev 21:245-273

Nishida Y., Arakawa S., Fujitani K., Yamaguchi H., Mizuta T., Kanaseki T., Komatsu M., Otsu K., Tsujimoto Y. and Shimizu S. (2009) *Discovery of Atg5/Atg7-independent Alternative Macroautophagy*. Nature 461:654-658

Noda T., Fujita N. And Yoshimori T. (2009) *The Late Stages of Autophagy: How Does the End Begin?* Cell Death Diff. 16:984-990

Ohsaki Y., Cheng J., Fujita A., Tokumoto T. and Fujimoto T. (2006) *Cytoplasmic Lipid Droplets are Sites of Convergence of Proteasomal and Autophagic Degradation of Apolipoprotein*. Mol Biol Cell 17:2674-2683

Orsi A., Polson H. and Tooze S. (2010) *Membrane Trafficking Events That Partake in Autophagy*. Curr Opin Cell Biol. 22:150-156

Pankiv S., Clausen T., Lamark T., Brech A., Bruun J., Outzen H., Overvatn A., Bjorkoy G. and Johansen T. (2007) *p62/SQSTM 1 Binds Directly to Atg8/LC3 to Facilitate Degradation of Ubiquitinated Protein Aggregates by Autophagy*. J Biol Chem 282, 33, p 24131 – 24145

Pattingre S., Espert L., Biard-Piechaczyk and Codogno P. (2008) *Regulation of Macroautophagy by mTOR and Beclin 1 Complexes*. Biochimie 90:313-323

Petiot A., Ogier-Denis E., Blommaart E., Meijer A. and Codogno P. (2000) *Distinct Classes of Phosphatidylinositol 3'-kinase are Involved in Signalling Pathways that Control Macroautophagy in HT-29 Cells*. J Biol Chem 275:992-998

Pierre P. (2005) *Dendritic Cells, DRiPs, and DALIS in the Control of Antigen Processing.* Immunol. Rev. 207: 184-190

Polson H., Lartigue J., Rigen D., Reedijk M., Urbe S., Clague M. and Tooze S. (2010) *Mammalian Atg18 (WIPI2) Localizes to Omegasome-anchored Phagophores and Positively Regulates Autophagy.* Autophagy 6:506-522

Poteryaev D., Datta S., Ackema K., Zerial M. and Spang A. (2010) *Identification of the Switch in Early-to-Late Endosome Transition*. Cell 141:497-508

Qin L., Wang Z., Tao L. and Wang Y. (2010) *ER Stress Negatively Regulates AKT/mTOR Pathway to Enhance Autophagy*. Autophagy 6:2-19

Ravikumar B., Moreau K., Jahreiss L., Puri C. and Rubinsztein D. (2010) *Plasma Membrane Contributes to the Formation of Pre-Autophagosomal Structures*. Nat Cell Biol 12:747-757

Ravikumar B., Imarisio S., Sakar S., O'Kane C. and Rubinsztein D. (2008) *Rab5 Modulates Aggregation and Toxicity of Huntingtin Through Macroautophagy in Cell and Fly Models of Huntington Disease*. J Cell Sci 121:1649-1660

Razi M., Chan E. and Tooze S. (2009) *Early Endosomes and Endosomal Coatomers are Required for Autophagy*. J Cell Biol. 185:305-321

Rejman J., Bragonzi A. and Conese M. (2005) *Role of Clathrin- and Caveolae- Mediated Endocytosis in Gene Transfer Mediated by Lipo- and Polyplexes.* Mol Ther. 12:468-474

Rouiller I., Brookes S., Hyatt A., Windsor M. and Wileman T. (1998) *African Swine Fever Virus is Wrapped by the Endoplasmic Reticulum*. J Virol 72:2373-2387

Sambrook J. and Russell D. (2000) *Molecular Cloning: A Laboratory Manual*. (3rd Edition) Cold Spring Harbour Laboratory Press, New York.

Sancak Y., Bar-Peled L., Zoncu R., Markhard A., Nada S. and Sabatini D. (2010) *Ragulator-Rag Complex Targets mTORC1 to the Lysosomal Surface and is Necessary for its Activation by Amino Acids*. Cell 141:290-303

Sancak Y., Peterson T., Shaul Y., Lindquist R., Thoreen C., Bar-Peled L and Sabatini D. (2008) *The Rag GTPases Bind Raptor and Mediate Amino Acid Signalling to mTORC1*. Science 320:1496-1501

Sarbassov D., Ali S., Sengupta S., Sheen J., Hsu P., Bagley A., Markhard A. and Sabatini D. (2006) *Prolonged Rapamycin Treatment Inhibits mTORC2 Assembly and Akt/PKB.* Mol Cell 22:159-168

Sarkar S., Korolchuk V., Renna M., Winslow A. and Rubinsztein D. (2009) *Methodological Considerations for Assessing Autophagy Modulators*. Autophagy 5:1-7

Scarlatti F., Maffei R., Beau I., Ghidoni R. and Codogna P. (2008) *Non-Canonical Autophagy*. Autophagy 4:1083–1085

Seibenhener M., Geetha T. and Wooten M. (2007) *Sequestosome 1/p62 – More Than Just a Scaffold*. FEBS Lett 581:175 – 179

Seleverstov O., Zabirnyk O., Zscharnack M., Bulavina L., Nowicki M., Heinrich J., Yezhelyev M., Emmrich F., O'Regan R. and Bader A. (2006) Quantum dots for Human Mesenchymal Stem Cells Labeling. A Size-dependent Autophagy Activation. Nano Lett 6:2826-2832.

Shibata M., Yoshimura K., Tamura H., Ueno T., Nishimura T., Inoue T., Saski M., Koike M., Arai H., Kominami E. and Uchiyama Y. (2010) *LC3, a Microtubule-Associated Protein 1A/B Light Chain3, is Involved in Cytoplasmic Lipid Droplet Formation*. Biochem Biophys Res Comm. 393:274-279

Shibata M., Yoshimori K., Furuya N., Koike M., Ueno T., Komatsu M., Arai H., Tanaka K., Kominami E. and Uchiyama Y. (2009) *The MAP1-LC3 Conjugation System is Involved in Lipid Droplet Formation*. Biochem Biophys Res Comm. 382:419-423

Simonsen A., Lippé R., Christoforidis S., Gaullier J., Brech A., Callaghan J., Toh B., Murphy C., Zerial M. and Stenmark H. (1998) *EEA1 links PI(3)K function to Rab5 Regulation of Endosome Function*. Nat 394:494-498

Shvets E., Fass E., Scherz-Shouval R. and Elazar Z. (2008) *The N-terminus and Phe52 Residue of LC3 Recruit p62/SQSTM1 into Autophagosomes*. J Cell Sci 121:2685-2695

Szeto J., Kaniuk N., Nisman R., Mizushima N., Yoshimori T., Bazett-Jones D. and Brumell J. (2006) *ALIS are Stress-Induced Protein Storage Compartments for Substrates of the Proteosome and Autophagy.* Autophagy 2, p 189-199

Takahashi K., Nakagawa M., Young S. and Yamanaka S. (2005) *Differential Membrane Localisation of ERas and Rheb, two Ras-related Proteins Involved in the Phosphatidylinositol 3-kinase/mTOR Pathway*. J Biol Chem 2:32768-32774

Tanida I., Minematsu-Ikeguchi N., Ueno T. and Kominami E. (2005) *Lysosomal Turnover, but not a Cellular Level, of Endogenous LC3 is a Marker for Autophagy*. Autophagy 1:84-91

Thoreen C., Kang S., Chang J., Liu Q., Zhang J., Gao Y., Reichling L., Sim T., Sabatini D. and Gray N. (2009) *An ATP-competitive Mammalian Target of Rapamycin Inhibitor Reveals Rapamycin-resistant Functions of mTORC1.* J Biol Chem 284:8023-8032

Tooze S. and Yoshimori T. (2010) *The Origin of the Autophagosomal Membrane*. Nat Cell Biol. 12:831-835

Tresset G. (2009) *The Multiple Faces of Self-Assembled Lipidic Systems*. PMC Biophys. 2:3

Wei Y., Pattingre S., Sinha S., Bassik M. and Levine B. (2008) *JNK-1-mediated Phosphorylation of Bcl-2 Regulates Starvation-induced Autophagy*. Mol Cell 30:678-688

Weichhart T. and Saemann M. (2009) *The Multiple Facets of mTOR in Immunity*. Trends Immunol. 30:218-226

Weidberg H., Shvets E., Shpilka T., Shimron F., Shinder V. and Elazar Z. (2010) *LC3 and GATE-16/GABARAP Subfamilies are both Essential yet Act Differently in Autophagosome Biogenesis*. EMBO J 29:1792-1802

Won Y., Sharma R. and Konieczny S. (2009) *Missing Pieces in Understanding the Intracellular Trafficking of Polycation/DNA Complexes*. J Control Release 139:88-93

Xie Z. and Klionsky D. (2007) *Autophagosome Formation: Core Machinery and Adaptations.* Nature Cell Biol. 9, p 1102 – 1108

Xu Y. and Szoka F. (1996) *Mechanism of DNA Release from Cationic Liposomes/DNA Complexes Used in Cell Transfection*. Biochemistry 35:5616-5623

Yamawaki H. and Iwai N. (2006) *Cytotoxicity of Water-Soluble Fullerene in Vascular Endothelial Cells*. Am J Physiol Cell Physiol. 290:C1495-C1502

Yorimitsu T. and Klionsky D. (2005) *Autophagy: Molecular Machinery For Self-eating*. Cell Death Differ. 12:1542-1552

Young A., Chan E., Hu X., Kochl R., Crawshaw S., High S., Hailey D., Lippincott-Schwartz J. and Tooze S. (2006) *Starvation and ULK1-dependent Cycling of Mammalian Atg9 Between TGN and Endosomes*. J Cell Sci 119:3888-3900

Yu L., McPhee C., Zheng L., Mardones G., Rong Y., Peng J., Mi N., Zhao . Liu Z., Hailey D., Oorschot V., Klumperman J, Baehrecke E. and Lenardo M. (2010) *Termination of Autophagy and Reformation of Lysosomes Regulated by mTOR*. Nat Lett. 465:942-947

Zhong Y., Wang Q., Li X., Yan Y., Backer J., Chait B., Heintz N. and Yue Z. (2009) *Distinct Regulation of Autophagic Activity by Atg14L and Rubicon Assoicated with Beclin 1-phosphatidyllinositol-3-kinase Complex.* Nat Cell Biol 11:468-477

Zhou X., Wang L., Hasegawa H., Amin P., Han B., Kaneko S., He Y. and Wang F. (2011) *Deletion of PIK3C3/Vps34 in Sensory Neurons Causes Rapid Neurodegeneration by Disrupting the Endosomal but not the Autophagic Pathway.* Proc Natl Acad Sci 107:9424-9249

Zidovska A., Ewert K., Quispe J., Carragher B., Potter C. and Safinya C. (2009) *The Effect of Salt and pH on Block Liposomes Studied by Cryogenic Transmission Electron Microscopy*. Biochim Biophys Acta 1788:1869-1876

Zuhorn I., Oberle V., Visser W., Engberts J., Bakowsky U., Polushkin E. and Hoekstra D. (2002) *Phase Behaviour of Cationic Amphiphiles and their Mixtures with Helper Lipids Influences Lipoplex Shape, DNA Translocation and Transfection Effeciency.* Biophys J. 83:2096-2108

Acknowledgements

First and foremost I offer my sincerest gratitude to my supervisors, Tom Wileman and Penny Powell, who have supported me throughout my thesis, and their encouragement and supervision have made this thesis possible. With their patience, guidance and knowledge I have developed research skills and techniques, whilst allowing me the room to work in my own way. I would also like to acknowledge and thank all of the Wileman/Powell lab members past and present – Eleanor, Roberto, Matt, Andras, Matthew, Maryam, Zhou, Jas and Laura who have not only provide support, motivation and interesting scientific discussions, but also for frequent coffee breaks and entertainment.

I would also like to thank everyone in the BMRC for anytime they have helped me with a technical difficulties in one shape or another – in particular Claire Butler for microscopy assistance, the McEwan and Clark lab with luciferase assays and the Mogensen lab for antibodies and microscopy expertise. I would like to thank Alba Warn and Jasmine Waters for the daily running of the BMRC laboratories. This journey would not have been as interesting without the fascinating people I met along the way, thank you all.

Furthermore I would like to say a huge thank you for all the support of Paul Thomas, and particularly his patience and guidance in setting up the live cell microscopy and various imaging assay for which has made this project possible.

Lastly, I would like to say thank you to my family for all the love and support for the duration of my studies. I owe a huge amount of gratitude to my partner, Jimmy, who has provided a great deal of physical and emotional support, as well as encouragement and motivation for the duration of my thesis. I know it has been tough!

"Long is the way, and hard, that out of hell leads up to light" – John Milton